Conditional Chemoconnectomics (cCCTomics): Conditional Targeting of Chemical Transmission Efficiently

Renbo Mao[a,b,#], Jianjun Yu[a,#], Bowen Deng[a], Xihuimin Dai[a], Yuyao Du[a], Sujie Du[a], Wenxia Zhang[a] and Yi Rao[a,1]

[a]Laboratory of Neurochemical Biology, Chinese Institute for Brain Research, Beijing; PKU-IDG/McGovern Institute for Brain Research, Peking-Tsinghua Center for Life Sciences, School of Life Sciences, Department of Chemical Biology, College of Chemistry and Chemical Engineering, School of Pharmaceutical Sciences, Peking University, Beijing 100871; Chinese Institutes for Medical Research, Capital Medical University; Changping Laboratory, Yard 28, Science Park Road, Changping District; and Research Unit of Medical Neurobiology, Chinese Academy of Medical Sciences, Beijing, China.

[b]National Institute of Biological Sciences, Chinese Academy of Medical Sciences & Peking Union Medical College, Beijing, China.

[#]Co-first authors

[1]Corresponding Author Yi Rao

Email: yrao@pku.edu.cn

Author Contributions: Y.R. supervised the project. R.M. and J.Y. performed majority of experiments and data analysis. B.D., J.Y., and R.M. found advanced morning activity phenotype and carried out experiments of CNMa/CNMaR. R.M., X.D., Y.D., and S.D. carried out experiments of cCCTomics fly generation.

R.M. and Y.R. wrote the manuscript.

Competing Interest Statement: The authors declare no competing interest.

Keywords: chemoconnectome, CRISPR/Cas9, CNMa, circadian rhythm, morning anticipation

Abstract

Dissection of neural circuitry underlying behaviors is a central theme in neurobiology. We have previously proposed the concept of chemoconnectome (CCT) to cover the entire chemical transmission between neurons and target cells in an organize and created tools for studying it (CCTomics) by targeting all genes related to the CCT in Drosophila. Here we have created lines targeting the CCT in conditional manners after modifying GFP RNA interference, Flp-out and CRISPR/Cas9 technologies. All three strategies are validated to be highly effective with the best using chromatin-peptide fused Cas9 variants and scaffold optimized sgRNAs. As a proof of principle, we conduct a comprehensive intersection analysis of CCT genes expression profiles in the clock neurons, uncovering 43 CCT genes present in clock neurons. Specific elimination of each from clock neurons revealed that loss of the neuropeptide CNMa in two posterior dorsal clock neurons (DN1ps) or its receptor (CNMaR) caused advanced morning activity, indicating a suppressive role of CNMa-CNMaR on morning anticipation, opposite to the promoting role of PDF-PDFR on morning anticipation. These results demonstrate the effectiveness of conditional CCTomics and its tools created by us here and establish an antagonistic relationship between CNMa-CNMaR and PDF-PDFR signaling in regulating morning anticipation.

52 **Introduction**

53 Much research efforts have been made to uncover the wiring and signaling
54 pathways of neural circuits underlying specific behaviors. Circuit dissection
55 strategies include genetic screening, genetic labelling, circuit tracing, live
56 imaging, genetic sensors and central nervous system (CNS) reconstruction via
57 electron microscopy (EM). Recently, we have developed chemoconnectomics
58 (CCTomics), focusing on building a comprehensive set of knockout and knockin
59 tool lines of chemoconnectome (CCT) genes, to dissect neural circuitry based
60 on chemical transmission (Deng et al., 2019).

61 Each strategy has advantages and disadvantages. For example, genetic
62 screening is less biased but inefficient; circuit tracing with viruses provides
63 information of connection, but is often prone to leaky expression and inaccurate
64 labelling; and EM reconstruction is anatomically accurate but does not allow for
65 manipulation of corresponding neurons. CCTomics overcomes limitations of
66 previous strategies by allowing for behavioral screening of CCT genes and
67 accurate labelling or manipulation of corresponding neurons. However, it is still
68 limited in that knockout of some CCT genes can be lethal during development
69 and that CCT genes may function differently in different neurons, which require
70 a cell type-specific manipulation. Thus, we decided to invent a conditional
71 CCTomics (cCCTomics) in which gene deletion was conditional.

72 There are three major strategies for somatic gene mutagenesis at the
73 DNA/RNA level: RNA interference, DNA site-specific recombination enzymes,

74 and CRISPR/Cas system. RNA interference targets RNAs conveniently and
75 efficiently (Martin and Caplen, 2007; Oberdoerffer et al., 2005). Libraries of
76 transgenic RNAi flies covering almost the entire fly genome have been
77 established (Ni et al., 2011; Perkins et al., 2015). DNA site specific
78 recombination enzymes such as Flp, B3 and Cre mediate specific and efficient
79 gene editing (Gaj et al., 2014; Grindley et al., 2006). These strategies require
80 flies with reverse repetitive sequences knocked into the corresponding genes,
81 which is time-consuming with relatively complex recombination for genetic
82 assays. CRISPR/Cas systems, particularly CRISPR/Cas9, which targets DNA
83 with a sgRNA/Cas protein complex, have been broadly applied in gene
84 manipulation over the last decade. The widespread use of CRIPSR/Cas9 in
85 Drosophila somatic gene manipulation began in 2014 (Xue et al., 2014). Later,
86 tRNA-flanking sgRNAs was designed and applied, which enabled multiple
87 sgRNAs to mature in a single transcript (Xie et al., 2015), accelerating the
88 application of this strategy in conditional gene manipulation in flies with
89 impressive efficiency (Delventhal et al., 2019; Port and Bullock, 2016; Port et
90 al., 2020; Schlichting et al., 2019; Schlichting et al., 2022). Additionally, libraries
91 of UAS-sgRNA targeting kinases (Port et al., 2020) and GPCRs (Schlichting et
92 al., 2022) have been established, but no sgRNA libraries covering all the CCT
93 genes exists yet. The efficiency of CRISPR/Cas9 has not been validated
94 systematically in the Drosophila nervous system.

95 The circadian rhythm can be used for proof of principle testing of

96 cCCTomics. Organisms evolve periodic behaviors and physiological traits in
97 response to cyclical environmental changes. The rhythmic locomotor behavior
98 of Drosophila, for instance, shows enhanced activity before the light is turned
99 on and off in a light-dark (LD) cycle, referred to as morning and evening
100 anticipations, respectively (Collins et al., 2005; Helfrich-Förster, 2001). Under
101 12 hours (h) dark-12 h dark (DD) conditions, the activities peaks regularly about
102 every 24 h (Konopka and Benzer, 1971). Approximately 150 clock neurons,
103 circadian output neurons and extra-clock electrical oscillators (xCEOs)
104 coordinate Drosophila circadian behaviors (Dubowy and Sehgal, 2017; Tang et
105 al., 2022). The regulation of morning and evening anticipations, the most
106 prominent features in the LD condition, is primarily mediated by four pairs of
107 sLNvs expressing pigment dispersing factor (PDF), six pairs of LNds and the
108 5th s-LNv (Grima et al., 2004; Rieger et al., 2006; Stoleru et al., 2004). At the
109 molecular level, Pdf and Pdf receptor (PDFR) are well-known, with their
110 mutants showing an advanced evening activity peak and no morning
111 anticipation (Hyun et al., 2005; Lear et al., 2005; Renn et al., 1999). Other
112 neuropeptides and their receptors, including AstC/AstC-R2 and neuropeptide F
113 (NPF) and its receptor (NPFR), have also been reported to modulate evening
114 activities (Díaz et al., 2019; He et al., 2013; Hermann et al., 2012), while
115 CCHa1/CCHa1-R and Dh31 regulate morning activities (Fujiwara et al., 2018;
116 Goda et al., 2019). To date, no advanced morning activity phenotype has been
117 reported in flies.

118 To develop a more efficient approach for somatic gene manipulation, we
119 have now generated two systems for conditional manipulation of CCT genes.
120 One is GFPi/Flp-out-based conditional knockout system of CCT genes
121 (cCCTomics) and another is CRISPR/Cas9-based (C-cCCTomics). Both
122 systems have achieved high efficiency of gene mutagenesis in the Drosophila
123 nervous system. C-cCCTomics, utilizing chromatin-peptide fused Cas9 and
124 scaffold optimized sgRNA, makes efficient conditional gene knockout as simple
125 as RNAi. Further application of C-cCCTomics in clock neurons revealed novel
126 roles of CCT genes in circadian behavior: CNMa-CNMaR modulates morning
127 anticipation as an antagonistic signal of PDF-PDFR.
128

129 **Results**

130 **Near Complete Disruption of Target Genes by GFPi and Flp-out Based**
131 **cCCTomics**

132 For the purpose of conditional chemoconnectomics (cCCTomics), we initially
133 leveraged the benefits of our previously generated CCTomics attP lines (Deng
134 et al., 2019), which enabled us to fuse enhanced GFP coding sequence at the
135 3' end of each gene's coding region and flank most or entire gene span with
136 FRT sequence through site-specific recombination (Fig. 1A, Table S1). We
137 designed this system so that it could be used to target genes tagged with GFP
138 by RNAi (Neumüller et al., 2012) and at the same time to enable flippase(Flp)
139 mediated DNA fragment excision between two FRT sequences when FRT

140 sequences are in the same orientation (Vetter et al., 1983)（Fig. 1A）.

141 To validate the efficiency of cCCTomics, we performed pan-neuronal
142 expression of either shRNA^{GFP} or flipase in cCCT flies. Immunofluorescent
143 imaging showed that constitutive expression of shRNA^{GFP} (Fig. 1B-1D, Fig.
144 S1A-S1I) or flipase (Fig. 1E-1G, Fig. S1J-S1U) almost completely eliminated
145 GFP signals of target genes, indicating high efficiency. Knocking out at the adult
146 stage using either hsFLP driven Flp-out (Golic and Lindquist, 1989) (Fig. 1H-
147 1J) or neural (elav-Switch) driven shRNA^{GFP} (Nicholson et al., 2008;
148 Osterwalder et al., 2001) (Fig. S2A-S2I) , also resulted in the elimination of most,
149 though not all, GFP signals. Notably, control group of CCT$^{EGFP.FRT}$; elav-
150 Switch/UAS-shRNAGFP flies fed with solvent (ethanol) showed obvious
151 decreased GFP (Fig. S2B, S2E, and S2H) comparing with UAS-
152 shRNA^{GFP}/CCT$^{EGFP.FRT}$ flies fed with RU486 (Fig. S2A, S2D, and S2G),
153 indicating leaky expression of elav-Switch.

154 We then applied cCCTomics in pan-neuronal knockout of nAChRβ2 which
155 is required for Drosophila sleep (Dai et al., 2021). Ablation of nAChRβ2 in the
156 nervous system dramatically decreased sleep of flies, mirroring the nAChRβ2
157 knockout phenotype (Fig. 1K, 1L). Therefore, cCCTomics is an effective toolkit
158 for manipulation of CCT genes and suitable for functional investigations of
159 genes. Expression of in-frame fused eGFP-labelled CCT genes highly co-
160 localized with signals revealed by immunocytochemistry (Fig. S3A-S3I),
161 allowing direct examination of gene expression without amplification, which is

162 different from the GAL4/UAS binary system.

163 We then checked the viability of cCCT lines and found that cCCT lines
164 including Capa$^{EGFP.FRT}$, ChAT$^{EGFP.FRT}$ and Eh$^{EGFP.FRT}$ were viable whereas their
165 CCT mutants were lethal. Gad1$^{EGFP.FRT}$, GluRIID$^{EGFP.FRT}$ and CapaR$^{EGFP.FRT}$
166 were still lethal as their CCT mutants were (Table S2). This indicates that some
167 of the cCCT knockin flies may functionally affect corresponding genes, which
168 are not suitable for conditional gene manipulation. Combination of cCCT
169 transgenic flies with UAS-flp, UAS-shRNA^{GFP} or specific drivers is complicated
170 and unfriendly for screen work, despite the almost 100% efficiency of gene
171 suppression when driven by a pan-neuronal driver. Because of the limitations
172 of this method, we further created a CRISPR/Cas9 based conditional knockout
173 system of chemoconnectomics (C-cCCTomics).

174

175 **CRISPR/Cas9-Based Conditional Knockout System for CCTomics**

176 To simplify effective manipulation of CCT genes, we designed a vector based
177 on pACU2 (Han et al., 2011) with tRNA flanking sgRNAs (Port and Bullock,
178 2016; Xie et al., 2015) targeting CCT genes (Fig. 2A). We also adopted an
179 optimized sgRNA scaffold “E+F” (E, stem extension; F, A-U flip) (Chen et al.,
180 2013), which facilitates Cas9-sgRNA complex formation and gene knockout
181 efficiency (Dang et al., 2015; Poe et al., 2019; Zhao et al., 2016), to all sgRNAs
182 to improve gene knockout efficiency. To balance efficiency and off-target effect,
183 we selected three sgRNAs for each CCT gene with highest predicted efficiency

184 and no predicted off-target effect based on previously reported models (Chu et
185 al., 2016; Doench et al., 2014; Graf et al., 2019; Gratz et al., 2014; Heigwer et
186 al., 2014; Stemmer et al., 2015; Xu et al., 2015) (see Table S3 and details at
187 Methods).

188 We generated UAS-sgRNA^{3x} transgenic lines for all 209 defined CCT
189 genes (Abruzzi et al., 2017; Dai et al., 2019; Deng et al., 2019) and UAS-
190 Cas9.HC (Cas9.HC) (Mali et al., 2013). We first verified that C-cCCTomics
191 mediated precise target DNA breaking by ubiquitous expression of Cas9.P2
192 (Port et al., 2014) and sgRNA by targeting Pdf or Dh31. Sanger sequencing
193 showed that indels were present exactly at the Cas9 cleavage sites (Fig. S4A-
194 S4H).

195 To determine the efficiency of C-cCCTomics, we employed pan-neuronal
196 expression of Cas9.HC with sgRNA^{Dh31} or sgRNA^{pdf}. Targeting by
197 Cas9.HC/sgRNA^{Dh31} eliminated most but not all of the GFP signal in
198 Dh31$^{EGFP.FRT}$ (Fig 2B-2D), whereas all anti-PDF signals were eliminated by
199 Cas9.HC/sgRNA^{pdf} (Fig 2E-2G). Furthermore, we used the C-cCCT strategy to
200 conditionally knockout genes for pdfr, nAChRβ2 and nAChRα2, which were
201 previously reported as essential for circadian rhythm or sleep (Dai et al., 2021;
202 Renn et al., 1999). Pan-neuronal knockout of Pdfr resulted in a tendency
203 towards advanced evening activity and weaker morning anticipation compared
204 to control flies (Fig. 2H-2I), which is similar to Pdfr-attpKO flies. These
205 phenotypes were not as pronounced as those reported previously, when

206 han^{5304} mutants exhibited a more obvious advanced evening peak and no
207 morning anticipation (Hyun et al., 2005). Furthermore, there was no significant
208 sleep decrease in these conditional knockout (cKO) flies (Fig. 2J-2K) when we
209 applied C-cCCTomics to manipulate nAChRβ2 or nAChRa2. Taken together, C-
210 cCCTomics (with Cas9.HC) achieved a relatively high gene knockout efficiency,
211 but it was not effective enough for all genes.
212

213 **Evaluation of Cas9 with Different Chromatin-Modulating Peptides**

214 Since the establishment of the CRISPR/Cas9 system a decade ago, many
215 groups have attempted to improve its efficiency in gene manipulation. Most
216 attempts have been focused on the two main components of this system, the
217 Cas9 protein (Ding et al., 2019; Ling et al., 2020; Liu et al., 2019; Zhao et al.,
218 2016; Zheng et al., 2020) and the single guide RNA (Chen et al., 2013; Chu et
219 al., 2016; Dang et al., 2015; Doench et al., 2014; Filippova et al., 2019; Graf et
220 al., 2019; Labuhn et al., 2018; Mu et al., 2019; Nahar et al., 2018; Scott et al.,
221 2019; Xu et al., 2015). At the beginning of C-cCCTomics design, we adopted
222 an optimized sgRNA scaffold and selected sgRNAs with predicted high
223 efficiency. We tried to further improve the efficacy by modifying Cas9 protein.
224 We fused a chromatin-modulating peptide (Ding et al., 2019), HMGN1 (High
225 mobility group nucleosome binding domain 1), at the N-terminus of Cas9 and
226 HMGB1 (High mobility group protein B1) at its C-terminus with GGSGP linker,
227 termed Cas9.M9 (Fig. 3A, Methods). We also obtained a modified Cas9.M6

228 with HMGN1 at the N-terminus and an undefined peptide (UDP) at the C-
229 terminus (Fig. 3A). We replaced the STARD linker between Cas9 and NLS in
230 Cas9.HC with GGSGP the linker (Zhao et al., 2016), termed Cas9.M0 (Fig 3A).
231 None of these modifications have been validated previously in flies.

232 To determine whether the modified Cas9 variants were more efficient, we
233 first pan-neuronally expressed each Cas9 variant and sgRNA^{ple}, and assessed
234 their efficiency by immunofluorescence imaging. By counting anti-TH positive
235 neurons in the brain (anterior view) after targeting by Cas9/sgRNA^{ple}, we found
236 that unmodified Cas9.HC/sgRNA^{ple} only achieved 69.58±3.04% (n=5) knockout
237 efficiency (Fig. 3G, 3K, 3L), while Cas9.M6/sgRNA^{ple} and Cas9.M9/sgRNA^{ple}
238 significantly improved efficiency to 87.53±3.06% (n=7) and 97.19±2.15% (n=8),
239 respectively (Fig. 3I-3L). Fourteen additional CCT genes were subjected to pan-
240 neuronal knockout, and the mRNA levels of the target genes were evaluated
241 using real-time quantitative PCR with at least one primer overlapping the
242 sgRNA targeting site (Fig. S5). Cas9.M6 and Cas9.M9 demonstrated
243 significantly higher gene disruption efficiency compared to the unmodified
244 Cas9.HC, achieving average efficiencies of 87.51%±2.24% and 89.59%±2.39%
245 for Cas9.M6 and Cas9.M9, respectively, in contrast to 70.72%±3.82% for
246 Cas9.HC. (Fig. 3M, Fig. S5). To rule out the possibility of the observed
247 variations in gene disruption efficiency being attributed to differential Cas9
248 expression levels, we quantified the Cas9 expression levels and noted that both
249 Cas9.M6 and Cas9.M9 exhibited lower mRNA levels than Cas9.HC under the

experiment condition (Fig. 3N). Subsequently, genomic DNA of Drosophila head was extracted, and libraries encompassing target sites were constructed for high-throughput sequencing to verify disparities in genetic editing efficiency among these three Cas9 variants (Fig. 3O). In almost all nineteen sites tested, the mutation ratio consistently showed a trend towards Cas9.M6 and Cas9.M9 having a higher gene disruption efficiency than Cas9.HC (Fig. 3P, Fig. S6). The single-site mutation rates varied from 5.81% to 43.47% for Cas9.HC, 22.40% to 53.54% for Cas9.M6, and 19.90% to 63.57% for Cas9.M9 (Fig. 3P, Fig. S6). It should be noted that genomic DNA extracted from fly heads contained glial cells, which did not express Cas9/sgRNA, leading to a larger denominator and consequently reducing the observed mutation rates. Unmodified Cas9 displayed mutation rates comparable to those previously reported by Schlichting et al., 2022. The findings indicated that both Cas9.M6 and Cas9.M9 displayed elevated efficiency compared to Cas9.HC, with Cas9.M9 exhibiting the highest mutagenesis proficiency. These results suggest that the implementation of modified C-cCCTomics using Cas9.M6 and Cas9.M9 achieved an elevated level of efficiency. While unmodified C-cCCTomics was not efficient enough to knockout nAChRβ2 and nAChRα2 to phenocopy their mutants, we employed Cas9.M9 in conditional knockout of these genes to verify its efficiency. Pan-neuronal knocking out of nAChRβ2 or nAChRa2 by Cas9.M9/sgRNA showed significant sleep decrease which was similar to their mutants (Fig. 3Q-3R) (Dai et al., 2021).

272 Taken together, our results support that we have created a high efficiency
273 toolkit for CCT gene manipulation in the nervous system, as well as more
274 efficient Cas9 variants, Cas9.M6 and Cas9.M9, which can also be applied to
275 genes other than those in the CCT.
276
277 **43 CCT Genes Detected in Clock Neurons by Genetic Intersection**
278 We analyzed the expression profile of CCT genes in circadian neurons with
279 CCTomics driver lines in all clock neurons expressing Clk856 (Gummadova et
280 al., 2009). With the Flp-out or split-lexA intersection strategy (Fig. 4A, 4B), we
281 found 43 out of 148 analyzed CCT genes expressed in circadian neurons (Fig.
282 4C, Fig S7-S8, Table S4, Table S5). In all eight subsets of clock neurons, 23
283 CCT genes were expressed in DN1s, 20 in DN2s, 22 in DN3s, 28 in LNds, 14
284 in l-LNvs, 12 in s-LNvs, 5 in 5th s-LNv and 3 in LPNs, with a total of 127 gene-
285 subsets.
286 To assess the accuracy of expression profiles using CCT drivers, we
287 compared our dissection results with previous reports. Initially, we confirmed
288 the expression of CCHa1 in two DN1s (Fujiwara et al., 2018), sNFP in four s-
289 LNvs and two LNds (Johard et al., 2009), and Trissin in two LNds (Ma et al.,
290 2021), aligning with previous findings. Additionally, we identified the expression
291 of nAChRα1, nAChRα2, nAChRβ2, GABA-B-R2, CCHa1-R, and Dh31-R in all
292 or subsets of LNvs, consistent with suggestions from studies using ligands or
293 agonists in LNvs (Duhart et al., 2020; Fujiwara et al., 2018; Lelito and Shafer,

294 2012; Shafer et al., 2008) (Table S4).

295 Regarding previously reported Nplp1 in two DN1as (Shafer et al., 2006),
296 we found approximately five DN1s positive for Nplp-KI-LexA, indicating a
297 broader expression than previously reported. A similar pattern emerged in our
298 analysis of Dh31-KI-LexA, where four DN1s, four s-LNvs, and two LNds were
299 identified, contrasting with the two DN1s found in immunocytochemical analysis
300 (Goda et al., 2016). Colocalization analysis of Dh31-KI-LexA and anti-PDF
301 revealed labeling of all PDF-positive s-LNvs but not l-LNvs (Fig. S9A),
302 suggesting that the differences may arise from the broader labeling of 3' end
303 knock-in LexA drivers or the amplitude effect of the binary expression system.
304 The low protein levels might go undetected in immunocytochemical analysis.
305 This aligns with transcriptome analysis findings showing Nplp1 positive in
306 DN1as, a cluster of CNMa-positive DN1ps, and a cluster of DN3s(Ma et al.,
307 2021), which is more consistent with our dissection.

308 Despite the well-known expression of PDF in LNvs and PDFR in s-LNvs
309 (Shafer et al., 2008), we did not observe stable positive signals for both in Flp-
310 out intersection experiments, although both Pdf-KI-LexA and Pdfr-KI-LexA label
311 LNvs as expected (Fig. S9B-S9C). We also noted fewer positive neurons in
312 certain clock neuron subsets compared to previous reports, such as NPF in
313 three LNds and some LNvs (Erion et al., 2016; He et al., 2013; Hermann et al.,
314 2012; Johard et al., 2009; Lee et al., 2006) and ChAT in four LNds and the 5th
315 s-LNv (Duhart et al., 2020; Johard et al., 2009) (Table S4). We attribute this

316 limitation to the inefficiency of LexAop-FRT-myr::GFP driven by LexA,
317 acknowledging that our intersection results may miss some positive signals.
318
319 **Conditional Knockout of CCT Genes in Clock Neurons**
320 To investigate the function of CCT genes in circadian neurons with our
321 conditional knockout system, we knocked out all 67 (genes identified above and
322 reported previously) CCT genes in Clk856-labeled clock neurons by C-
323 cCCTomics.
324 In the pilot screen, we monitored fly activity by video recording (Dai et al.,
325 2019) and analyzed rhythmic behavior under LD and DD conditions. We
326 analyzed morning anticipation index (MAI) and evening anticipation index (EAI)
327 under the LD condition (Harrisingh et al., 2007; Im and Taghert, 2010; Seluzicki
328 et al., 2014) (Fig. 5A), power, period and arrhythmic rate (AR) under the DD
329 condition. Fly activities tended to rise rapidly after ZT22.5 at dawn and ZT10 at
330 dusk. Thus, we added two more parameters to describe the anticipatory activity
331 patterns of LD condition. Morning anticipation pattern index (MAPI) was defined
332 as the difference between Pi_a[arctan(ZT20.5~ZT22.5 activity increasing slope)]
333 and Pi_p[arctan(ZT22.5 ~ZT24 activity increasing slope)], M(Pi_a-Pi_p). Evening
334 anticipation pattern index (EAPI) was defined similar to MAPI (Fig. 5A, see
335 Methods). Pi_a and Pi_p were positive, while MAPI and EAPI were negative, for
336 wild type (wt) flies as their activities gradually increases at dawn or dusk at
337 increasing rates.

338 Knocking out Pdf or Pdfr in clock neurons phenocopied their mutants with
339 lower MAI, advanced evening activity, low power, high arrhythmic rate and
340 shorter period (Hyun et al., 2005; Lear et al., 2005; Renn et al., 1999) (Table
341 S6, Fig S10A-S10D). The MAI-decreasing phenotype of Dh31 knockout was
342 also reproduced in this pilot screen (Goda et al., 2019) (Table S6). All the above
343 results verified the effectiveness of C-cCCTomics. Unexpectedly, additional
344 experimental replications with full controls using Cas9.M9 revealed that leaky
345 expression of Cas9.M9 and sgRNA might have caused disruption of Dh31,
346 Dh44, Pdf and Pdfr (Fig. S10A-S10D) (see DISCUSSION), which was not
347 suitable for neuronal specific mutagenesis of some genes. Therefore, in the
348 following work we primarily focused on Cas9.M6 instead.
349 Analysis of the newly defined parameters MAPI and EAPI showed that control
350 flies (Clk856-GLA4>UAS-Cas9.M9) had negative EAPI but slightly positive
351 MAPI. The positive MAPI of control flies in this screen might be caused by
352 Cas9.M9 toxicity. Only the Pdf and Pdfr clock-neuron knockout flies showed
353 positive EAPIs, indicating an advanced evening activity (Table S6, Fig S10A,
354 S10C). nAChRα1, MsR1, mAChR-B, and CNMa cKO flies had highest MAPI
355 values (Table S6). We further confirmed their phenotypes using Cas9.M6 which
356 revealed that CNMa plays a role in regulating morning anticipatory activity (Fig.
357 S11A).
358
359 **Regulation of Morning Anticipation by CNMa-positive DN1p Neurons**

360 Conditionally knocking out CNMa in clock neurons advanced morning activity
361 (Fig. 5B, Fig. S11B) and increased MAPI (Fig. 5C, Fig S11A, S11C), leaving the
362 power and period intact in male flies (Fig. 5D, 5E). The same advanced morning
363 activity phenotype were also observed in female flies (Fig. S11D-S11G). To
364 further validate this phenotype, we generated a CNMa knockout ($CNMa^{KO}$) line
365 by replacing its whole coding region with an attP-splicing adaptor element
366 (Deng et al., 2019) (Fig. 5F). Both male and female $CNMa^{KO}$ flies exhibited the
367 same phenotypes as seen in the CNMa cKO (Fig. 5G-5I).

368 Previous studies have found CNMa expression in DN1 neurons (Abruzzi et
369 al., 2017; Jin et al., 2021; Ma et al., 2021). Our intersection showed four DN1p
370 and one DN3 CNMa positive neurons in Clk856 labelled neurons (Fig. S8 - 16,
371 Fig. 4C, Table S4). Analysis with an endogenous CNMa-KI-GAL4 knockin driver
372 showed that six pairs of CNMa neurons located in the DN1p region and three
373 pairs located in the subesophageal ganglion (SOG) had the brightest GFP
374 signals (Fig. 6A). The anatomical features of CNMa neurons were further
375 confirmed using stingerRed and more neurons were found in regions, the
376 anterior ventrolateral protocerebrum (AVLP), and the antennal
377 mechanosensory and motor center (AMMC) (Fig. S12A). Dendrites of CNMa
378 neurons were concentrated in DN1p and SOG, with their axons distributed
379 around DN1p region, lateral horn (LH), and prow region (PRW) (Fig. 6B, 6C).
380 Using the Trans-tango strategy (Talay et al., 2017), we also found that
381 downstream of CNMa neurons were about fifteen pairs of neurons in the SOG,

382 five pairs of LNd neurons, one pair of DN3 neurons and six intercerebralis (PI)
383 neurons (Fig. 6D, arrowhead).

384 Because we had found that knocking out CNMa in Clk856-GAL4 labeled
385 neurons produced advanced morning activity, and that CNMa intersected with
386 Clk856-Gal4 labeled neurons in 4 pairs of DN1ps and one pair of DN3 neurons
387 (Fig. S8-16), we focused on these neurons and performed more intersections.
388 Taking advantage of a series of clock neuron subset-labeled drivers (Sekiguchi
389 et al., 2020), we intersected CNMa-p65AD with 4 DN1 labelling drivers:
390 GMR51H05-GAL4, GMR91F02-GAL4, Pdfr-KI-GAL4 and GMR79A11-GAL4
391 (Fig. 6E-6H). We found two arborization patterns: Type I with two neurons
392 whose branches projecting to the anterior region, as observed in
393 CNMa∩GMR51H05, CNMa∩Pdfr, and CNMa∩GMR79A11 (Fig 6E, 6G, 6H),
394 and type II with four neurons branching on the posterior side with few
395 projections to the anterior region, as observed in CNMa∩GMR91F02 (Fig. 6F).
396 These two types of DN1ps' subsets have been previously reported and
397 profound discussed (Lamaze et al., 2018; Reinhard et al., 2022).

398 CNMa knockout in Type I or Type II neurons (GMR51H05-GAL4, GMR91F02-
399 GAL4, and GMR79A11-GAL4) all reproduced the MAPI-increased phenotype
400 of clk856 specific CNMa knockout (Fig. 6I). However, Type II neurons-specific
401 CNMa knockout (CNMa ∩ GMR91F02) showed weaker advanced morning
402 activity without advanced morning peak (Fig. 6N), while Type I neurons-specific
403 CNMa knockout did (Fig. 6J), indicating a possibility that these two type I CNMa

404 neurons are the main functional subset regulating the morning anticipation
405 activity of fruit fly.
406 Pdf or Pdfr mutants exhibit weak or no morning anticipation, which is related
407 to the phenotype of CNMa knockout flies. We also identified two Pdfr and CNMa
408 double-positive DN1ps, which have a type I projection pattern (Fig. 6G).
409 Reintroduction of Pdfr in Pdfr knockout background revealed that GMR51H05
410 and GMR79A11 Gal4 drivers, which covered the main functional CNMa-positive
411 subset, could partially rescue the morning anticipation and power phenotype of
412 Pdfr knockout flies to a considerably larger extent than the GMR91F02 driver
413 (Fig. 6Q-6S, Fig. S13A, Table S7). Moreover, knocking out Pdfr by GMR51H05,
414 GMR79A11 and CNMa GAL4, which cover type I CNMa neurons, decreased
415 morning anticipation of flies (Fig. 6T, Fig. S13B). However, the decrease in
416 morning anticipation observed in the Pdfr knockout by CNMa-GAL4 was not as
417 pronounced as with the other two drivers. Because the presumptive main
418 subset of functional CNMa is also PDFR-positive, there is a possibility that
419 CNMa secretion is regulated by PDF/PDFR signal.
420

421 **Role of Neuronal CNMaR in Morning Anticipation**

422 There is only one CNMa receptor reported in the fly genome (Jung et al., 2014).
423 We generated a CNMaR$^{KO\text{-}p65AD}$ line by CRISPR/Cas9 (Fig. 7A) and this
424 knockout showed advanced morning activity (Fig. 7B, 7D) and increased MAPI
425 (Fig. 7C, 7E) in both sexes. CNMaR$^{KI\text{-}Gal4}$/UAS-mCD8::GFP and CNMaR$^{KI\text{-}}$

426 ^{Gal4}/UAS-stinger::Red showed expression of CNMaR across the whole brain
427 (Fig. 7F, Fig S12B), especially in DN1p, DN3 , the PI and the SOG. The dendrite
428 arborization and synaptic projections of CNMaR neurons also covered broad
429 regions (Fig. 7G, 7H), at the PI, the SOG, the posterior ventrolateral
430 protocerebrum (PVLP) and the central complex (CC). Further conditional
431 knockout of CNMaR in neurons by C-cCCTomics phenocopied CNMaR$^{KO\text{-}p65AD}$
432 phenotype (Fig. 7I-7L). These results indicate that CNMaR is similar to CNMa
433 in regulating morning anticipation.
434

435 **DISCUSSION**

436 **Conditional CCTomics Strategies and Toolkit**

437 We have generated conditional gene manipulation systems based on Flp-
438 out/GFPi or CRISPR/Cas9. cCCT based gene deletion after heat-shock or
439 mifepristone (RU486) eliminated most GFP signals, and pan-neuronal
440 constitutive expression of shRNA^{GFP} or flippase disrupted seven out of eight
441 tested genes completely while targeting of SIFa$^{EGFP.FRT}$ achieved 96±3%
442 efficiency. Although the recombination of genetic elements is relatively
443 cumbersome when using cCCTomics, it is worthwhile to apply this method to
444 specific genes given its high level of efficiency. While two UAS-sgRNA libraries
445 have been established, one primarily targeting kinases (Port et al., 2020) and
446 the other targeting GPCRs (Schlichting et al., 2022), both libraries only cover a
447 portion of CCT genes, and are thus insufficient for manipulating all CCT genes.

448 The development of C-cCCTomics, however, makes CCT gene manipulation
449 as simple as RNA interference. Furthermore, the use of modified Cas9.M6 or
450 Cas9.M9 highly enhances the efficiency of gene disruption in the nervous
451 system, allowing for efficient manipulation of all CCT genes in a cell-specific
452 manner.

453 The toxicity of CRISPR/Cas9 depends on the Cas9 protein (Port et al.,
454 2014). When expressed pan-neuronally in nSyb-GAL4 (R57C10-GAL4,
455 attP40) , Cas9.M9 slightly reduced viability, while the expression of other Cas9
456 variants had no significant effect on viability (Fig. S14). Although Cas9.M9
457 showed leaky-expression- efficiency, this was not a problem with Cas9.M6,
458 which successfully disrupted Dh31, Dh44, Pdf, and Pdfr (Fig. S9). A more
459 restricted expression of Cas9.M9 with lower toxicity is necessary for better
460 somatic gene manipulation in the future.

461

462 **CCT of Clock Neurons**

463 Intersecting Clk856-Gal4 or Clk856-p6AD with CCTomics, we identified 45 CCT
464 genes in Clk856 labelled clock neurons. Clock neurons appear highly
465 heterogeneous both in our intersection dissection and in a previous
466 transcriptomic analysis (Abruzzi et al., 2017; Ma et al., 2021). Comparing these
467 two CCT gene expression profiles in clock neurons, 41 out of 127 gene-subsets
468 are identical. The accuracy of our genetic intersection is limited by two
469 possibilities: 1) KI-LexA may not fully represent the expression pattern of the

470 corresponding gene, and 2) the efficiency of STOP cassette removal in the Flp-
471 out strategy is limited or the efficiency of LexA>LexAop::myrGFP. Moreover, the
472 leakage of LexAop-GFP may result in unreliable labelling in split-lexA strategy.
473 Both genetic drivers and transcriptomic analysis contribute to our knowledge of
474 the expression profile of neurons. The physiological significance of each gene
475 in particular neurons should be further investigated by genetic manipulation.
476

477 **Regulation of Rhythmic Behavior by CCT genes**

478 Multiple attractive genes have been identified in our functional screen of CCT
479 genes in clock neurons: for example, knocking out of VGlut weakens morning
480 anticipation (Table S8). In further screening of brain regions, we have narrowed
481 down the morning anticipation regulation role of VGlut in R18H11-GAL4 labeled
482 neurons (Table S9). VGlut in these neurons has also been reported to regulate
483 sleep in Drosophila (Guo et al., 2016). Its downstream neurons may be the PI
484 neurons or LNvs (Barber et al., 2021; Guo et al., 2016).

485 Moreover, the deficiency of the neuropeptide CNMa results in advanced
486 morning activity. We have validated that two Pdfr and CNMa double-positive
487 DN1p neurons may play a major role in regulating this process through
488 intersectional manipulation of CNMa. Knockout and reintroduction of Pdfr in
489 these neurons have verified that Pdfr partially functions in DN1p CNMa neurons,
490 and PDF increases cAMP level in Pdfr positive neurons (Shafer et al., 2008),
491 suggesting a possibility of the regulation of CNMa signaling by PDF signaling.

492 Furthermore, given that the morning anticipation vanishing phenotype of Pdf or
493 Pdfr mutant indicates a promoting role of PDF-PDFR signal, while the
494 enhanced morning anticipation phenotype of CNMa mutant suggests an
495 inhibiting role of CNMa signal, we consider the two signals to be antagonistic.
496 However, knocking out CNMaR in Clk856 labelled clock neurons showed no
497 significant phenotype (Table S6), whereas the mutant and pan-neuronal
498 knockout flies had similar phenotypes to CNMa knockout flies, suggesting its
499 role in the circadian output neurons. Previous studies have indicated that CNMa
500 integrate thermosensory inputs to promote wakefulness, and CNMaR is
501 thought to function in Dh44 positive PI neurons (Jin et al., 2021), a subset of
502 circadian output neurons. To gain a deeper understanding of the downstream
503 effects of DN1p CNMa positive neurons, further analysis focusing on specific
504 brain regions is necessary.

505 We have also reproduced phenotypes of Pdf, Pdfr, and Dh31 mutant flies
506 with C-cCCTomics as previous studies. Surprisingly, only five genes are
507 functional among all sixty-seven CCT genes in this prior screen. This may be
508 caused by limitations of the simple behavioral paradigm, single gene
509 manipulation, and single GAL4 driver. For example, switching of light condition
510 from L: D = 12h: 12h to L: D = 6h:18h, AstC/AstC-R2 would suppress flies'
511 evening activity intensity to adapt to the environmental change (Díaz et al.,
512 2019), and only double knockout of AChRs and mGluRs in PI neurons can
513 possibly result in alteration in behavioral rhythms (Barber et al., 2021). Further

514 diversified functional analysis of CCT genes in clock neurons is required for

515 clock circuit dissection.

516 **Methods**

517 **Fly Lines and Rearing Conditions**

518 Flies were reared on standard corn meal at 25 ℃, 60% humidity, 12 h light: 12
519 h dark (LD) cycle. For flies used in behavior assays, they were backcrossed
520 into our isogenized Canton S background for 5 to 7 generations. For heat
521 induced assays, flies were reared at 20℃. All CCT attP KO lines and CCT KI
522 driver lines were previous generated at our lab (Deng et al., 2019). Clk856-
523 GAL4 and GMR57C10-GAL4 driver lines were gifts from Donggen Luo Lab
524 (Peking University). 13XLexAop2 (FRT.stop) myr::GFP was gift from Rubin Lab.

525

526 **C-cCCTomics sgRNAs design**

527 All sgRNAs target at or before functional coding regions (e.g. GPCR
528 transmembrane domain, synthetase substrate binding domain) of each CCT
529 genes. For each gene, about 20 sgRNAs with specific score ≥ 12 were firstly
530 designed at CRISPRgold website (Chu et al., 2016; Graf et al., 2019), then their
531 specificity and efficacy were further valued in Optimal CRISPR target
532 finder(Gratz et al., 2014), E-CRISPR(Heigwer et al., 2014) and CCTop
533 (Stemmer et al., 2015) system. The first three highest efficacy sgRNAs with no
534 predicted off-target effect were selected. All selected sgRNAs are listed in Table
535 S3.

536

537 **Molecular Biology**

538 All cCCTomics knockin (KI) lines and C-cCCTomics transgenic flies were

539 generated through phiC31 mediated attB/attP recombination, and the miniwhite
540 gene was used as selection marker.

541 For cCCTomics KI lines, backbone pBSK-attB-FRT-*Hpa*I-T2A-EGFP-FRT
542 was modified from pBSK-attB-loxP-myc-T2A-Gal4-GMR-miniwhite (Deng et al.,
543 2019). Myc-T2A-GAL4 cassette was removed by PCR amplification while first
544 FRT cassette was introduced. Second FRT cassette was inserted by T4 ligation
545 between *SpeI* and *BamHI*. T2A-EGFP was cloned from pEC14 and was
546 inserted into the backbone between two FRT cassettes. All gene spans, except
547 for stop codon, deleted in CCT attP KO lines were cloned into pBSK-attB-FRT-
548 *Hpa*I-T2A-EGFP-FRT at *Hpa*I site.

549 For C-cCCTomics UAS-sgRNA lines, backbone pMsgNull was modified
550 from pACU2 (Han et al., 2011). Synthetic partial fly $tRNA^{Gly}$ sequence was
551 inserted between *EcoR*I and *Kpn*I. An irrelevant 1749 bp cassette amplified
552 from pAAV-Efla-DIO-mScarlet (addgeen#130999) was inserted between *Eag*I
553 and *Kpn*I. All sgRNA spacers were synthesized at primers, and “E+F” sgRNA
554 scaffold and rice $tRNA^{Gly}$ was amplified from a synthetic backbone PM04.
555 Finally, gRNA-$tRNA^{Gly}$ cassettes were cloned into pMsgNull between *Eag*I and
556 *Kpn*I by Gibson Assembly.

557 All UAS-Cas9 variants generated in this research were cloned into vector
558 pACU2 and all Cas9 sequence were amplified from hCas9 (addgene#41815).
559 Human codon optimized Cas9 was cloned into pACU2 to generate UAS-
560 Cas9.HC. UAS-Cas9.M0 was modified from UAS-Cas9.HC by introduce a 3x

561 HA tag after NSL and replace the SARD linker with the 3×GGSGP linker (Zhao
562 et al., 2016). UAS-Cas9.M6 and UAS-Cas9.M9 were designed as HMGN1-
563 Cas9-UPD and HMGN1-Cas9-HB1 respectively. All these chromatin-
564 modulating peptides were linked with Cas9 by 3x GGSGP linker.

565 CNMaR$^{KO\text{-}p65AD}$ is generated by replace the coding region of the first exon
566 with T2A-p65AD by CRISPR/Cas9, the T2A-p65AD was linked in frame after
567 first ten amino acids. Spacers of gRNAs used to break the targeted CNMaR
568 region were 5'-GCAGATTTCAGTTCATCTTT-3', 5'-GGCTTGGCAATGAC
569 TATATA-3'.

570

571 **Gene expression quantitation and high-throughput sequencing**

572 Female flies were gathered six to eight days post-eclosion for gene expression
573 quantification and high-throughput sequencing. Fly heads were isolated by
574 chilling them on liquid nitrogen and subsequent shaking. mRNA extraction was
575 performed using Trizol according to a previously established protocol (Green
576 and Sambrook, 2020). Genomic DNA was removed, and cDNA was
577 synthesized using a commercial kit (TIANGEN#DP419). For real-time
578 quantitative PCR, at least one PCR primer was designed to overlap with the
579 sgRNA target site.

580 Genomic DNA from fly heads was extracted using a standard alkali lysis
581 protocol(Huang et al., 2009). Genomic regions approximately 130 to 230 bp in
582 length, centered around the sgRNA target site, were amplified by PCR

583 employing Q5 polymerase (NEB#M0494). Subsequently, libraries were
584 prepared using the BTseq kit (Beijing Tsingke Biotech Co., Ltd.). These libraries
585 were pooled and subjected to sequencing on the MiSeq platform (Illumina).
586 Analysis of the libraries was conducted using Crispresso2(Clement et al., 2019).

587 **Generation of KI and Transgenic lines**

588 Generation of cCCTomics KI, CNMa$^{KI\text{-}p65AD}$ and CNMaR$^{KO\text{-}p65AD}$ lines are the
589 same as generation of CCTomics KI driver lines as previously described (Deng
590 et al., 2019). To generate C-cCCTomics UAS-sgRNA or UAS-Cas9 variants
591 lines, attB vectors were injected and integrated into the attP40, attP2 or
592 VK00005 through phiC31 mediated gene integration.

593 All flies generated in this research were selected by mini-white and
594 confirmed by PCR.

595

596 **Behavioral assays**

597 Unmated male or female flies of 4 to 5 days were used in circadian rhythm
598 assays. Before measurement, flies were entrained under 12 h light: 12 h dark
599 cycle at 25℃ for at least 3 days and then transferred to dark-dark condition for
600 7 days.

601 Virgin flies of 4 to 5 days were used in sleep assays. Flies were entrained
602 to a 12 h light: 12 h dark cycle at 25℃ for 2 days to eliminate the effect of CO2
603 anesthesia before sleep record. Sleep was defined as 5 min or longer
604 immobility (Hendricks et al., 2000; Shaw et al., 2000) and analyzed by in-house

605 scripts as previously described ((Dai et al., 2021; Dai et al., 2019; Deng et al.,
606 2019).
607 Locomotion was obtained as previously described (Dai et al., 2021).
608 Locomotion activity was measured and analyzed by Actogram J plugin (Dai et
609 al., 2019). Morning anticipation index and evening anticipation index were
610 defined as the ratio of last 3 hours activity before light-on or light-off accounts
611 to last 6 hours activity before light-on or light-off, further subtracted by
612 0.5(Index=sum(3hrs)/sum(6hrs)-0.5) (Harrisingh et al., 2007; Im and Taghert,
613 2010; Seluzicki et al., 2014) and analyzed by an in-house python script.
614

615 **Heat Shock and Drug Treatment**

616 For hsFLP mediated conditional knockout, flies of 4 to 6 days were heat shock
617 at 37℃ during ZT10 to ZT12 for 4 days. And they were reared at 20℃ for
618 another 4-days and then dissected.
619 For mifepristone (RU486) induced conditional knockout, flies of 4 to 6 days
620 were treated with 500 μM RU486 mixed in corn food and then dissected 4 days
621 later.
622

623 **Immunohistochemistry and Confocal Imaging**

624 For all imaging without staining, adult flies were anesthetized on ice and
625 dissected in cold phosphate-buffer saline (PBS). Brains or ventral nerve codes
626 (VNC) were fixed in 2% paraformaldehyde (weight/volume) for 30 min, washed

627 with washing buffer (PBS with 1% Triton X-100, v/v, 3% NaCl, g/mL) for 7 min
628 three times and mounted in Focusclear (Cell Explorer Labs, FC-101).
629 For imaging with staining, brains and VNCs were fixed for 30 min, washed
630 for 15 min three times. Then they were blocked in PBSTS, incubated with
631 primary antibodies, washed with washing buffer, incubated with second
632 antibodies and mounted as described previously(Dai et al., 2021; Dai et al.,
633 2019).
634 All brains or VNCs were imaged on Zeiss LSM710 or Zeiss LSM880
635 confocal microscope and processed by Imaris.
636 The following primary antibodies were used: mouse anti-PDF (1:200,
637 DSHB), rabbit anti-TH (1:1000, Novus Biologicals), rabbit anti-LK (1:1000,
638 RaoLab, this paper). Rabbit anti-DSK (1:1000) was a gift from Dr. C. Zhou Lab
639 (Institute of Zoology, Chinese Academy of Science) (Wu et al., 2020). The
640 following secondary antibodies were used: AlexaFluor goat anti-mouse 488
641 (1:1000, Invitrogen), AlexaFlour goat anti-rabbit 488/633 (1:1000, Invitrogen).
642 For Fig 2, number of TH positive neurons were counted with Imaris Spots
643 plugin.
644
645 **Quantification and Statistics**
646 MAI, MAPI, EAI, EAPI, power and period were calculated by python or R scripts.
647 ZT0 was set as the time point when light was on and ZT12 was set as the time
648 point for light-off. Activity bins started at ZT0 and each was calculated as a sum

649 of the total activity within 30min. Flies were regarded as death and removed if
650 their activity value within last 2 bins was 0. A representative 24hr activity pattern
651 was the average between corresponding activity bins from 2 consecutive days.
652 To minimize effects from singular values, each flies` activity was normalized
653 using the following formula:

654 $$Nor_b_i = \frac{b_i - \min(b_0, \dots, b_{48})}{\max(b_0, \dots, b_{48}) - \min(b_0, \dots, b_{48})}$$

655 bi means the activity value for a certain bin. min(b0,...,b48) means the minimal
656 bin value within 24hr and max(b0,...,b48) means the maximal bin value within
657 24hr. Nor_bi means the final normalized bin value for a certain bin from a given
658 fly. Normalized activity was used for following analysis.

659 Morning activity arise (M_arise) was defined as the radian between the
660 activity curve (ZT21-ZT22) and the time coordinate. Morning activity plateau
661 (M_plateau) was defined as the radian between the activity curve (ZT22.5-ZT24)
662 and the time coordinate. Evening activity arise (E_arise) was defined as the
663 radian between the activty curve (ZT8-ZT11.5) and the time coordinate.
664 Evening activity plateau (E_plateau) was defined as the radian between the
665 activity curve (ZT10.5-ZT12) and the time coordinate. Morning anticipation
666 pattern index (MAPI) was calculated by subtracting M_arise from M_plateau
667 and Evening anticipation pattern index (EAPI) was calculated by subtracting
668 E_arise from E_plateau.

669 The original activity data from 7 consecutive days in dark-dark condition was
670 used for power and period calculation as described (Geissmann et al., 2019).

671 Each flies` periodogram was calculated based on Chi-Square algorithm
672 (Sokolove and Bushell, 1978) and flies with a null power value were regarded
673 as arrhythmic.
674 All statistical analyses were carried out with Prism 8 (Graphpad software).
675 The Kruskal-Wallis ANOVA test followed by Dunn's posttest was used to
676 compare multiple columns.
677

678 **ACKNOWLEDGEMENTS.**

679 We are grateful to Xiaofei Liu, Xueying Wang and Yile Jiao for sgRNA design
680 and cloning, to Linyi Zhang, Wenli Xu, Yuqing Gong and Quiquan Chen for
681 assistance with behavior assays, to Xiao Dong for cloning, to Xinwei Gao for
682 assistance with imaging, to Pingping Yan, Lan Wang, Yonghui Zhang and
683 Haixia Zeng for fly rearing, to Enxing Zhou and Wei Yang for Drosophila activity
684 tracing scripts, to Yujie Li for cartoon illustration, to Donggen Luo, Chuan Zhou,
685 Gerald M. Rubin, Vienna Drosophila RNAi Center and Bloomington Drosophila
686 Stock Center for flies, to Yuh-Nung Jan for pACU2 construct.
687

688 **REFERENCES**

689 Abruzzi, K.C., Zadina, A., Luo, W., Wiyanto, E., Rahman, R., Guo, F., Shafer, O., and Rosbash,
690 M. (2017). RNA-seq analysis of Drosophila clock and non-clock neurons reveals neuron-
691 specific cycling and novel candidate neuropeptides. PLoS genetics *13*, e1006613.

692 Barber, A.F., Fong, S.Y., Kolesnik, A., Fetchko, M., and Sehgal, A. (2021). Drosophila clock cells
693 use multiple mechanisms to transmit time-of-day signals in the brain. Proc Natl Acad Sci USA
694 *118*, e2019826118.

695 Chen, B., Gilbert, L.A., Cimini, B.A., Schnitzbauer, J., Zhang, W., Li, G.W., Park, J., Blackburn,
696 E.H., Weissman, J.S., Qi, L.S.*, et al.* (2013). Dynamic imaging of genomic loci in living human
697 cells by an optimized CRISPR/Cas system. Cell *155*, 1479-1491.

698 Chu, V.T., Graf, R., Wirtz, T., Weber, T., Favret, J., Li, X., Petsch, K., Tran, N.T., Sieweke, M.H.,
699 Berek, C.*, et al.* (2016). Efficient CRISPR-mediated mutagenesis in primary immune cells using
700 CrispRGold and a C57BL/6 Cas9 transgenic mouse line. Proc Natl Acad Sci USA *113*, 12514-
701 12519.

702 Clement, K., Rees, H., Canver, M.C., Gehrke, J.M., Farouni, R., Hsu, J.Y., Cole, M.A., Liu, D.R.,
703 Joung, J.K., Bauer, D.E.*, et al.* (2019). CRISPResso2 provides accurate and rapid genome
704 editing sequence analysis. Nature Biotechnology *37*, 224-226.

705 Collins, B.H., Dissel, S., Gaten, E., Rosato, E., and Kyriacou, C.P. (2005). Disruption of
706 Cryptochrome partially restores circadian rhythmicity to the arrhythmic period mutant of
707 Drosophila. Proc Natl Acad Sci USA *102*, 19021-19026.

708 Dai, X., Zhou, E., Yang, W., Mao, R., Zhang, W., and Rao, Y. (2021). Molecular resolution of a
709 behavioral paradox: sleep and arousal are regulated by distinct acetylcholine receptors in
710 different neuronal types in Drosophila. Sleep *44*, zsab017.

711 Dai, X., Zhou, E., Yang, W., Zhang, X., Zhang, W., and Rao, Y. (2019). D-Serine made by serine
712 racemase in Drosophila intestine plays a physiological role in sleep. Nat Commun *10*, 1986.

713 Dang, Y., Jia, G., Choi, J., Ma, H., Anaya, E., Ye, C., Shankar, P., and Wu, H. (2015). Optimizing
714 sgRNA structure to improve CRISPR-Cas9 knockout efficiency. Genome Biol *16*, 280.

715 Delventhal, R., O'Connor, R.M., Pantalia, M.M., Ulgherait, M., Kim, H.X., Basturk, M.K.,
716 Canman, J.C., and Shirasu-Hiza, M. (2019). Dissection of central clock function in Drosophila

through cell-specific CRISPR-mediated clock gene disruption. eLife *8*, e48308.

Deng, B., Li, Q., Liu, X., Cao, Y., Li, B., Qian, Y., Xu, R., Mao, R., Zhou, E., Zhang, W.*, et al.* (2019). Chemoconnectomics: mapping chemical transmission in Drosophila. Neuron *101*, 876-893.e874.

Díaz, M.M., Schlichting, M., Abruzzi, K.C., Long, X., and Rosbash, M. (2019). Allatostatin-C/AstC-R2 is a novel pathway to modulate the circadian activity pattern in Drosophila. Curr Biol *29*, 13-22.

Ding, X., Seebeck, T., Feng, Y., Jiang, Y., Davis, G.D., and Chen, F. (2019). Improving CRISPR-Cas9 genome editing efficiency by fusion with chromatin-modulating peptides. Crispr j *2*, 51-63.

Doench, J.G., Hartenian, E., Graham, D.B., Tothova, Z., Hegde, M., Smith, I., Sullender, M., Ebert, B.L., Xavier, R.J., and Root, D.E. (2014). Rational design of highly active sgRNAs for CRISPR-Cas9-mediated gene inactivation. Nat Biotechnol *32*, 1262-1267.

Dubowy, C., and Sehgal, A. (2017). Circadian Rhythms and Sleep in Drosophila melanogaster. Genetics *205*, 1373-1397.

Duhart, J.M., Herrero, A., de la Cruz, G., Ispizua, J.I., Pírez, N., and Ceriani, M.F. (2020). Circadian Structural Plasticity Drives Remodeling of E Cell Output. Curr Biol *30*, 5040-5048.e5045.

Erion, R., King, A.N., Wu, G., Hogenesch, J.B., and Sehgal, A. (2016). Neural clocks and Neuropeptide F/Y regulate circadian gene expression in a peripheral metabolic tissue. eLife *5*, e13552.

Filippova, J., Matveeva, A., Zhuravlev, E., and Stepanov, G. (2019). Guide RNA modification as a way to improve CRISPR/Cas9-based genome-editing systems. Biochimie *167*, 49-60.

Fujiwara, Y., Hermann-Luibl, C., Katsura, M., Sekiguchi, M., Ida, T., Helfrich-Förster, C., and Yoshii, T. (2018). The CCHamide1 neuropeptide expressed in the anterior dorsal neuron 1 conveys a circadian signal to the ventral lateral neurons in Drosophila melanogaster. Front Physiol *9*, 1276.

Gaj, T., Sirk, S.J., and Barbas, C.F., 3rd (2014). Expanding the scope of site-specific recombinases for genetic and metabolic engineering. Biotechnol Bioeng *111*, 1-15.

Geissmann, Q., Garcia Rodriguez, L., Beckwith, E.J., and Gilestro, G.F. (2019). Rethomics: An R framework to analyse high-throughput behavioural data. PLoS One *14*, e0209331.

Goda, T., Tang, X., Umezaki, Y., Chu, M.L., Kunst, M., Nitabach, M.N.N., and Hamada, F.N. (2016). Drosophila DH31 neuropeptide and PDF receptor regulate night-onset temperature preference. J Neurosci *36*, 11739-11754.

Goda, T., Umezaki, Y., Alwattari, F., Seo, H.W., and Hamada, F.N. (2019). Neuropeptides PDF and DH31 hierarchically regulate free-running rhythmicity in Drosophila circadian locomotor activity. Sci Rep *9*, 838.

Golic, K.G., and Lindquist, S. (1989). The FLP recombinase of yeast catalyzes site-specific recombination in the Drosophila genome. Cell *59*, 499-509.

Graf, R., Li, X., Chu, V.T., and Rajewsky, K. (2019). sgRNA Sequence Motifs Blocking Efficient CRISPR/Cas9-Mediated Gene Editing. Cell Rep *26*, 1098-1103.e1093.

Gratz, S.J., Ukken, F.P., Rubinstein, C.D., Thiede, G., Donohue, L.K., Cummings, A.M., and O'Connor-Giles, K.M. (2014). Highly specific and efficient CRISPR/Cas9-catalyzed homology-directed repair in Drosophila. Genetics *196*, 961-971.

Green, M.R., and Sambrook, J. (2020). Total RNA Isolation from Drosophila melanogaster. *2020*, pdb.prot101675.

Grima, B., Chélot, E., Xia, R., and Rouyer, F. (2004). Morning and evening peaks of activity rely on different clock neurons of the Drosophila brain. Nature *431*, 869-873.

Grindley, N.D., Whiteson, K.L., and Rice, P.A. (2006). Mechanisms of site-specific recombination. Annu Rev Biochem *75*, 567-605.

Gummadova, J.O., Coutts, G.A., and Glossop, N.R. (2009). Analysis of the Drosophila clock promoter reveals heterogeneity in expression between subgroups of central oscillator cells and identifies a novel enhancer region. J Biol Rhythms *24*, 353-367.

Guo, F., Yu, J., Jung, H.J., Abruzzi, K.C., Luo, W., Griffith, L.C., and Rosbash, M. (2016). Circadian neuron feedback controls the Drosophila sleep--activity profile. Nature *536*, 292-297.

Han, C., Jan, L.Y., and Jan, Y.-N. (2011). Enhancer-driven membrane markers for analysis of nonautonomous mechanisms reveal neuron-glia interactions in Drosophila. Proc Natl Acad Sci USA *108*, 9673-9678.

775 Harrisingh, M.C., Wu, Y., Lnenicka, G.A., and Nitabach, M.N. (2007). Intracellular Ca2+
776 regulates free-running circadian clock oscillation in vivo. J Neurosci *27*, 12489-12499.
777 He, C., Cong, X., Zhang, R., Wu, D., An, C., and Zhao, Z. (2013). Regulation of circadian
778 locomotor rhythm by neuropeptide Y-like system in Drosophila melanogaster. Insect Mol Biol
779 *22*, 376-388.
780 Heigwer, F., Kerr, G., and Boutros, M. (2014). E-CRISP: fast CRISPR target site identification.
781 Nat Methods *11*, 122-123.
782 Helfrich-Förster, C. (2001). The locomotor activity rhythm of Drosophila melanogaster is
783 controlled by a dual oscillator system. J Insect Physiol *47*, 877-887.
784 Hendricks, J.C., Finn, S.M., Panckeri, K.A., Chavkin, J., Williams, J.A., Sehgal, A., and Pack,
785 A.I. (2000). Rest in Drosophila Is a Sleep-like State. Neuron *25*, 129-138.
786 Hermann, C., Yoshii, T., Dusik, V., and Helfrich-Förster, C. (2012). Neuropeptide F
787 immunoreactive clock neurons modify evening locomotor activity and free-running period in
788 Drosophila melanogaster. J Comp Neurol *520*, 970-987.
789 Huang, A.M., Rehm, E.J., and Rubin, G.M. (2009). Quick preparation of genomic DNA from
790 Drosophila. Cold Spring Harb Protoc *2009*, pdb.prot5198.
791 Hyun, S., Lee, Y., Hong, S.T., Bang, S., Paik, D., Kang, J., Shin, J., Lee, J., Jeon, K., Hwang,
792 S., *et al.* (2005). Drosophila GPCR Han is a receptor for the circadian clock neuropeptide PDF.
793 Neuron *48*, 267-278.
794 Im, S.H., and Taghert, P.H. (2010). PDF receptor expression reveals direct interactions between
795 circadian oscillators in Drosophila. J Comp Neurol *518*, 1925-1945.
796 Jin, X., Tian, Y., Zhang, Z.C., Gu, P., Liu, C., and Han, J. (2021). A subset of DN1p neurons
797 integrates thermosensory inputs to promote wakefulness via CNMa signaling. Curr Biol.
798 Johard, H.A., Yoishii, T., Dircksen, H., Cusumano, P., Rouyer, F., Helfrich-Förster, C., and
799 Nässel, D.R. (2009). Peptidergic clock neurons in Drosophila: ion transport peptide and short
800 neuropeptide F in subsets of dorsal and ventral lateral neurons. J Comp Neurol *516*, 59-73.
801 Jung, S.H., Lee, J.H., Chae, H.S., Seong, J.Y., Park, Y., Park, Z.Y., and Kim, Y.J. (2014).
802 Identification of a novel insect neuropeptide, CNMa and its receptor. FEBS Lett *588*, 2037-2041.
803 Konopka, R.J., and Benzer, S. (1971). Clock mutants of Drosophila melanogaster. Proc Natl

Acad Sci USA *68*, 2112-2116.

Labuhn, M., Adams, F.F., Ng, M., Knoess, S., Schambach, A., Charpentier, E.M., Schwarzer, A., Mateo, J.L., Klusmann, J.H., and Heckl, D. (2018). Refined sgRNA efficacy prediction improves large- and small-scale CRISPR-Cas9 applications. Nucleic Acids Res *46*, 1375-1385.

Lamaze, A., Krätschmer, P., Chen, K.F., Lowe, S., and Jepson, J.E.C. (2018). A Wake-Promoting Circadian Output Circuit in Drosophila. Curr Biol *28*, 3098-3105.e3093.

Lear, B.C., Merrill, C.E., Lin, J.-M., Schroeder, A., Zhang, L., and Allada, R. (2005). A G protein-coupled receptor, groom-of-PDF, is required for PDF neuron action in circadian behavior. Neuron *48*, 221-227.

Lee, G., Bahn, J.H., and Park, J.H. (2006). Sex- and clock-controlled expression of the neuropeptide F gene in Drosophila. *103*, 12580-12585.

Lelito, K.R., and Shafer, O.T. (2012). Reciprocal cholinergic and GABAergic modulation of the small ventrolateral pacemaker neurons of Drosophila's circadian clock neuron network. J Neurophysiol *107*, 2096-2108.

Ling, X., Xie, B., Gao, X., Chang, L., Zheng, W., Chen, H., Huang, Y., Tan, L., Li, M., and Liu, T. (2020). Improving the efficiency of precise genome editing with site-specific Cas9-oligonucleotide conjugates. Sci Adv *6*, eaaz0051.

Liu, G., Yin, K., Zhang, Q., Gao, C., and Qiu, J.L. (2019). Modulating chromatin accessibility by transactivation and targeting proximal dsgRNAs enhances Cas9 editing efficiency in vivo. Genome Biol *20*, 145.

Ma, D., Przybylski, D., Abruzzi, K.C., Schlichting, M., Li, Q., Long, X., and Rosbash, M. (2021). A transcriptomic taxonomy of Drosophila circadian neurons around the clock. Elife *10*.

Mali, P., Yang, L., Esvelt, K.M., Aach, J., Guell, M., DiCarlo, J.E., Norville, J.E., and Church, G.M. (2013). RNA-guided human genome engineering via Cas9. Science *339*, 823-826.

Martin, S.E., and Caplen, N.J. (2007). Applications of RNA interference in mammalian systems. Annu Rev Genomics Hum Genet *8*, 81-108.

Mu, W., Zhang, Y., Xue, X., Liu, L., Wei, X., and Wang, H. (2019). 5' capped and 3' polyA-tailed sgRNAs enhance the efficiency of CRISPR-Cas9 system. Protein Cell *10*, 223-228.

Nahar, S., Sehgal, P., Azhar, M., Rai, M., Singh, A., Sivasubbu, S., Chakraborty, D., and Maiti,

833 S. (2018). A G-quadruplex motif at the 3' end of sgRNAs improves CRISPR-Cas9 based
834 genome editing efficiency. Chem Commun (Camb) *54*, 2377-2380.
835 Neumüller, R.A., Wirtz-Peitz, F., Lee, S., Kwon, Y., Buckner, M., Hoskins, R.A., Venken, K.J.,
836 Bellen, H.J., Mohr, S.E., and Perrimon, N. (2012). Stringent analysis of gene function and
837 protein-protein interactions using fluorescently tagged genes. Genetics *190*, 931-940.
838 Ni, J.Q., Zhou, R., Czech, B., Liu, L.P., Holderbaum, L., Yang-Zhou, D., Shim, H.S., Tao, R.,
839 Handler, D., Karpowicz, P.*, et al.* (2011). A genome-scale shRNA resource for transgenic RNAi
840 in Drosophila. Nat Methods *8*, 405-407.
841 Nicholson, L., Singh, G.K., Osterwalder, T., Roman, G.W., Davis, R.L., and Keshishian, H.
842 (2008). Spatial and temporal control of gene expression in Drosophila using the inducible
843 GeneSwitch GAL4 system. I. Screen for larval nervous system drivers. Genetics *178*, 215-234.
844 Oberdoerffer, P., Kanellopoulou, C., Heissmeyer, V., Paeper, C., Borowski, C., Aifantis, I., Rao,
845 A., and Rajewsky, K. (2005). Efficiency of RNA interference in the mouse hematopoietic system
846 varies between cell types and developmental stages. Mol Cell Biol *25*, 3896-3905.
847 Osterwalder, T., Yoon, K.S., White, B.H., and Keshishian, H. (2001). A conditional tissue-specific
848 transgene expression system using inducible GAL4. Proc Natl Acad Sci USA *98*, 12596-12601.
849 Perkins, L.A., Holderbaum, L., Tao, R., Hu, Y., Sopko, R., McCall, K., Yang-Zhou, D., Flockhart,
850 I., Binari, R., Shim, H.S.*, et al.* (2015). The Transgenic RNAi project at harvard medical school:
851 resources and validation. Genetics *201*, 843-852.
852 Poe, A.R., Wang, B., Sapar, M.L., Ji, H., Li, K., Onabajo, T., Fazliyeva, R., Gibbs, M., Qiu, Y.,
853 Hu, Y.*, et al.* (2019). Robust CRISPR/Cas9-mediated tissue-specific mutagenesis reveals gene
854 redundancy and perdurance in Drosophila. Genetics *211*, 459-472.
855 Port, F., and Bullock, S.L. (2016). Augmenting CRISPR applications in Drosophila with tRNA-
856 flanked sgRNAs. Nature Methods *13*, 852-854.
857 Port, F., Chen, H.M., Lee, T., and Bullock, S.L. (2014). Optimized CRISPR/Cas tools for efficient
858 germline and somatic genome engineering in Drosophila. Proc Natl Acad Sci USA *111*, E2967-
859 2976.
860 Port, F., Strein, C., Stricker, M., Rauscher, B., Heigwer, F., Zhou, J., Beyersdörffer, C., Frei, J.,
861 Hess, A., Kern, K.*, et al.* (2020). A large-scale resource for tissue-specific CRISPR mutagenesis

in Drosophila. eLife *9*, e53865.

Reinhard, N., Schubert, F.K., Bertolini, E., Hagedorn, N., Manoli, G., Sekiguchi, M., Yoshii, T., Rieger, D., and Helfrich-Förster, C. (2022). The Neuronal Circuit of the Dorsal Circadian Clock Neurons in Drosophila melanogaster. Front Physiol *13*, 886432.

Renn, S.C., Park, J.H., Rosbash, M., Hall, J.C., and Taghert, P.H. (1999). A pdf neuropeptide gene mutation and ablation of PDF neurons each cause severe abnormalities of behavioral circadian rhythms in Drosophila. Cell *99*, 791-802.

Rieger, D., Shafer, O.T., Tomioka, K., and Helfrich-Förster, C. (2006). Functional analysis of circadian pacemaker neurons in Drosophila melanogaster. J Neurosci *26*, 2531-2543.

Schlichting, M., Díaz, M.M., Xin, J., and Rosbash, M. (2019). Neuron-specific knockouts indicate the importance of network communication to Drosophila rhythmicity. eLife *8*, e48301.

Schlichting, M., Richhariya, S., Herndon, N., Ma, D., Xin, J., Lenh, W., Abruzzi, K., and Rosbash, M. (2022). Dopamine and GPCR-mediated modulation of DN1 clock neurons gates the circadian timing of sleep. Proc Natl Acad Sci USA *119*, e2206066119.

Scott, T., Urak, R., Soemardy, C., and Morris, K.V. (2019). Improved Cas9 activity by specific modifications of the tracrRNA. Sci Rep *9*, 16104.

Sekiguchi, M., Inoue, K., Yang, T., Luo, D.G., and Yoshii, T. (2020). A Catalog of GAL4 Drivers for Labeling and Manipulating Circadian Clock Neurons in Drosophila melanogaster. J Biol Rhythms *35*, 207-213.

Seluzicki, A., Flourakis, M., Kula-Eversole, E., Zhang, L., Kilman, V., and Allada, R. (2014). Dual PDF signaling pathways reset clocks via TIMELESS and acutely excite target neurons to control circadian behavior. PLoS Biol *12*, e1001810.

Shafer, O.T., Helfrich-Förster, C., Renn, S.C., and Taghert, P.H. (2006). Reevaluation of Drosophila melanogaster's neuronal circadian pacemakers reveals new neuronal classes. J Comp Neurol *498*, 180-193.

Shafer, O.T., Kim, D.J., Dunbar-Yaffe, R., Nikolaev, V.O., Lohse, M.J., and Taghert, P.H. (2008). Widespread receptivity to neuropeptide PDF throughout the neuronal circadian clock network of Drosophila revealed by real-time cyclic AMP imaging. Neuron *58*, 223-237.

Shaw, P.J., Cirelli, C., Greenspan, R.J., and Tononi, G. (2000). Correlates of sleep and waking

in Drosophila melanogaster. Science *287*, 1834-1837.

Sokolove, P.G., and Bushell, W.N. (1978). The chi square periodogram: Its utility for analysis of circadian rhythms. Journal of Theoretical Biology *72*, 131-160.

Stemmer, M., Thumberger, T., Del Sol Keyer, M., Wittbrodt, J., and Mateo, J.L. (2015). CCTop: An Intuitive, Flexible and Reliable CRISPR/Cas9 Target Prediction Tool. PLoS One *10*, e0124633.

Stoleru, D., Peng, Y., Agosto, J., and Rosbash, M. (2004). Coupled oscillators control morning and evening locomotor behaviour of Drosophila. Nature *431*, 862-868.

Talay, M., Richman, E.B., Snell, N.J., Hartmann, G.G., Fisher, J.D., Sorkaç, A., Santoyo, J.F., Chou-Freed, C., Nair, N., Johnson, M.*, et al.* (2017). Transsynaptic Mapping of Second-Order Taste Neurons in Flies by trans-Tango. Neuron *96*, 783-795.e784.

Tang, M., Cao, L.-H., Yang, T., Ma, S.-X., Jing, B.-Y., Xiao, N., Xu, S., Leng, K.-R., Yang, D., Li, M.-T.*, et al.* (2022). An extra-clock ultradian brain oscillator sustains circadian timekeeping. Sci Adv *8*, eabo5506.

Vetter, D., Andrews, B.J., Roberts-Beatty, L., and Sadowski, P.D. (1983). Site-specific recombination of yeast 2-micron DNA in vitro. Proc Natl Acad Sci U S A *80*, 7284-7288.

Wu, F., Deng, B., Xiao, N., Wang, T., Li, Y., Wang, R., Shi, K., Luo, D.G., Rao, Y., and Zhou, C. (2020). A neuropeptide regulates fighting behavior in Drosophila melanogaster. Elife *9*, e54229.

Xie, K., Minkenberg, B., and Yang, Y. (2015). Boosting CRISPR/Cas9 multiplex editing capability with the endogenous tRNA-processing system. Proc Natl Acad Sci U S A *112*, 3570-3575.

Xu, H., Xiao, T., Chen, C.H., Li, W., Meyer, C.A., Wu, Q., Wu, D., Cong, L., Zhang, F., Liu, J.S.*, et al.* (2015). Sequence determinants of improved CRISPR sgRNA design. Genome Res *25*, 1147-1157.

Xue, Z., Wu, M., Wen, K., Ren, M., Long, L., Zhang, X., and Gao, G. (2014). CRISPR/Cas9 mediates efficient conditional mutagenesis in Drosophila. G3 (Bethesda) *4*, 2167-2173.

Zhao, P., Zhang, Z., Lv, X., Zhao, X., Suehiro, Y., Jiang, Y., Wang, X., Mitani, S., Gong, H., and Xue, D. (2016). One-step homozygosity in precise gene editing by an improved CRISPR/Cas9 system. Cell Res *26*, 633-636.

920 Zheng, X., Qi, C., Yang, L., Quan, Q., Liu, B., Zhong, Z., Tang, X., Fan, T., Zhou, J., and Zhang,
921 Y. (2020). The Improvement of CRISPR-Cas9 system with ubiquitin-associated domain fusion
922 for efficient plant genome editing. Front Plant Sci *11*, 621.
923

924 **FIGURE Legends**

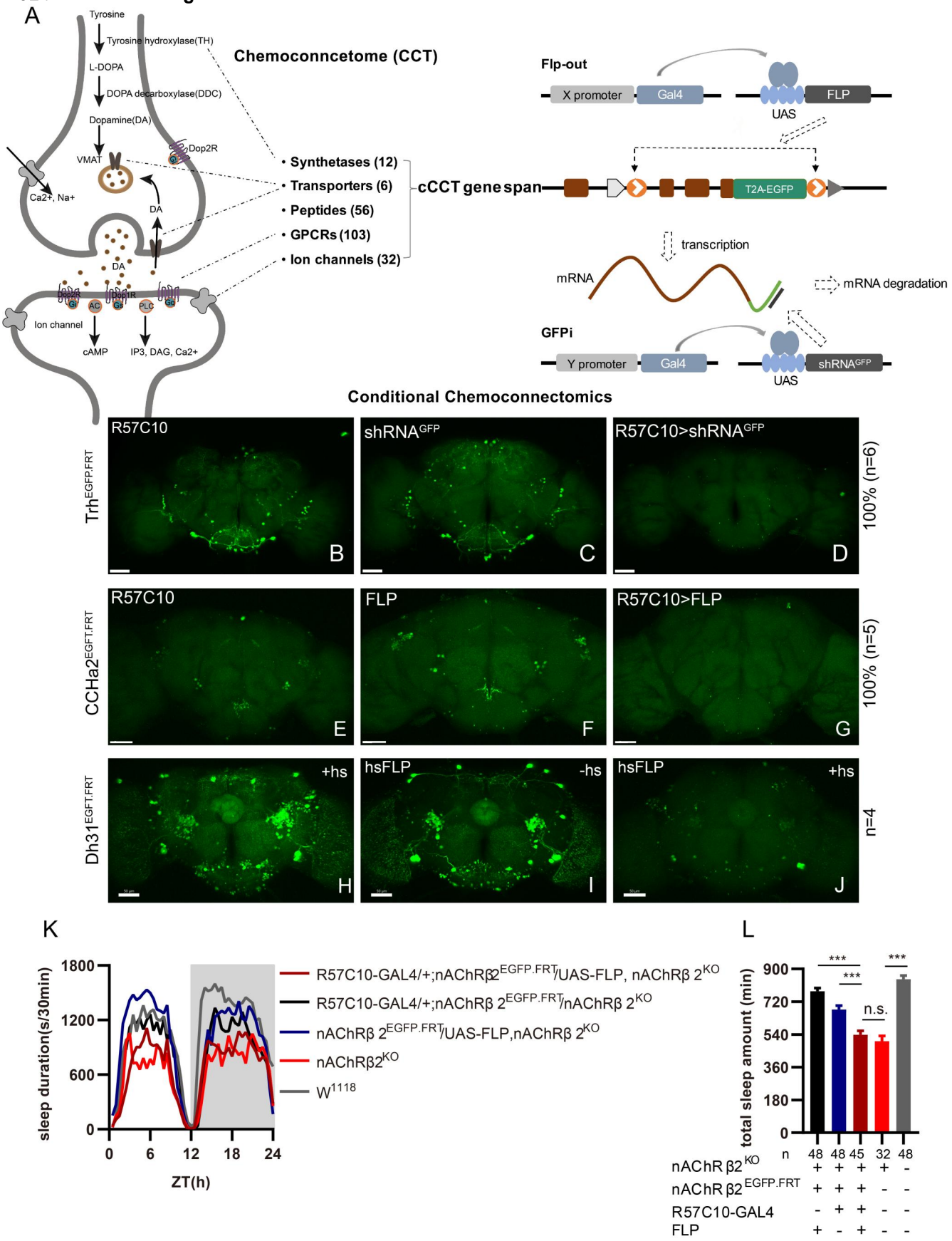

926 **Fig. 1. cCCTomics Mediates Efficient Conditional Disruption of CCT Genes**

927 (A) Schematic of cCCT gene span and principle of cCCTomics. A T2A-EGFP sequence was
928 introduced at the 3' end of CCT genes and their most or all coding regions (depending on attP-
929 KO lines) were flanked by 34 bp FRT sequence. Both Flp-out (top) and GFP RNAi (down) could
930 mediate CCT gene manipulation. (B-J) Expression of Trh (B-D), CCHa2 (E-G), and Dh31 (H-J)
931 are efficiently disrupted by pan-neuronal expression of GFP-RNAi (B-D), pan-neuronal
932 expression of Flp-out (E-G), and heatshock-Flp (H-J) respectively. Representative fluorescence
933 images of R57C10-Gal4/+;Trh$^{EGFP.FRT}$/+ (B), UAS-shRNA^{GFP}/Trh$^{EGFP.FRT}$ (C), R57C10-Gal4/+;
934 UAS-shRNA^{GFP}/Trh$^{EGFP.FRT}$ (D), R57C10-Gal4/+;CCHa2$^{EGFP.FRT}$/+; (E), UAS-
935 Flp/CCHa2$^{EGFP.FRT}$ (F), R57C10-Gal4/+; UAS-Flp/CCHa2$^{EGFP.FRT}$ (G), Dh31$^{EGFP.FRT}$ with
936 heatshock (H), hs-Flp/Dh31$^{EGFP.FRT}$ without heatshock (I), and hs-Flp/Dh31$^{EGFP.FRT}$ with
937 heatshock are shown. Manipulation efficiency and experiment group fly number is noted on the
938 right. Scale bar, 50um. (K-L) sleep profiles (K) and statistical analysis (L) of Flp-out induced
939 nAChRβ2 neuronal knockout flies (dark red), nAChRβ2 knockout flies, and genotype controls
940 (dark and blue). Sleep profiles are plotted in 30 min bins. In this and other figures, blank
941 background indicates the light phase (ZT 0-12); shaded background indicates the dark phase
942 (ZT 12-24). Daily sleep duration were significantly reduced in nAChRβ2 neuronal knockout files
943 which is comparable to nAChRβ2 knockout.
944 In all statistical panels, unless otherwise noted, 1) Numbers below each bar represent the
945 number of flies tested. 2) Mean ± SEM is shown. 3) The Kruskal-Wallis test followed by Dunn's
946 post test was used. ***$p < 0.001$. ** $p < 0.01$. * $p < 0.05$. n.s. $p > 0.05$. Male flies were used
947 unless otherwise noted.
948

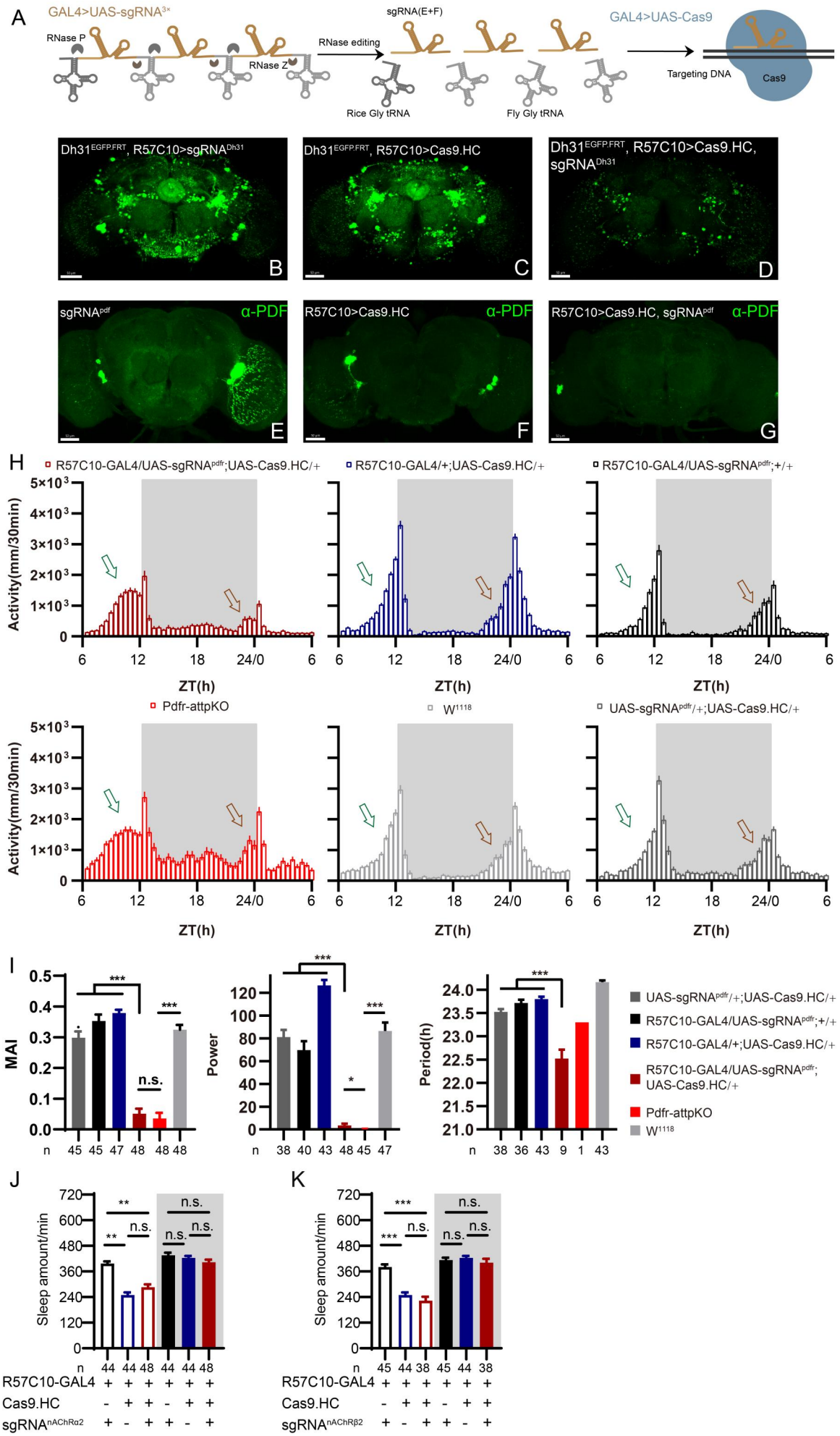

Fig. 2. C-cCCTomics Mediates Efficient Conditional Knockout of CCT Genes

(A) Schematic of C-cCCTomics principle. Cas9 and three sgRNAs are driven by GAL4/UAS system. Three tandem sgRNAs are segregated by fly $tRNA^{Gly}$ and matured by RNase Z and RNase P. (B-G) Pan-neuronal knockout of Dh31 (D) and Pdf (G) by C-cCCTomics strategy. Representative fluorescence images presented expression of Dh31 (B-D) or anti-PDF (E-G). Pan-neuronal expression of Cas9 and sgRNA eliminated most (D) or all (G) fluorescent signal compared to control fly brains (B-C, E-F). Scale bar, 50 μm. (H) Activity profiles of pan-neuronal knockout of Pdfr and Pdfr-attpKO. Activity profiles were centered of the 12h darkness in all figures with evening activity on the left and morning activity on the right, which is different from general circadian literatures. Plotted in 30 min bins. (I) Statistical analysis of morning anticipation index (MAI), power, and period for pan-neuronal Pdf knockout and Pdfr-attpKO flies. Knocking out of Pdfr in neurons reduced both morning anticipation index, power and period significantly. (J-K) Statistical analysis of nAChRα2 (J) and nAChRβ2 (K) pan-neuronal knockout flies' sleep phenotype. Sleep of these flies were not disrupted.

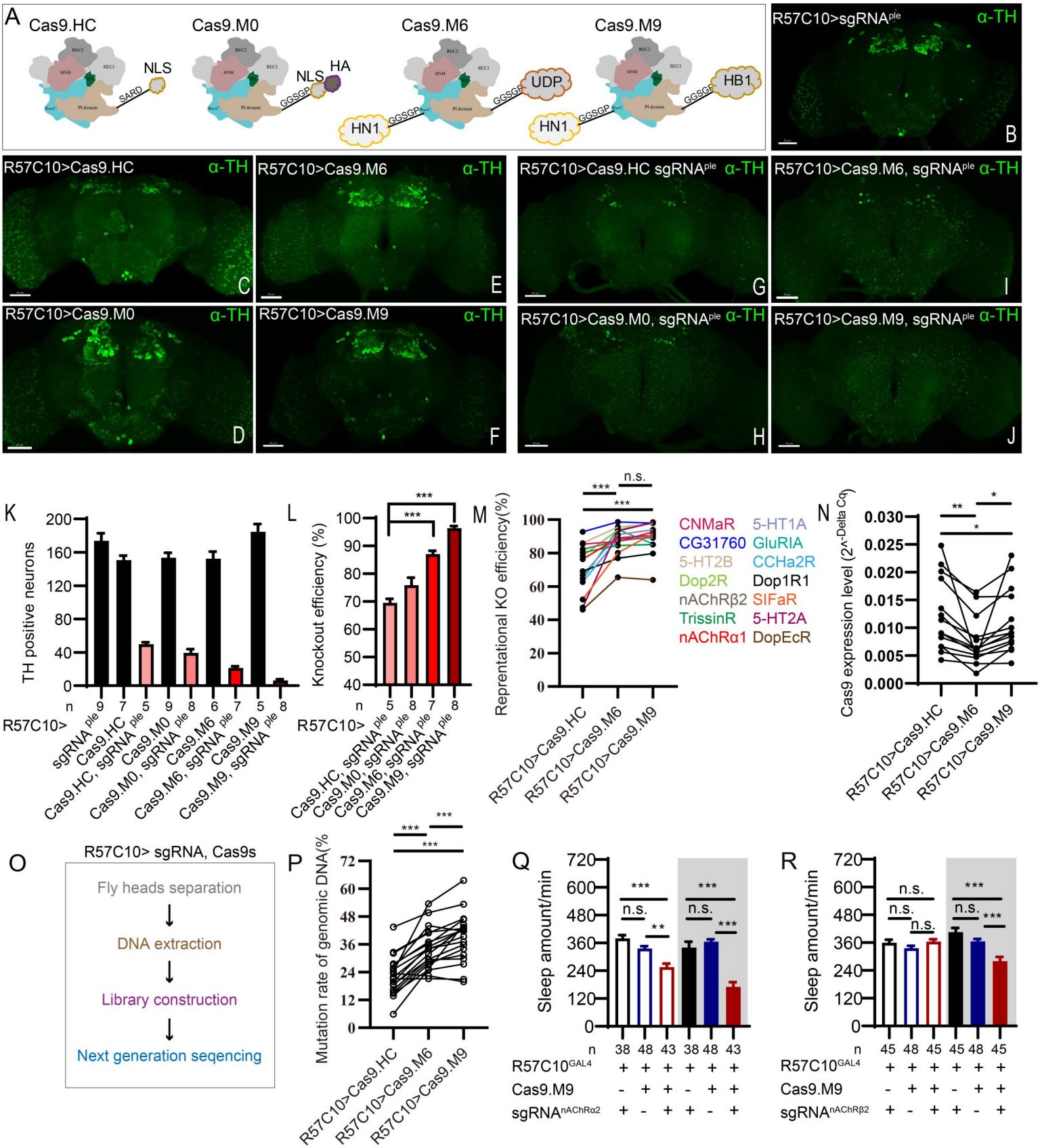

966 **Fig. 3. Efficiency Evaluation of Variations of Chromatin-Modulating Peptides Modified**

967 **Cas9.**

968 (A) Schematics of chromatin-modulating peptides modified Cas9. (B-J) Efficiency evaluation

969 of Cas9 variants. Fluorescence imaging of R57C10-Gal4>UAS-sgRNA^{ple} (B), R57C10-

970 Gal4>UAS-Cas9 (C-F), and R57C10-Gal4>UAS-Cas9, UAS-sgRNA^{ple} (G-J) flies are shown.

971 Brains were stained with anti-TH (green). Scale bar is 50μm. (K) Anterior TH positive neurons

972 numbers of (K-U). (L) Statistical analysis of ple knockout efficiency related to (K). Modified

973 Cas9.M6 and Cas9.M9 showed an improved efficiency comparing to Cas9.HC. Student's t

974 test was used. (M) Statistical analysis of representational KO efficiency of Cas9 variants as

975 related to Figure S5. Gene symbols on the right indicate tested genes. (N) Statistical analysis

976 of Cas9 expression level. (O-P) Workflow of efficiency validation by next-generation

977 sequencing (O) and Statistical analysis of single-site mutation ratios induced by Cas9 variants

978 (P). Paired t test was used in (M), (N) and (P). (Q-R) Statistical analysis of sleep amount for

979 nAChRα2 (Q) or nAChRβ2 (R) pan-neuronal knockout flies. Knockout of nAChRα2 and

980 nAChRβ2 by modified Cas9.M9 significantly decreased flies' sleep amount.

981

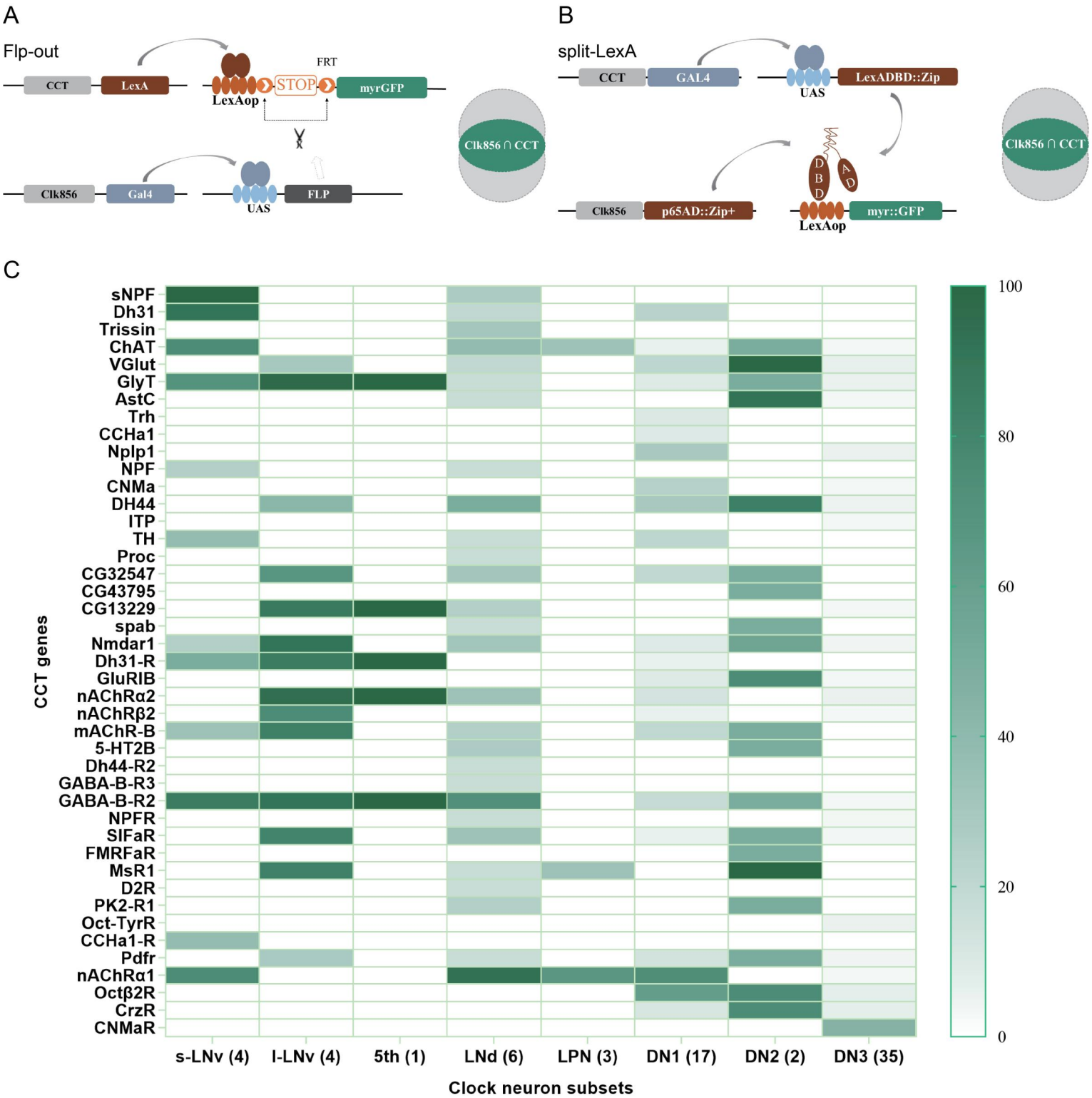

983 **Fig 4. Genetic Dissection of Clk856 Labelled Clock Neurons.**

984 (A-B) Schematic of intersection strategies used in Clk856 labelled clock neurons dissection,

985 Flp-out strategy (A) and split-LexA strategy (B). The exact strategy used for each gene is

986 annotated in Table S5. (C) Expression profiles of CCT genes in clock neurons. Gradient color

987 denotes proportion of neurons that were positive for the CCT gene within each subset. The

988 exact cell number for each subset is annotated in Table S4.

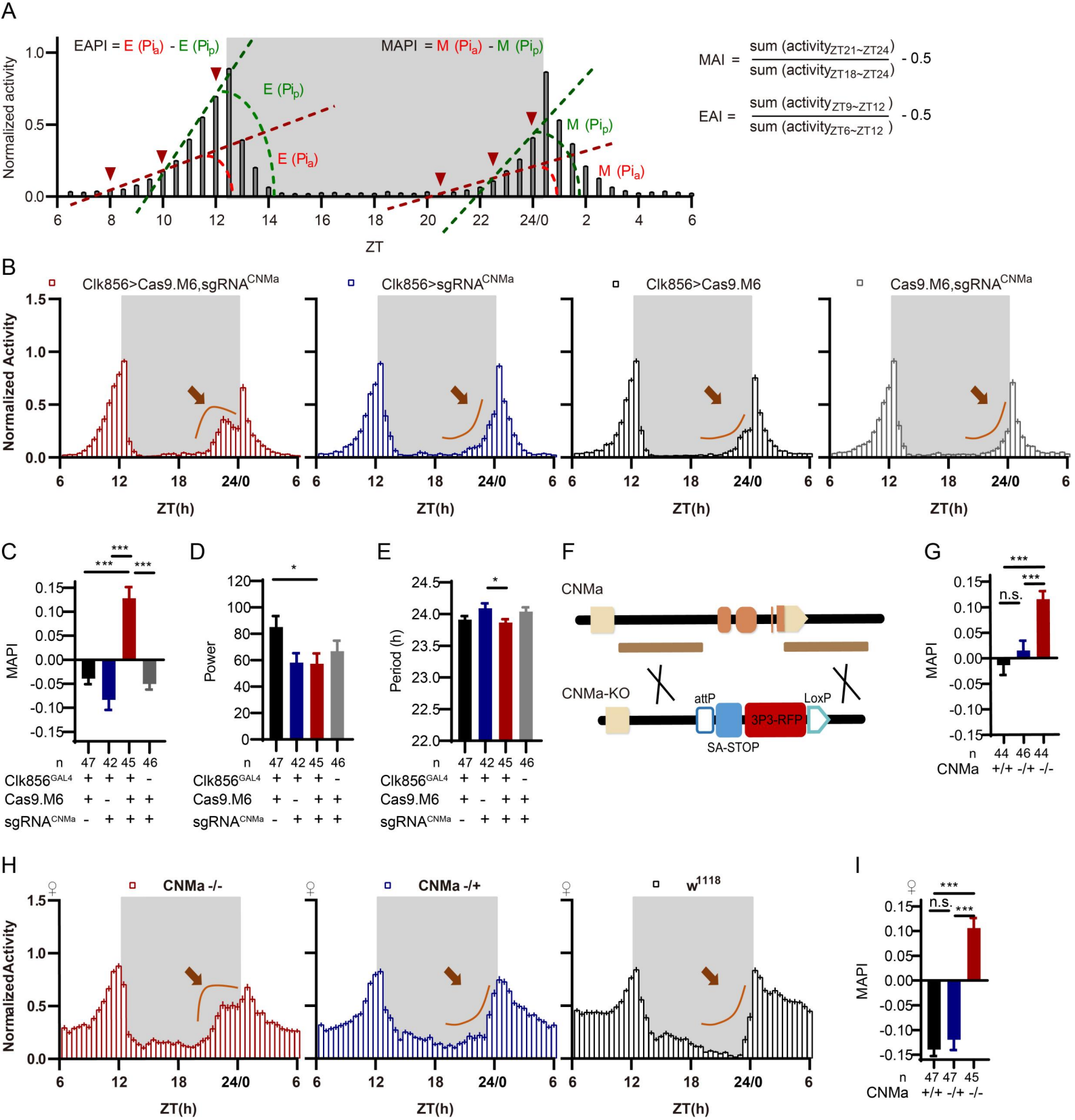

Fig. 5. CNMa Regulation of Morning Anticipation in Clock Neuron

(A)Schematic of MAI, EAI, MAPI and EAPI definition. (B) Activity plots of male flies with CNMa knockout in clock neurons (red) and controls (blue, black and grey), plotted in 30 min bins. An advancement of morning activity peak was presented in CNMa clock-neuron-specific mutants (brown arrowhead). (C-E) Statistical analyses of MAPI, power, and period of flies in (B). MAPI

995 was significantly increased in clock neurons-specific CNMa deficient flies (C) while power (D)

996 and period (E) were not changed. (F) Schematic of $CNMa^{KO}$ generation. The entire encoding

997 region of CNMa was replaced by an attP-SAstop-3P3-RFP-loxP cassette using CRISPR-Cas9

998 strategy. (G) Statistical analysis of MAPI of male $CNMa^{KO}$ flies (red) and controls (blue and

999 black). MAPI significantly increased in male $CNMa^{KO}$ flies. (H) Activity plots of female $CNMa^{KO}$

1000 flies (red) and controls (blue and black). (I) Statistical analysis of MAPI of female $CNMa^{KO}$ flies

1001 (red) and controls (blue and black). MAPI was significantly increased in female $CNMa^{KO}$ flies.

1002

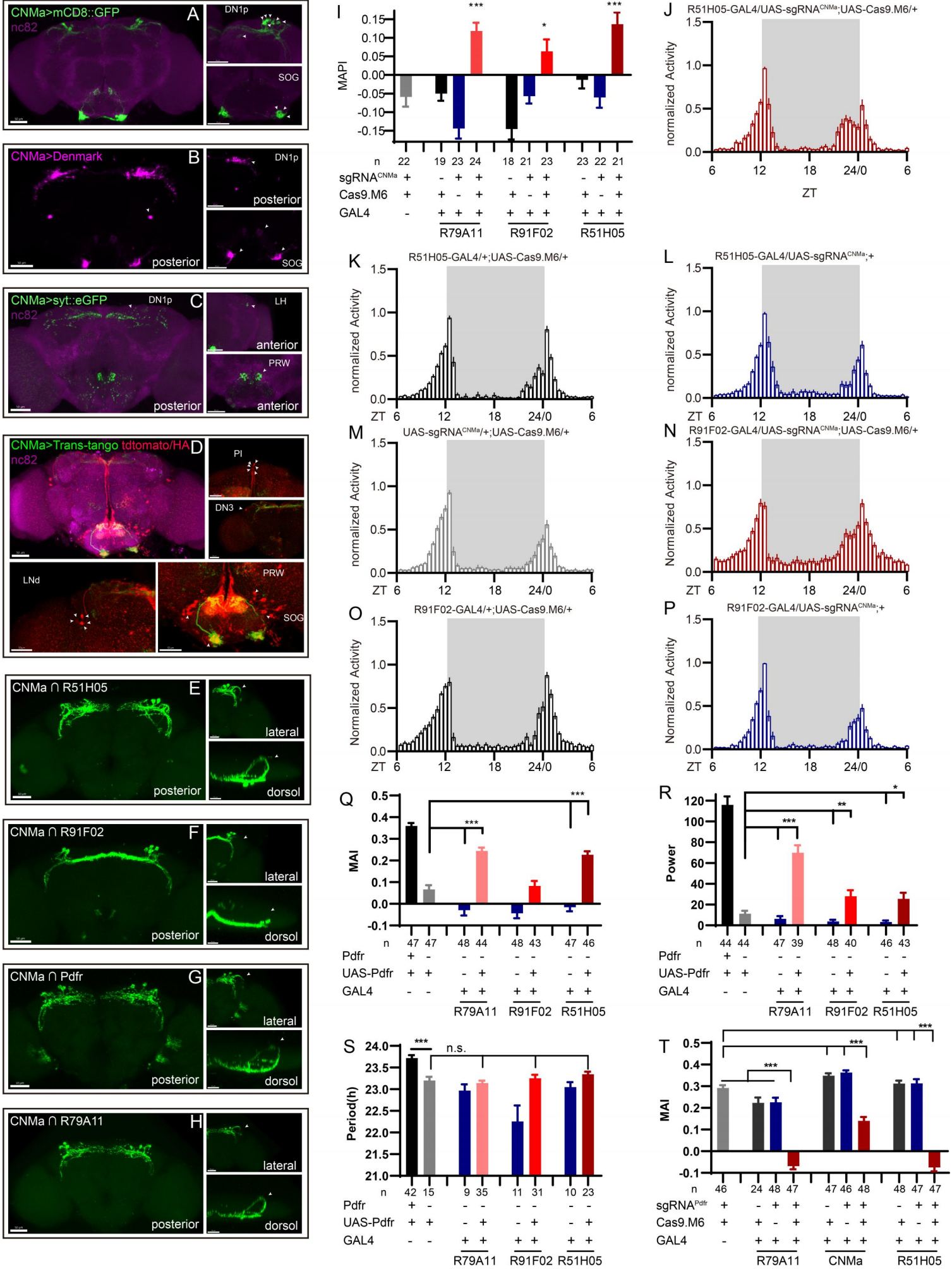

1004 **Fig. 6. Expression, Projection and Trans-projection Feature of CNMa Neurons and Its**

1005 **Functional Subset**

1006 (A-C) Expression and projection patterns of CNMa-KI-Gal4 in the brain. Membrane, dendrites,
1007 and axon projections are labelled by mCD8::GFP (A), Denmark (B), and syt::eGFP (C)
1008 respectively. (D) Downstream neurons labelled through trans-tango driven by CNMa-KI-GAL4.
1009 Arrowheads indicate candidate downstream neurons: six neurons in PI, one pair in DN3, five
1010 pairs in LNd and about 15 pairs in SOG. (E-H) Intersection of DN1p CNMa neurons with DN1p
1011 labelled drivers. GMR51H05-GAL4 (E), GMR91F02-GAL4 (F), Pdfr-KI-GAL4 (G) and
1012 GMR79A11-GAL4 (H) were intersected with CNMa-p65AD, UAS-LexADBD, LexAop-myr::GFP.
1013 Two type I (E, G, H) neurons projected to anterior region and four type II (F) neurons had fewer
1014 projections to anterior region. Scale bar, 50μm. (I) MAPIs were significantly increased in all
1015 three DN1p drivers mediated CNMa knockout. (J-K) Activity plots of CNMa knockout in
1016 R51H05-GAL4 (J) and R91F02-GAL4 (N) neurons. R51H05-GAL4 mediated CNMa knockout
1017 flies showed an advanced morning activity peak (J), while R91F02-Gal4 mediated CNMa
1018 knockout flies did not (N). (Q-S) Statistical analyses of MAI, power and Period. Pdfr
1019 reintroduction in R79A11 and R51H05 neurons could partially rescue the MAI-decreased
1020 phenotype of Pdfr knockout flies. (T) Statistical analyses of MAI of Pdfr knocking out in R79A11-
1021 GAL4, CNMa-GAL4 and R51H05-GAL4 labelled neurons.
1022

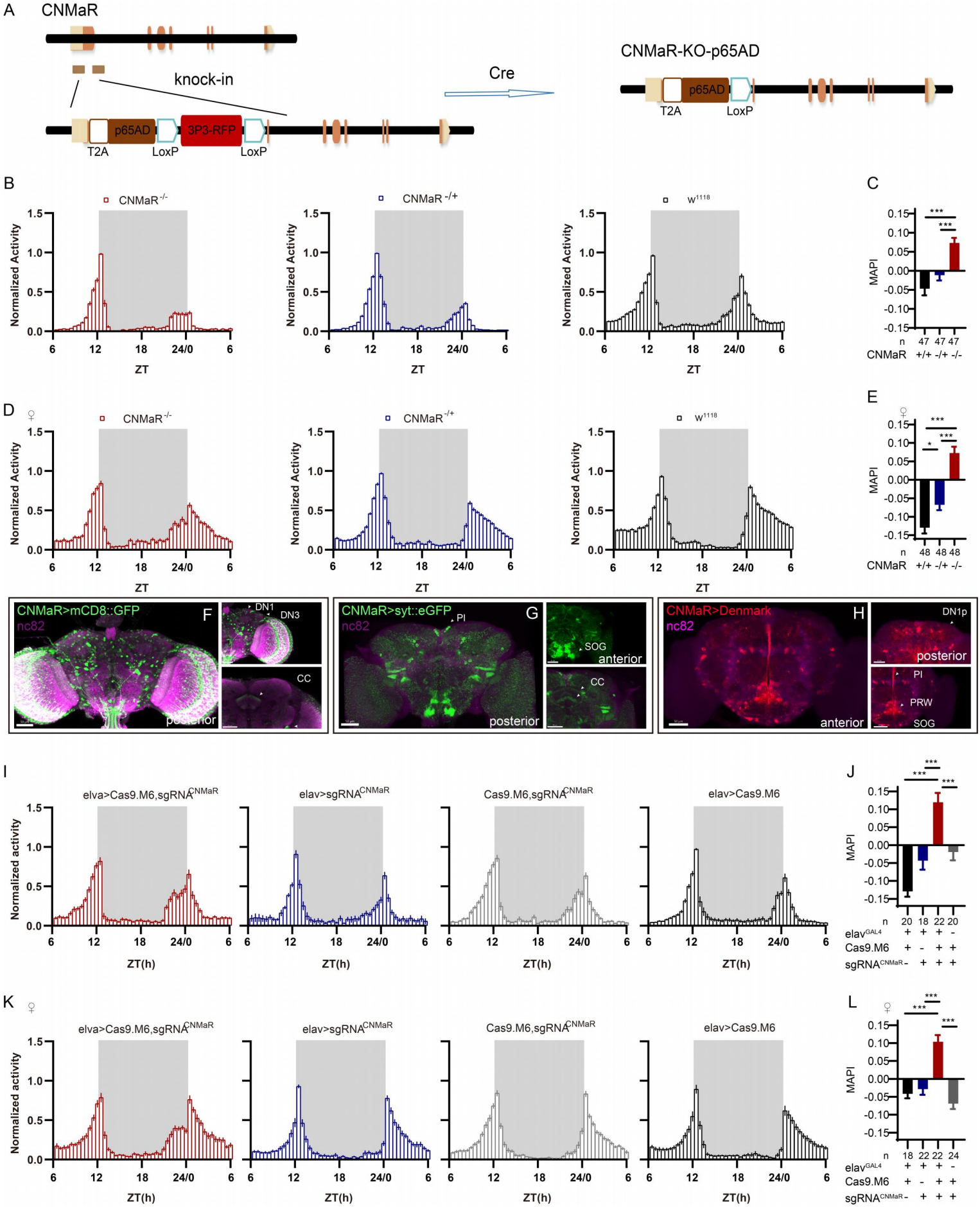

Fig. 7. CNMaR Regulation of Morning Anticipation

(A) Schematic of CNMaR$^{KO\text{-}p65AD}$ generation. Most of the first exon in CNMaR was replaced by

1026 a T2A-p65AD-loxP-3P3-RFP-loxP cassette using CRISPR-Cas9 strategy and the T2A-p65AD
1027 was inserted in the reading frame of the remaining CNMaR codon. 3P3-RFP was removed
1028 latterly by Cre mediated recombination. (B-E) Activity plot (B, D) and statistical analysis (C, E)
1029 of male (B-C) or female (D-E) $CNMaR^{KO\text{-}p65AD}$ flies (red) and genotypical controls (blue and
1030 black). MAPI was significantly increased in both male and female $CNMaR^{KO\text{-}p65AD}$ flies. In this
1031 and other figures, "♀" denotes female flies. (F-H) Expression and projection patterns of
1032 CNMaR-KI-Gal4 in the brain. Scale bars, 50μm. (I-L) Activity plots (I, K) and statistical analyses
1033 (J, L) of CNMaR pan-neuronal knockout flies. Neuronal knockout of CNMaR increased MAPI
1034 (J, L).
1035

1036 **Supplementary Information**

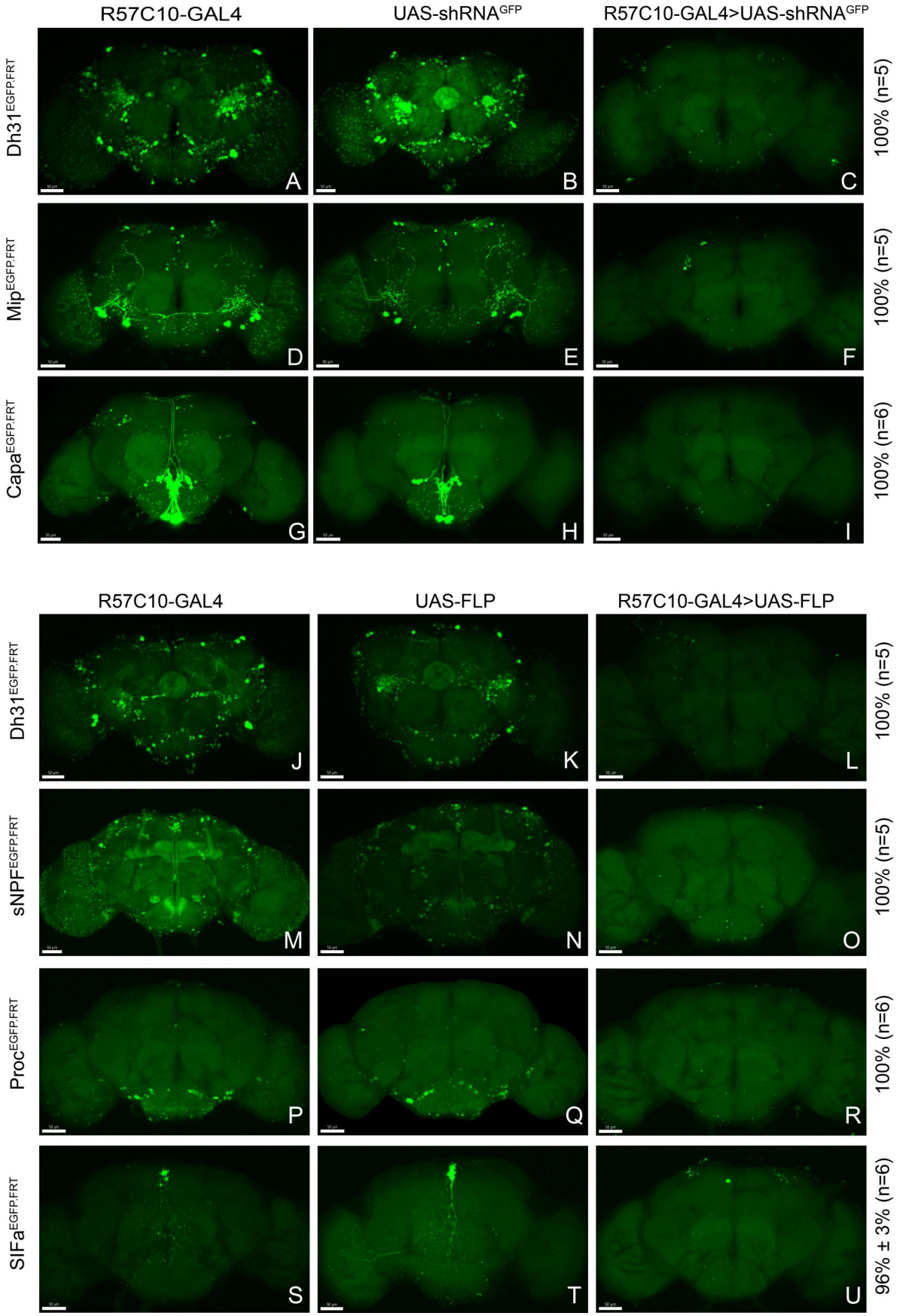

1037

1038 **Fig. S1. Efficient Conditional Disruption of CCT Genes by cCCTomics**

1039 (A-I) Pan-neuronal knockdown of Dh31 (A-C), Mip (D-F) and Capa (G-I) by GFPi. All
1040 experimental fly brains (C, F, I) showed no GFP signal after knockdown by GFPi. As described
1041 in Fig 1, all percentages in the right represent gene disruption efficiency and n represent number
1042 of experimental flies. (J-U) Pan-neuronal knock out of Dh31, sNPF, Proc and SIFa by Flp-out
1043 strategy. No obvious GFP signal was found in the experimental fly brains (L, O, R), excepting
1044 one GFP positive neurons in SIFa flp-out group (U).
1045

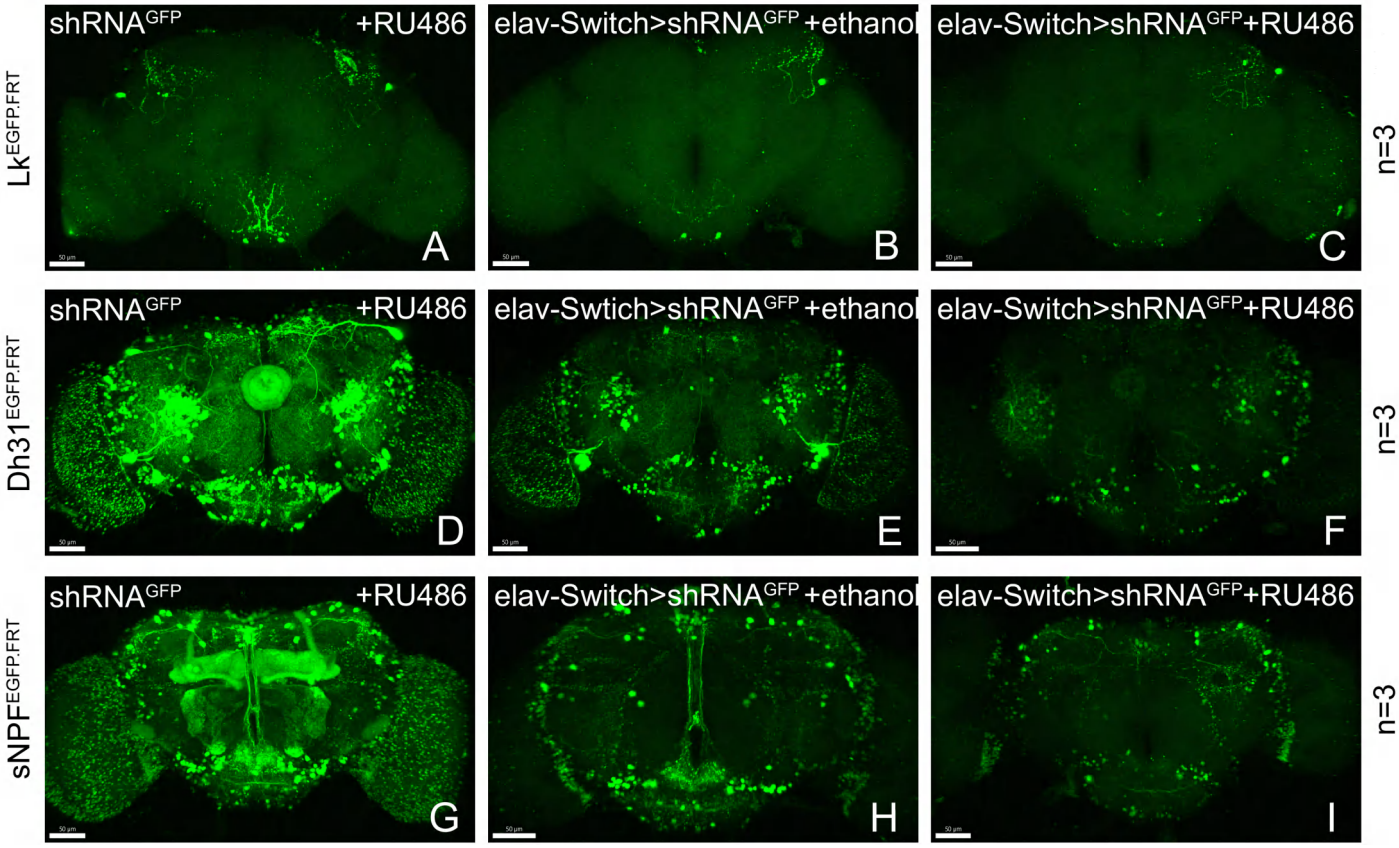

1047 **Fig. S2. Gene Disruption of Target Genes by Induced shRNA**

1048 (A-J) Knockdown of Lk, Dh31 and sNPF by elav-Switch. Most GFP signal is lost in the

1049 experimental group (C, F, I).

1050

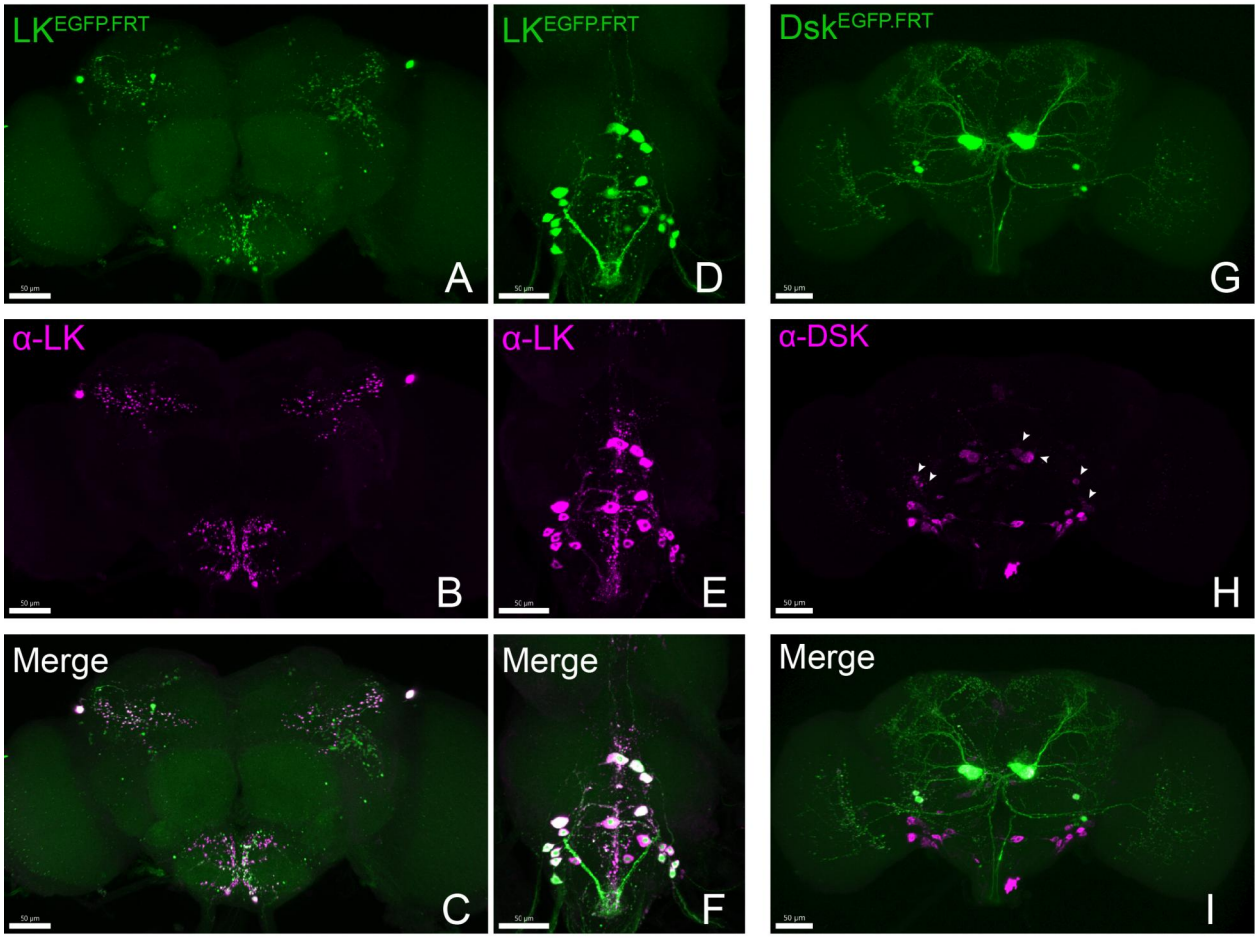

Fig. S3. Accurate Labeling of Target Genes by cCCT Lines

(A-J) Co-localization of fused EGFP labelled CCT genes and corresponding antibodies. All the EGFP labelled Lk (A, D) and Dsk (G) neurons (Green) were co-localized with anti-LK (B, E; merge C, F) and anti-DSK (H, merge I) signal (purple). Arrowheads represent specific anti-DSK signal (Wu et al., 2020).

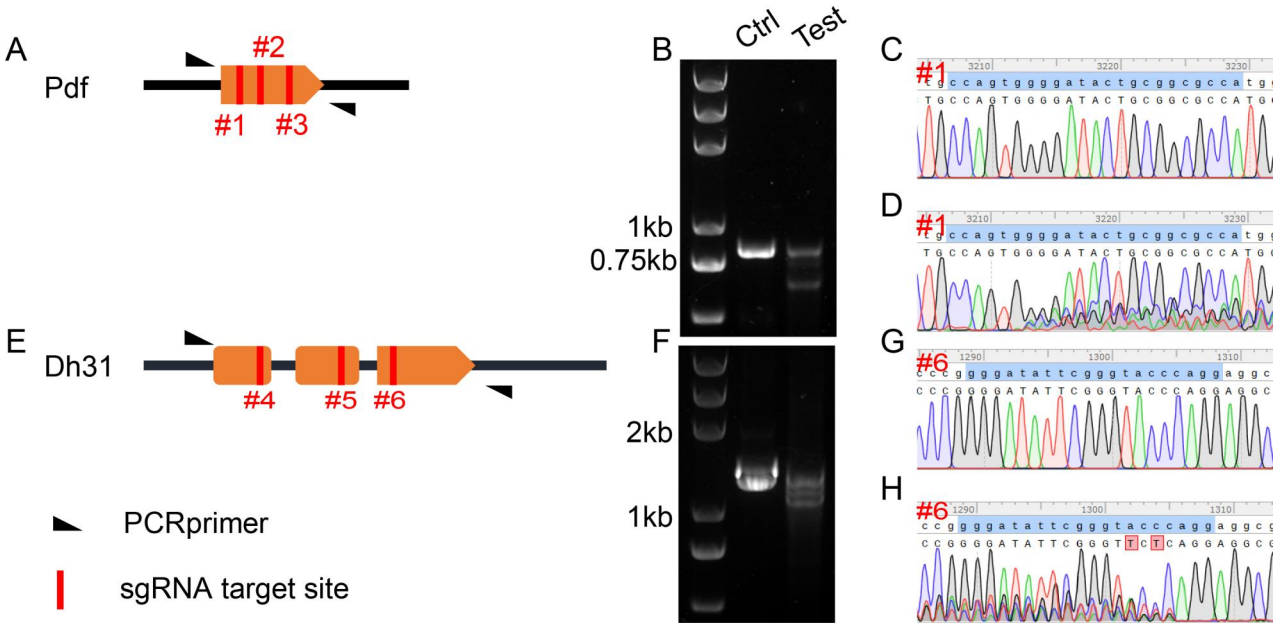

1059 **Fig. S4. Validation of Primary C-cCCTomics**

1060 (A) Gene span of Pdf. #1, #2 and #3 with red lines denote sgRNA targets regions in Pdf coding

1061 sequence. (B) DNA gel electrophoresis of PCR products after *pdf* KO by C-cCCTomics. "Ctrl"

1062 denotes PCR products from genomic DNA mixture of Act5C-GAL4/+; UAS-Cas9.P2/+ flies and

1063 UAS-sRNA^{Pdf} flies. "Test" denotes PCR products from Act5C-GAL4/ UAS-sRNA^{Pdf}; UAS-

1064 Cas9.P2 flies. (C-D) Sanger sequencing results of Ctrl (C) and Test (D) PCR products at #1

1065 sgRNA target site. (E-H) Similar to (A-D) with Dh31 as target.

1066

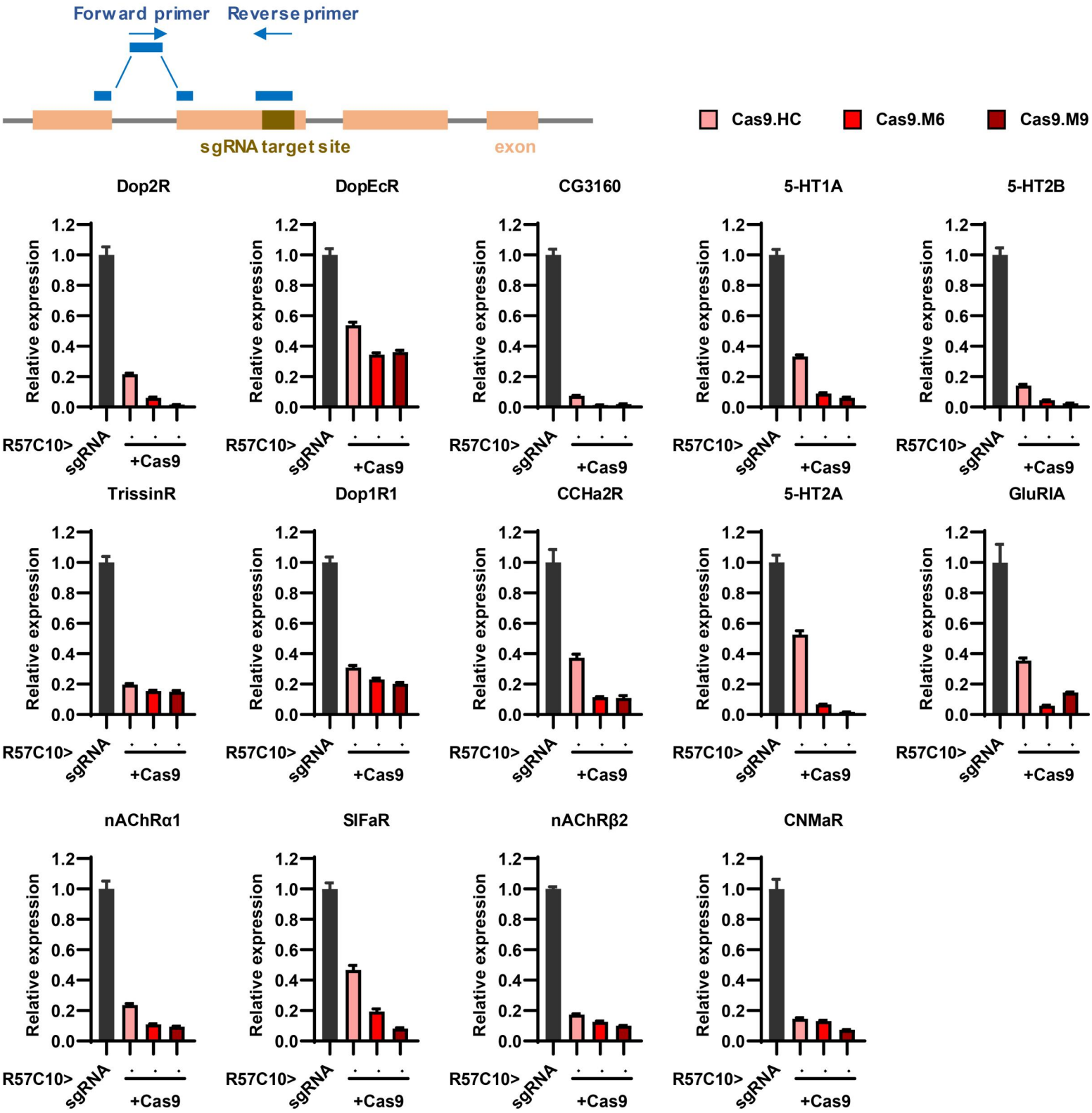

1068 **Fig. S5. Efficiency validation by real-time quantitative PCR.**

1069 This figure corresponds to Fig 3M. The schematic at the top illustrates the principle of primer
1070 design. The gene symbol above each panel indicates the target of sgRNAs. The expression
1071 of the target gene in the experimental groups (where R57C10-GAL4 drives the expression of
1072 both Cas9 variants and sgRNA) was normalized to the control group (where R57C10-GAL4
1073 drives sgRNA expression only).
1074

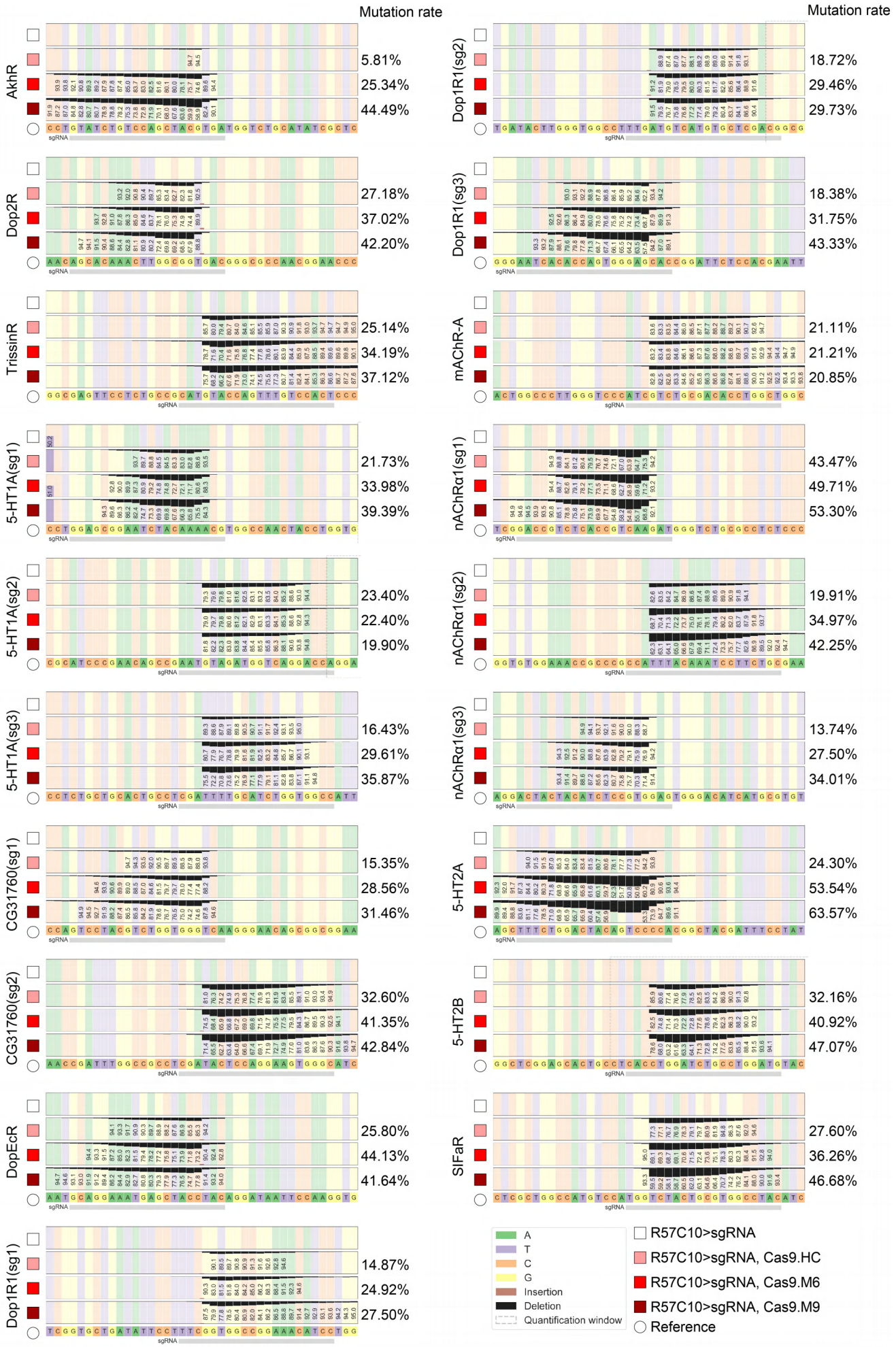

Fig. S6. Efficiency validation by high-throughput sequencing

1077 This figure corresponds to Fig 3P. Gene symbol on the left side of each panel denotes the target

1078 gene, while the percentages on the right denotes mutation rate as calculated by CRISPResso2.

1079 A minimum of 10,000 reads were analyzed for each genotype.

1080

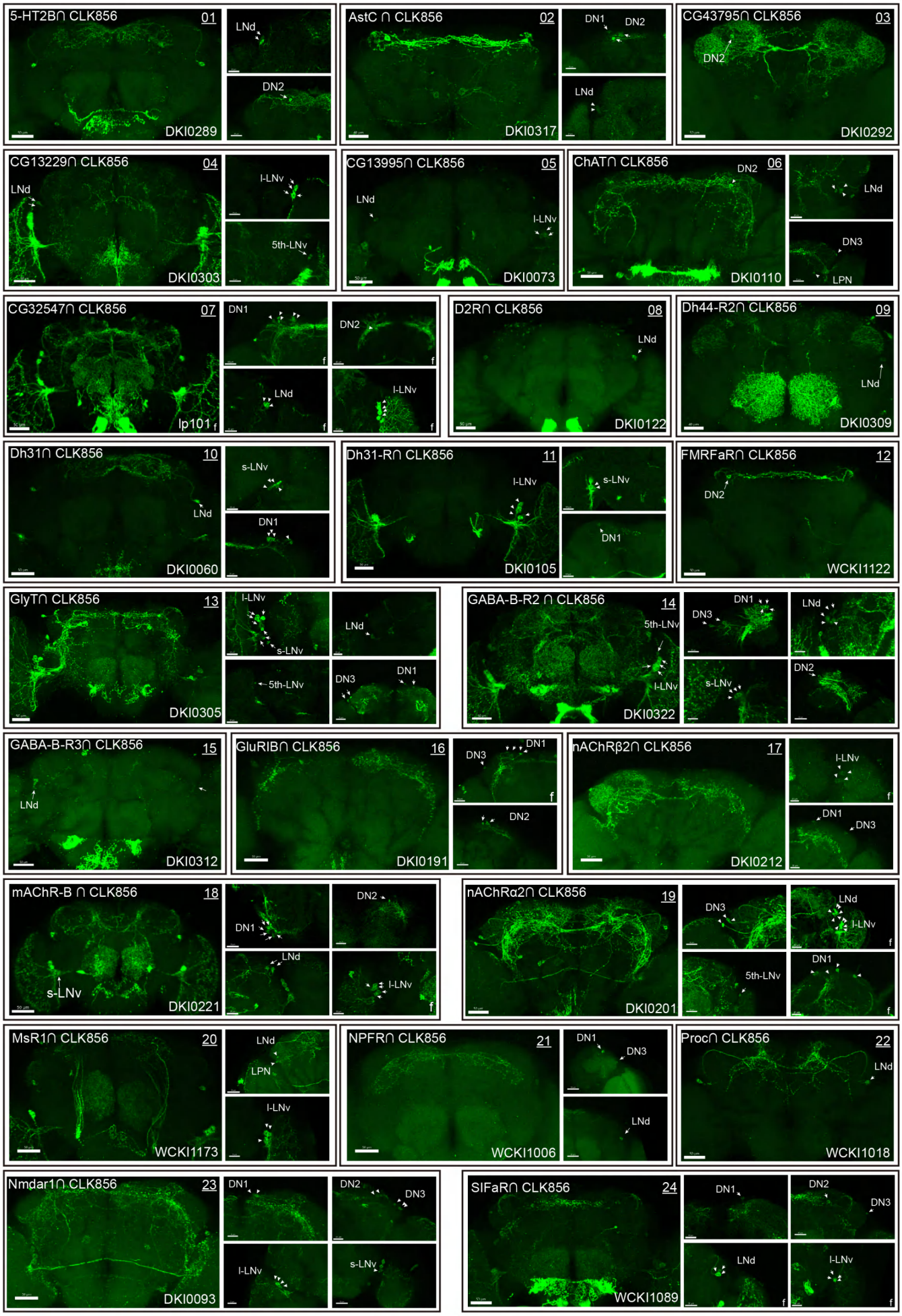

1082 **Fig. S7. Co-expression of Clk856 with CCT Genes**

1083 (01-24) Intersectional expression patterns of CCT drivers with Clk856. The exact strategy used

1084 for each gene is annotated in Table S5. Maximum neuron numbers were presented in each

1085 image. Note at the bottom right corner is category ID of CCT drivers in Rao Lab fly stock library.

1086 “f” denotes female fly brain, otherwise male brain is shown.

1087

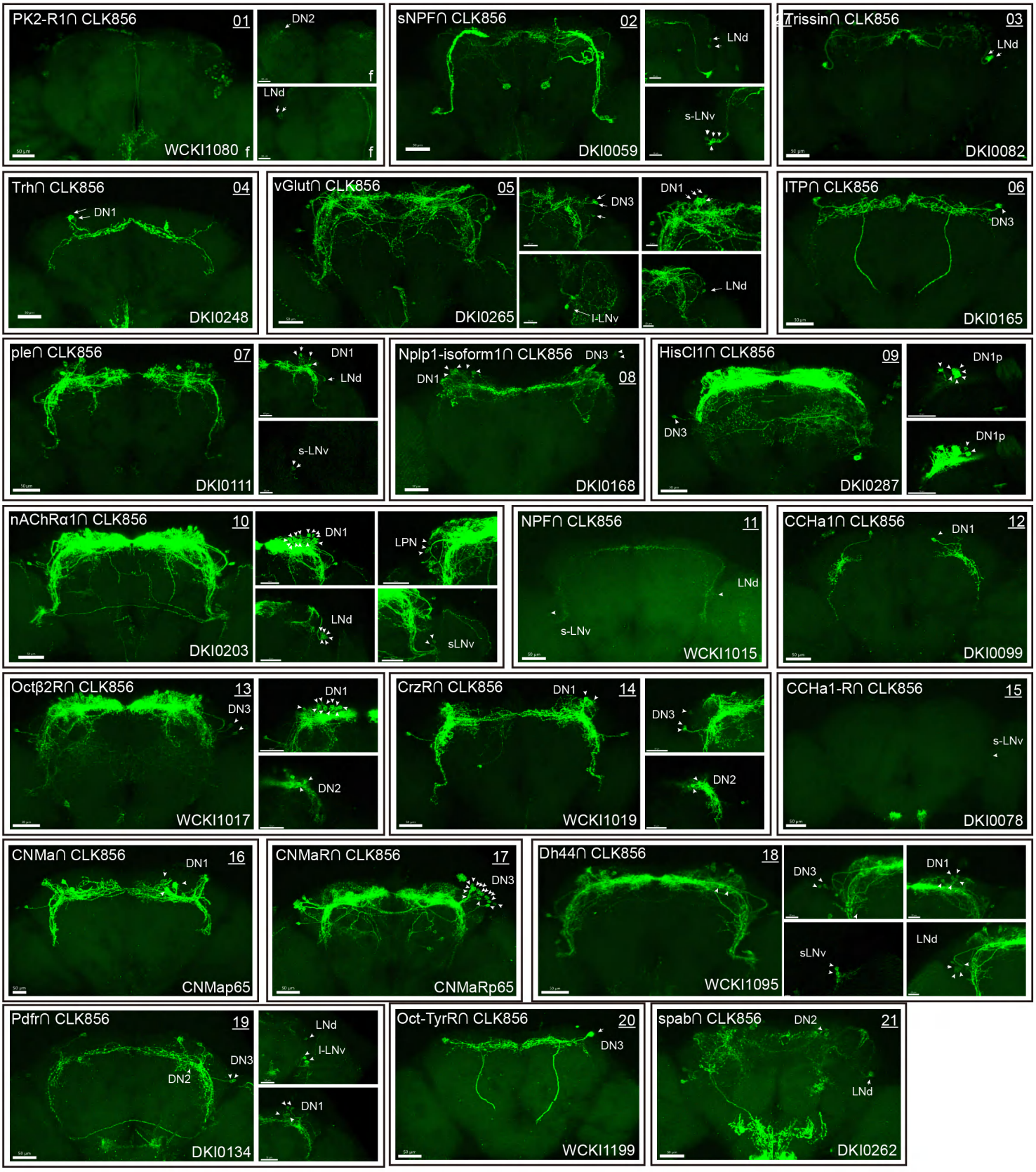

Fig. S8 Co-expression of Clk856 with CCT Genes

(01-21) Intersectional expression patterns of CCT drivers with Clk856. The exact strategy used for each gene is annotated in Table S5. Maximum neuron numbers were presented in each image. Note at the bottom right corner is category ID of CCT drivers in Rao Lab fly stock library.

1093 “f” denotes female fly brain, otherwise male brain is shown.

1094

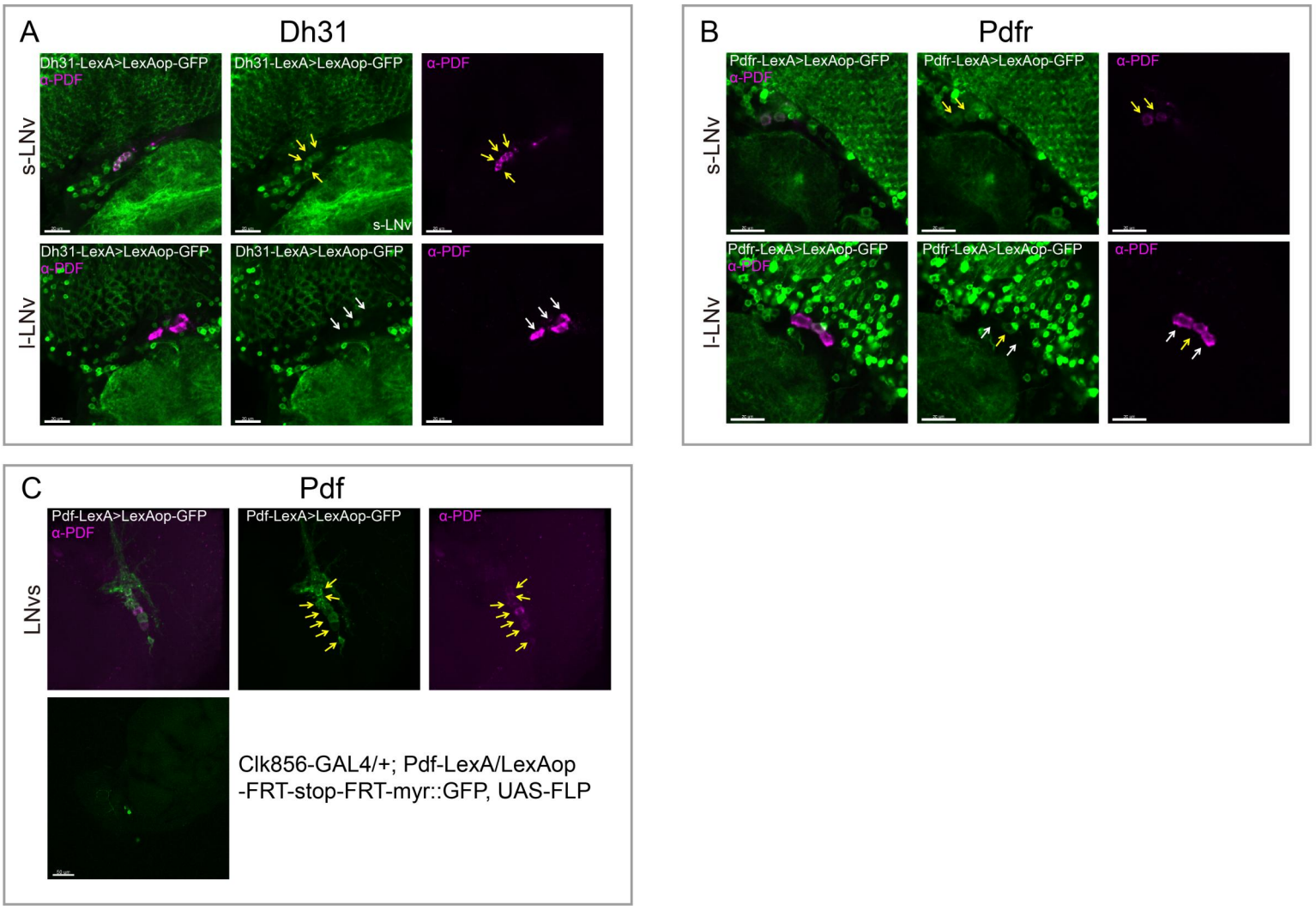

Fig. S9 Colocalization analyse of Dh31, Pdfr, and Pdf -KI-LexA with LNvs

LNvs are labels by anti-PDF. Yellow arrow heads indicate KI-LexA (Green, A, B) colocalized with anti-PDF (violet, A, B, C) and white arrow heads indicate KI-LexA did not colocalized with anti-PDF. (C) Pdf-KI-LexA labels all PDF positive LNvs but only scattered signal observed when intersect with CLK856-GAL4.

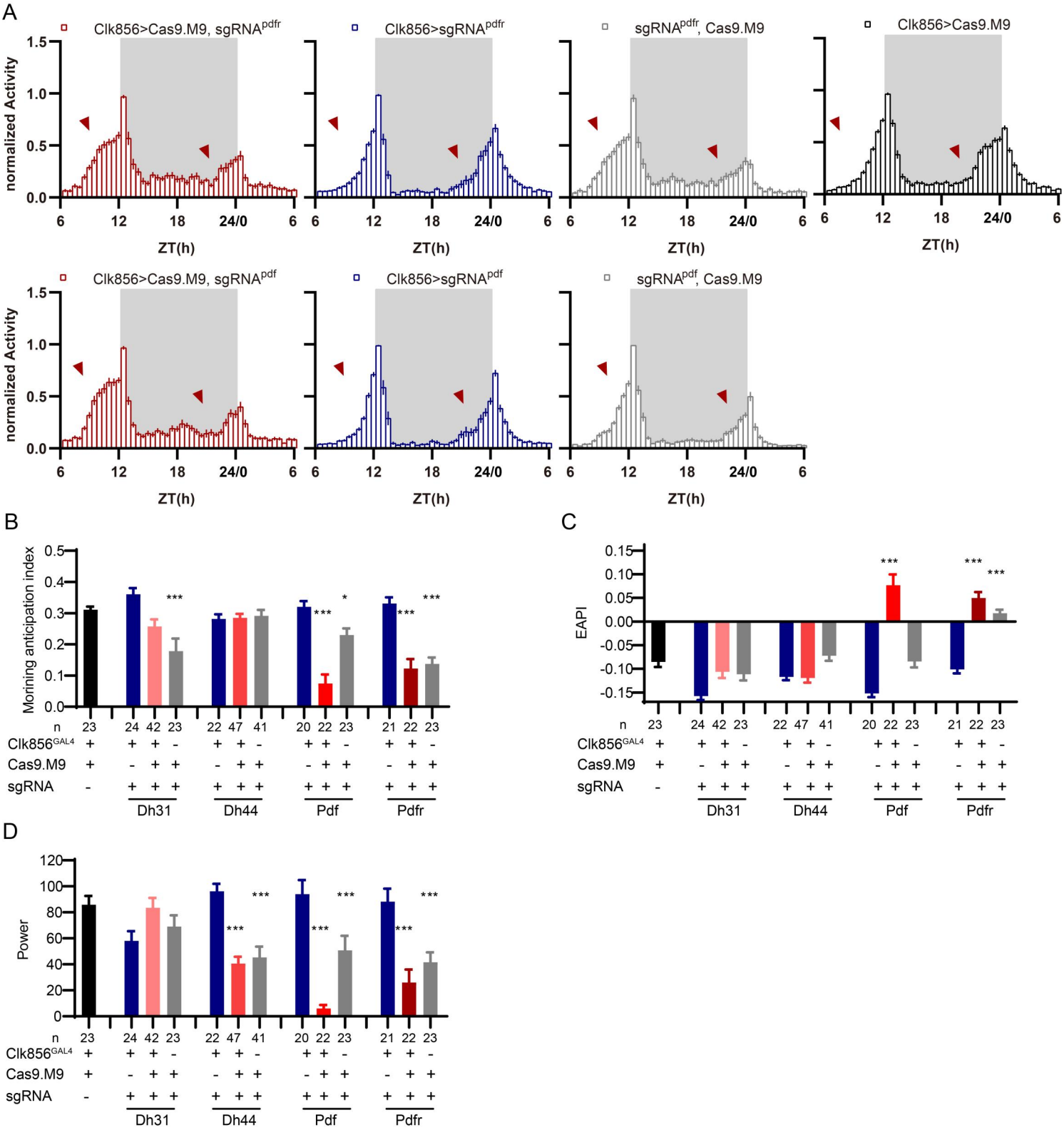

Fig. S10. Disruption of CCT Genes due to Leaky Expression of Cas9.M9

(A) Activity plots of Pdfr or Pdf clock-neuron knockout flies (red) and control groups (blue, black, and gray). (B-D) Statistical analyses of morning anticipation index (B), EAPI (C) and power (D) after CCT genes were knockdown by Cas9.M9/sgRNAs. Leakage expression of Cas9.M9 and sgRNAs might disrupt target genes at certain levels (grey bar). Cas9.M9 denotes UAS-Cas9.M9. sgRNA denotes UAS-sgRNA.

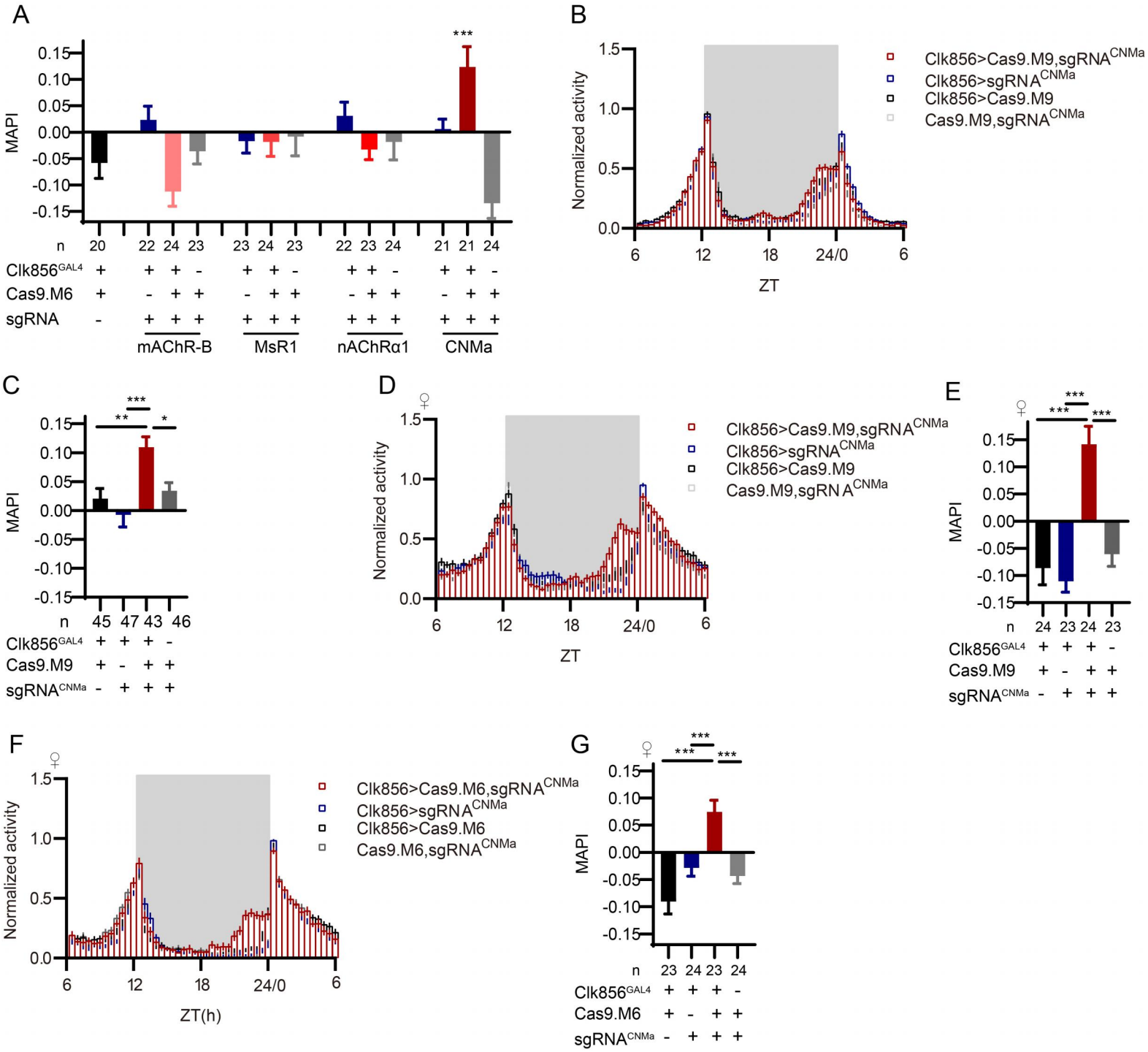

Fig. S11. Morning Activity Advanced by Loss of CNMa

(A) MAPI statistical analyses after mAChR-B, MsR1, nAChRα1 and CNMa knockout in clock neurons. Only the CNMa knockout in clock neurons increased MAPI significantly. (B-E) Activity plots (B, D) and statistical analyses (C, E) of male (B, C) and female (D, E) flies with CNMa knockout in clock neurons. Both male and female flies showed advanced morning activity patterns B, C) and increased MAPIs (D, E). UAS-sgRNA^{CNMa}/UAS-Cas9.M9 flies showed a slightly increased MAPI which indicate possible leakage expression. (F-G) Activity plots (F) and

1119 statistical analyses (G) of female flies with CNMa deficient in clock neurons with Cas9.M6 used.

1120

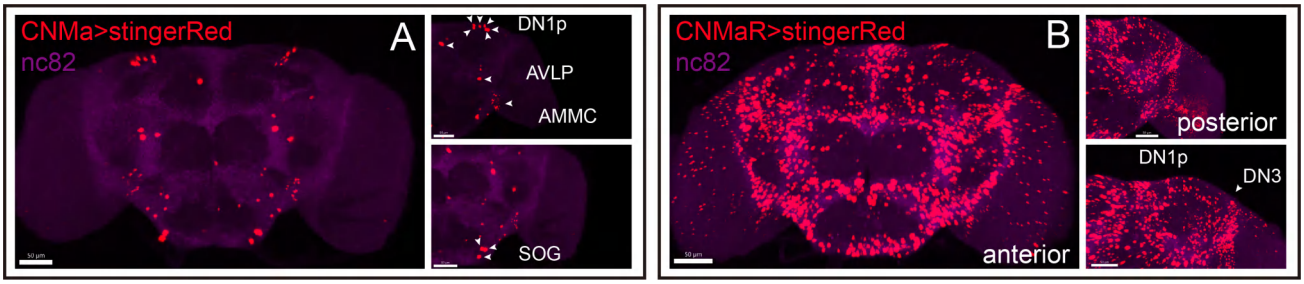

Fig. S12. Expression of CNMa and CNMaR

(A-B) Stinger::Red labeled neurons in brain driven by CNMa-KI-GAL4 (A) and CNMaR-KI-GAL4 (B)

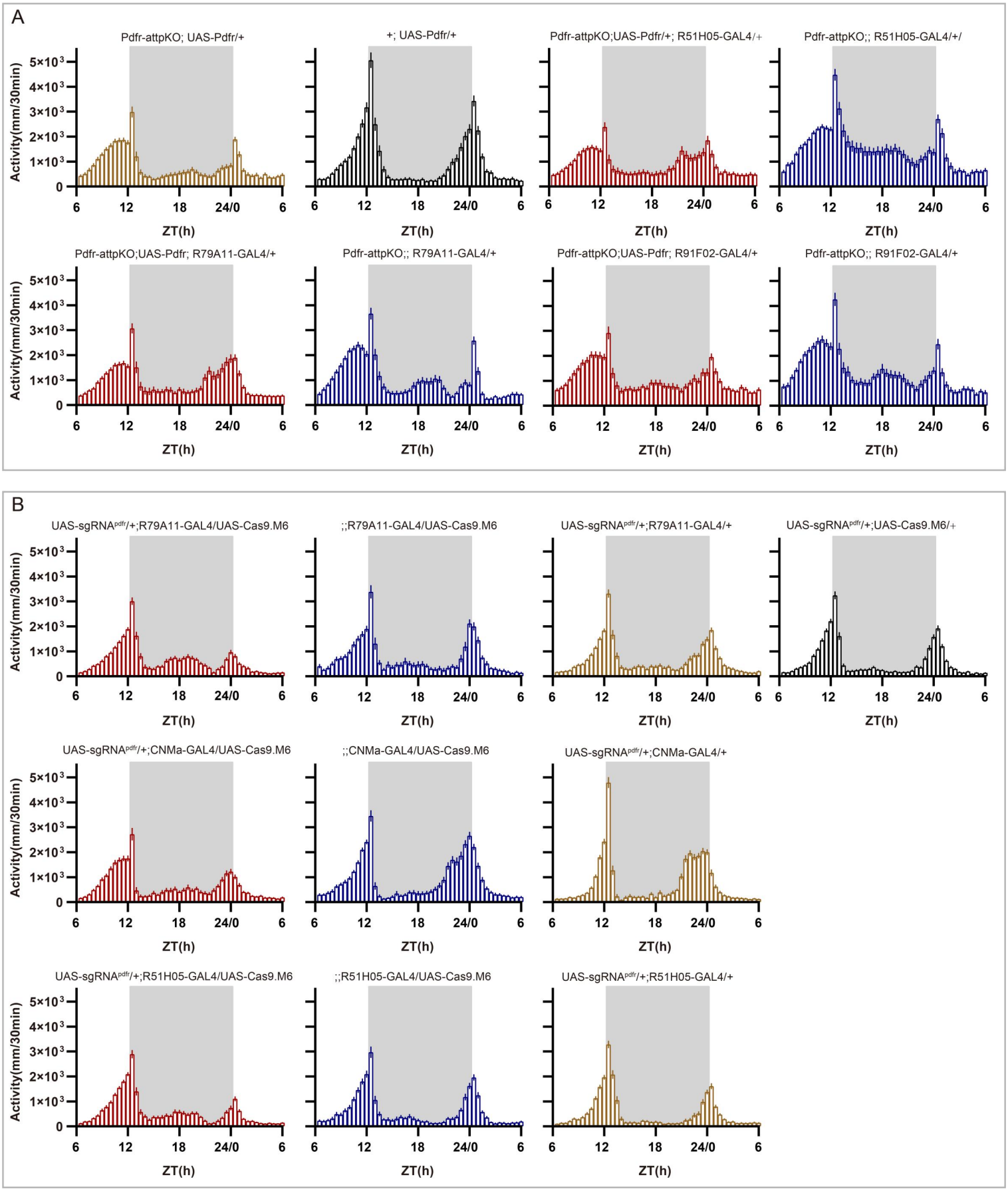

Fig. S13.Activity plots related to Fig 6

(A-B) Activity plots of reintroducing Pdfr (A, related to Fig 6Q) or mutating Pdfr (B, related to Fig 6T) in DN1p subset neurons. 30 min per bin is plotted.

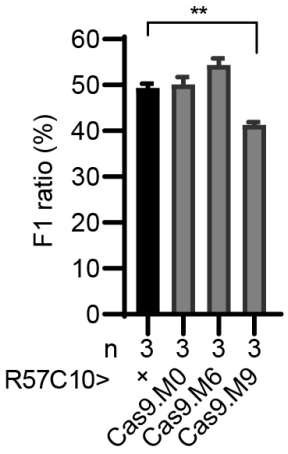

Fig. S14. Impact on Viability of Cas9 Variants Expression by GMR57C10-GAL4

F1 ratio of UAS-Cas9 variants (male) cross GMR57C10-GAL4/cyo (virgin female). Expression of Cas9.M9 decreased progeny viability slightly.

** $p < 0.01$. Two-student test was used.

Table S1 cCCT Knockin fly list

cCCT NO.	CG number	Gene Symbol	cCCT NO.	CG number	Gene Symbol
CCT1002C	CG11325	AkhR	CCT1087C	CG42244	Octβ3R
CCT1003C	CG14375	CCHa2	CCT1088C	CG7411	Ort
CCT1004C	CG14593	CCHa2-R	CCT1089C	CG1543	TβH
CCT1007C	CG6936	mth	CCT1093C	CG13968	sNPF
CCT1008C	CG31147	mthl11	CCT1097C	CG15520	Capa
CCT1009C	CG17084	mthl9	CCT1098C	CG4910	CCAP
CCT1010C	CG6496	Pdf	CCT1099C	CG11318	CG11318
CCT1011C	CG8784	PK2-R1	CCT1102C	CG13229	CG13229
CCT1012C	CG13687	Ptth	CCT1103C	CG15556	CG15556
CCT1013C	CG14734	Tk	CCT1107C	CG30340	CG30340
CCT1014C	CG6515	TkR86C	CCT1108C	CG32447	CG32447
CCT1016C	CG13633	AstA	CCT1109C	CG33639	CG33639
CCT1019C	CG3302	Crz	CCT1110C	CG33696	CNMaR
CCT1020C	CG10698	CrzR	CCT1111C	CG34411	Lgr4
CCT1021C	CG2902	Nmdar1	CCT1113C	CG43795	CG43795
CCT1024C	CG32540	CCKLR-17D3	CCT1114C	CG44153	CG44153
CCT1025C	CG33517	D2R	CCT1117C	CG12345	Cha
CCT1026C	CG13094	Dh31	CCT1118C	CG13936	CNMamide
CCT1027C	CG32843	Dh31-R	CCT1119C	CG8380	DAT
CCT1028C	CG18090	Dsk	CCT1120C	CG9887	dVGLUT
CCT1029C	CG6440	Ms	CCT1121C	CG5400	Eh
CCT1030C	CG43745	MsR2	CCT1122C	CG18105	ETH
CCT1034C	CG13480	Lk	CCT1123C	CG5911	ETHR
CCT1035C	CG10626	Lkr	CCT1124C	CG2346	FMRFa
CCT1036C	CG4128	nAChR α6	CCT1126C	CG15274	GABA-B-R1
CCT1037C	CG33976	Octβ2R	CCT1128C	CG14994	gad1
CCT1039C	CG14358	CCHa1	CCT1129C	CG8442	GluRIA
CCT1040C	CG30106	CCHa1-R	CCT1130C	CG43743	GluRIB
CCT1041C	CG13575	CG13575	CCT1131C	CG6992	GluRIIA
CCT1042C	CG13995	CG13995	CCT1133C	CG4226	GluRIIC
CCT1043C	CG33495	Dup99B	CCT1134C	CG18039	GluRIID
CCT1044C	CG31720	mthl15	CCT1135C	CG31201	GluRIIE
CCT1047C	CG1147	NPFr	CCT1136C	CG14723	HisCl1
CCT1050C	CG16752	SPR	CCT1137C	CG13586	ITP
CCT1051C	CG14871	Trissin	CCT1138C	CG7665	Lgr1
CCT1052C	CG34381	TrissinR	CCT1143C	CG8985	MsR1
CCT1053C	CG16720	5-HT1A	CCT1145C	CG32853	mthl12
CCT1055C	CG12073	5HT7	CCT1147C	CG30018	mthl13
CCT1056C	CG14919	AstC	CCT1148C	CG17795	mthl2
CCT1057C	CG14575	CapaR	CCT1149C	CG6536	mthl4
CCT1058C	CG33344	CCAP-R	CCT1150C	CG6965	mthl5
CCT1059C	CG13579	CG13579	CCT1151C	CG16992	mthl6

CCT1060C	CG31760	CG31760	CCT1152C	CG7476	mthl7
CCT1061C	CG32547	CG32547	CCT1153C	CG32475	mthl8
CCT1062C	CG18314	DopEcR	CCT1156C	CG32538	nAChR α7
CCT1065C	CG3454	HDC	CCT1158C	CG34388	natalisin
CCT1066C	CG4395	hec	CCT1159C	CG3441	Nplp1
CCT1068C	CG6456	Mip	CCT1161C	CG15361	Nplp4
CCT1070C	CG6530	mthl3	CCT1164C	CG13565	Orcokinin
CCT1071C	CG5610	nAChR α1	CCT1165C	CG15284	Pburs
CCT1072C	CG6844	nAChR α2	CCT1166C	CG31660	pog
CCT1073C	CG2302	nAChR α3	CCT1167C	CG7105	Proc
CCT1074C	CG11348	nAChRβ1	CCT1168C	CG6986	Proc-R
CCT1075C	CG6798	nAChRβ2	CCT1169C	CG10537	Rdl
CCT1076C	CG6919	oa2	CCT1170C	CG8930	rk
CCT1078C	CG7395	sNPF-R	CCT1172C	CG5811	RYa-R
CCT1079C	CG11895	stan	CCT1174C	CG33527	SIFa
CCT1080C	CG9122	TRH	CCT1175C	CG10823	SIFaR
CCT1081C	CG1056	5-HT2A	CCT1176C	CG3171	Tre1
CCT1082C	CG42796	5HT2B	CCT1177C	CG7431	TyrR
CCT1083C	CG9753	AdoR	CCT1179C	CG8394	vGAT
CCT1084C	CG18208	Octα2R	CCT1183C	CG5621	Grik
CCT1085C	CG18741	DopR2	CCT1186C	CG8681	clumsy
CCT1086C	CG32476	mthl14	CCT1189C	CG12344	CG12344

Table S2 cCCT knockin strategy can't rescue all knockout phenotype

CG No.	Gene Symbol	attP KO phenotype	cCCT phenotype
CG15520	Capa	lethal	viable
CG12345	ChAT	lethal	viable
CG5400	Eh	lethal	viable
CG5911	ETHR	lethal	viable
CG10537	Rdl	lethal	viable
CG14575	CapaR	lethal	lethal
CG14994	gad1	lethal	lethal
CG18039	GluRIID	lethal	lethal
CG33976	Octβ2R	sterile	fertile
Rescue Rate		6/9	

Table S3 C-cCCTomics sgRNAs list

CCTsgEF No.	CG No.	Spacer + PAM	CCTsgEF No.	CG No.	Spacer + PAM
CCT1001sgEF	CG1171	GGCCAGCAGCATGAAGAGCACGG	CCT1108sgEF	CG32447	GATGGCCCCCAAACTAGCGCAGG
CCT1001sgEF	CG1171	TTGACCTTCTCGCCGGATTGGGG	CCT1108sgEF	CG32447	TGGGTGGACACTATACTGGGCGG
CCT1001sgEF	CG1171	TGCAATGAGGACTTCGCTCTTGG	CCT1108sgEF	CG32447	CACGCCCCGTCGGAGTTCAGGGG
CCT1002sgEF	CG11325	GTATCTGTCCAGCTACGTGATGG	CCT1109sgEF	CG33639	TCCCTCAGCGATTCCGTCCGCGG
CCT1002sgEF	CG11325	ACACGGTGATGGACAATCGGTGG	CCT1109sgEF	CG33639	GCCCAGATAAAGCTCCAGGTGGG
CCT1002sgEF	CG11325	CTTGGTCAGCAGATACAGCACGG	CCT1109sgEF	CG33639	CCGTCTTCAGCAGCGACCTGAGG
CCT1003sgEF	CG14375	ACTGGTCGTTATCTGCACCGTGG	CCT1110sgEF	CG33696	TGTATTGTATTCCGTGACATTGG
CCT1003sgEF	CG14375	TTTCGCTTGGCTCTGTTGCGCGG	CCT1110sgEF	CG33696	CTGCTCCGTCTGGTTTGTGGTGG
CCT1003sgEF	CG14375	TCAGAGGGATGCCAGGCCTACGG	CCT1110sgEF	CG33696	AGTGAGCGACACCTGCTTCCTGG
CCT1004sgEF	CG14593	ACGGTGACAATGTACGTCTCCGG	CCT1111sgEF	CG34411	GCCGGAACACTTCTTCCCCGAGG
CCT1004sgEF	CG14593	GCCGTCGCTATCCGCCAGCCTGG	CCT1111sgEF	CG34411	ACTGTGCCGTTGTATTGCAGTGG
CCT1004sgEF	CG14593	CTCCTGCTCCAGACCTTGTCCGG	CCT1111sgEF	CG34411	CTAAGCTCTCTGCTCCTAACGGG
CCT1005sgEF	CG4313	GATGCACGGCACCATGAAGGCGG	CCT1113sgEF	CG43795	GGAGAGCTCATTCGTGACGGCGG
CCT1005sgEF	CG4313	GATCAGGAAAAGGTCAGCCTGGG	CCT1113sgEF	CG43795	AATGCGACCGAGAGCGCCCGTGG
CCT1005sgEF	CG4313	GATCGCAGGACGACCCTTTGTGG	CCT1113sgEF	CG43795	GGAACCTGTCCTGAGCATACCGG
CCT1006sgEF	CG6371	AGCAGGTAATAGGTCAGTGGCGG	CCT1114sgEF	CG44153	GGTATGCTAAAGGCACGCCATGG
CCT1006sgEF	CG6371	GGCACGTCAAAAGCGCGCCATGG	CCT1114sgEF	CG44153	CCTCGGTGAGCGTGAAGACGCGG
CCT1006sgEF	CG6371	TTGCACACTGCTGCTAATCGCGG	CCT1114sgEF	CG44153	CGAAATAAACGAGACTACGCAGG
CCT1007sgEF	CG6936	GCCATCAATTACCGGTCAGACGG	CCT1115sgEF	CG7497	TTTGCATAGAGCGCTTTCGGAGG
CCT1007sgEF	CG6936	GACCTACCGATGCCGTGTGACGG	CCT1115sgEF	CG7497	ATGCATTGCAGCAGTTATGGCGG
CCT1007sgEF	CG6936	TATCCATGATATGGTCGTGAGGG	CCT1115sgEF	CG7497	CCACTCGGATGAACGACTGCAGG
CCT1008sgEF	CG31147	AATGAATAGTGTCTCTCGCAGGG	CCT1116sgEF	CG8216	GTTTGCGTCAGCACATACGGCGG
CCT1008sgEF	CG31147	GCAAACTGAAGACATGCATCCGG	CCT1116sgEF	CG8216	GATGCGGACGCCGCGAGCGAGGG
CCT1008sgEF	CG31147	TAGTTCTTACCGGTACTTGTCGG	CCT1116sgEF	CG8216	CTGGGCCTTGACGAATACCTGGG
CCT1009sgEF	CG17084	GCTCCACGTGAGTGGACTCGCGG	CCT1117sgEF	CG12345	AGGCAGTTCTCGGCTCCCCAGGG
CCT1009sgEF	CG17084	TGAGTATTGCTTTAGCCCGTTGG	CCT1117sgEF	CG12345	GGCCGACTATATCCGCGCCCTGG
CCT1009sgEF	CG17084	CACTACTCCAGCGTATGAGTAGG	CCT1117sgEF	CG12345	TTGAACAGGCCTATTACTACTGG
CCT1010sgEF	CG6496	GTTGCGCTTCCTGATGGGCACGG	CCT1118sgEF	CG13936	GATTGGACCGGGAGACGCCATGG
CCT1010sgEF	CG6496	CCTCGACTGGTTCAACAACGTGG	CCT1118sgEF	CG13936	GAGCAACAGATCCCTCAGCGAGG
CCT1010sgEF	CG6496	TGGCGCCGCAGTATCCCCACTGG	CCT1118sgEF	CG13936	CACAGGCTCGGCGATAATGGAGG
CCT1011sgEF	CG8784	GTATTAAGTCGGAAACCGCCAGG	CCT1119sgEF	CG8380	GACGAGCGCGAAACATGGAGCGG
CCT1011sgEF	CG8784	GATACATATCCGGATACCAAAGG	CCT1119sgEF	CG8380	CTTACGATTGTGCTGACCCAGGG
CCT1011sgEF	CG8784	GCTCGCATTTGTGCCGTTCGTGG	CCT1119sgEF	CG8380	GGTGCTGATAGCCTTCTATGTGG
CCT1012sgEF	CG13687	GAGTCTGGAACACCGCGCGGAGG	CCT1120sgEF	CG9887	CACGAAGAGATGCAGCGTGGCGG
CCT1012sgEF	CG13687	GCCATTGCCATAATGGAAATGGG	CCT1120sgEF	CG9887	TCTGACGGCGTTTAAGGAGAAGG
CCT1012sgEF	CG13687	GTACATGGGCGGCAGCTGATGGG	CCT1120sgEF	CG9887	TCATGATCGCCTTCGGCATGAGG
CCT1013sgEF	CG14734	GCTGACGGCACCATCGAGTGCGG	CCT1121sgEF	CG5400	GTGCGTATAATGACTTATGGCGG
CCT1013sgEF	CG14734	CATCCAATGCGCCCTCTGAGCGG	CCT1121sgEF	CG5400	TTTCTTGCAGACTCCATGGGTGG
CCT1013sgEF	CG14734	GCCCGCTTTACCACCCGACGCGG	CCT1121sgEF	CG5400	CTTGATTTTGTGCACCTTTGTGG
CCT1014sgEF	CG6515	ATTGTGAACACCACGCTCCTGGG	CCT1122sgEF	CG18105	TGCTCACTGCGTCCTATGCGAGG
CCT1014sgEF	CG6515	CAACGTCACGGTCTCTACGTCGG	CCT1122sgEF	CG18105	ACCAAGAACGTACCGCGGCTGGG
CCT1014sgEF	CG6515	CAAGACCGTACGAGTTGCCATGG	CCT1122sgEF	CG18105	CTGTCTGTTTCGCTCTTGGTGGG

CCT1015sgEF	CG7887	ATGGTCATTGTGGCGACGGGCGG	CCT1123sgEF	CG5911	GACTATGCAGAAGAACATGGCGG
CCT1015sgEF	CG7887	GTCTTCCACGTCCCCGACGGCGG	CCT1123sgEF	CG5911	CACGCCCACCGTCCTCGTGGAGG
CCT1015sgEF	CG7887	GTTGAAGGTGACGTTCAGGCTGG	CCT1123sgEF	CG5911	CATCTCGTGGCCAAGTACCCAGG
CCT1016sgEF	CG13633	GACGAGATGGCCGACAACGGTGG	CCT1124sgEF	CG2346	ACTTCATGCACTTCGGCAAGAGG
CCT1016sgEF	CG13633	GCAGTAGGAGGTGGGCGTGAAGG	CCT1124sgEF	CG2346	CGATGCCAATCACAGAGATGGGG
CCT1016sgEF	CG13633	CAGCTCCCCGGTAATTGGCCAGG	CCT1124sgEF	CG2346	GGCCGACTGCATCTGGTACAGGG
CCT1017sgEF	CG2872	CGAATGATCCGTGTGTTCCGAGG	CCT1125sgEF	CG2114	AATCGTCCTTAACCACACGGAGG
CCT1017sgEF	CG2872	GACGAACAGAATGTCCGAGACGG	CCT1125sgEF	CG2114	AGAACAATCGCATTGAGTTCTGG
CCT1017sgEF	CG2872	TTGTGGATACGATCCGTTCGAGG	CCT1125sgEF	CG2114	TGGATTGGCCCGCTGTGATACGG
CCT1018sgEF	CG10001	ACTGGCCATATGGAAGGTTCTGG	CCT1126sgEF	CG15274	GGATCTCGAGAATCGATGCATGG
CCT1018sgEF	CG10001	GATTACGAACATCAGATCAGCGG	CCT1126sgEF	CG15274	GCCTGCCGCAAGACTGGCGTTGG
CCT1018sgEF	CG10001	AAGAAGAATCCCACTATCCACGG	CCT1126sgEF	CG15274	TGCAGGATGAGCTTGAAGCCCGG
CCT1019sgEF	CG3302	TCTTGCCGTTGGTCCATCCGCGG	CCT1127sgEF	CG6706	GGCGTGGAAAACTCCTACACCGG
CCT1019sgEF	CG3302	GAAGGTCTGGCCCATGCACATGG	CCT1127sgEF	CG6706	GAAGGACGTGAGGATCATTCTGG
CCT1019sgEF	CG3302	CCATCCGCGGGAGTACTGGAAGG	CCT1127sgEF	CG6706	TCTACGTAATACATCCTTCGAGG
CCT1020sgEF	CG10698	CTCCCCGATAATGCAGAACCAGG	CCT1128sgEF	CG14994	CGAGTAATGGCACTGATCCGAGG
CCT1020sgEF	CG10698	TGGTGCTTCATGGCGACTATTGG	CCT1128sgEF	CG14994	ACGGGTATAAACTGTCCGAGAGG
CCT1020sgEF	CG10698	GGTCAGCAATTGGTCCACACTGG	CCT1128sgEF	CG14994	GCTTCATGTCCTCGGGATGGTGG
CCT1021sgEF	CG2902	AATGGTGACCGAATCTACGCCGG	CCT1129sgEF	CG8442	GCCAAAGCCAGAACGCAGGGGGG
CCT1021sgEF	CG2902	ACGAGAGTACTCGATCGTGACGG	CCT1129sgEF	CG8442	GTACACCTACGGAGAATCATTGG
CCT1021sgEF	CG2902	GAATCCGCTTGTATAACTCACGG	CCT1129sgEF	CG8442	ATCGATACCATCCAGTACTACGG
CCT1022sgEF	CG33513	GGACGGGGACCTGCGCTCGGCGG	CCT1130sgEF	CG43743	ATTCGTCCGGATACAGACCTCGG
CCT1022sgEF	CG33513	CACTGTTAACAAGCTCCATGAGG	CCT1130sgEF	CG43743	GCCGTGCAGCTTCTCACCAAAGG
CCT1022sgEF	CG33513	GGAGGCCTACCTAACGGATCCGG	CCT1130sgEF	CG43743	GGGGAACCAGGGCGTCACGAAGG
CCT1023sgEF	CG42301	AGCTGTAACCGTCAGGACACCGG	CCT1131sgEF	CG6992	AAGCTTGCTAATGAGATCCACGG
CCT1023sgEF	CG42301	GCTCGGCGTATTCTGCATGCCGG	CCT1131sgEF	CG6992	TCTGCACTACAAGAGTCCTCCGG
CCT1023sgEF	CG42301	CTTAGGTCGGGATTGAGTGTCGG	CCT1131sgEF	CG6992	ACGCGAGAGTACTGACAAGGAGG
CCT1024sgEF	CG32540	GTAGTCGAGCAGTGCCCTATAGG	CCT1132sgEF	CG7234	CCTTAATCCGTATAATGCCGAGG
CCT1024sgEF	CG32540	TGGACTTGAACTGGTGCCCAGGG	CCT1132sgEF	CG7234	GCATCCCCAGCAGTCGAACAGGG
CCT1024sgEF	CG32540	GAGCAGGAACACGTTGGTTATGG	CCT1132sgEF	CG7234	AGTCATATTATATCCAATCGAGG
CCT1025sgEF	CG33517	CTACAATGGGAGCACGGTTTCGG	CCT1133sgEF	CG4226	GCTGCGTTATCTGACCCCGAGGG
CCT1025sgEF	CG33517	ACGGTGGCGCGCGAGACGCTGGG	CCT1133sgEF	CG4226	CCTCTATCAAGGATATGCCGTGG
CCT1025sgEF	CG33517	AGCACAAACTTGGCGGTGACGGG	CCT1133sgEF	CG4226	AATGACCCTTAACCTCTACCCGG
CCT1026sgEF	CG13094	GGGATATTCGGGTACCCAGGAGG	CCT1134sgEF	CG18039	GATCACCTAATGACCCGATACGG
CCT1026sgEF	CG13094	CTTGGCCATCTCGAGCATCGAGG	CCT1134sgEF	CG18039	GGATGCAGATTGAAACCATCCGG
CCT1026sgEF	CG13094	GCTTTGGACGCACCATCATACGG	CCT1134sgEF	CG18039	GTCATTGCCACCGTCGCGGAAGG
CCT1027sgEF	CG32843	GAGGTCTTCGAGATTTACGCAGG	CCT1135sgEF	CG31201	GAGTGTTTGGACCCTCGTCGCGG
CCT1027sgEF	CG32843	GTCCGGGCAGAGTTCGTAGGCGG	CCT1135sgEF	CG31201	CCGGCGGGTTCGAAAGTCCGTGG
CCT1027sgEF	CG32843	TCGCTGCCAATAACTCGTTGTGG	CCT1135sgEF	CG31201	TCGCATGTAATTCTTGAAGGAGG
CCT1028sgEF	CG18090	GACTAGTCTACAGAACGCTAAGG	CCT1136sgEF	CG14723	GATTTGCGTGTCATGCGGATAGG
CCT1028sgEF	CG18090	CATTCTCTCTATTCGGGGACAGG	CCT1136sgEF	CG14723	CCAGGGAGAGGACCGTGACATGG
CCT1028sgEF	CG18090	CACGCTGTTTATGCCACTCTGGG	CCT1136sgEF	CG14723	GGCAATATATTTGCACGCGCTGG
CCT1029sgEF	CG6440	CAGTTGATCGGAGTTCTCCAGGG	CCT1137sgEF	CG13586	CCGACTGGACCGCATCTGCGAGG
CCT1029sgEF	CG6440	TCCTGGCCGTGTCCAACACACGG	CCT1137sgEF	CG13586	TTCTTCGACCTGGAGTGCAAGGG

CCT1029sgEF	CG6440	GCTTGTTGTAGTTCTTCAACAGG	CCT1137sgEF	CG13586	CCACCGAGATCTTTATGTTGCGG
CCT1030sgEF	CG43745	ATGCCGGTGCCGCAATAATGCGG	CCT1138sgEF	CG7665	CGATGTCTACCCCAATCTCACGG
CCT1030sgEF	CG43745	GGCAGTTTGGCGGTACATAGCGG	CCT1138sgEF	CG7665	CTGCTGCTAACGTCGCTGAGTGG
CCT1030sgEF	CG43745	CTCGCGGCAGCCTTACACTGAGG	CCT1138sgEF	CG7665	AGCACCCGAGTCTGTCCCAGCGG
CCT1031sgEF	CG8348	GTTCCATCCGGGTAGTCCAGAGG	CCT1139sgEF	CG31096	GTGACCTCCGAACTGAGACGCGG
CCT1031sgEF	CG8348	GCTGTCCATTGTCAATCCGCTGG	CCT1139sgEF	CG31096	GGTCATCAGACAGAAGCCTACGG
CCT1031sgEF	CG8348	GGCCGTGCAGACGAGCCTTGTGG	CCT1139sgEF	CG31096	TAGAGGAGACCGCACTCCACCGG
CCT1032sgEF	CG8422	CTGCACAACCTAGATGGCATCGG	CCT1140sgEF	CG7918	TGTATCATTCTTACGGTGGGCGG
CCT1032sgEF	CG8422	GCCACTATCGTTGCCATAGGTGG	CCT1140sgEF	CG7918	CAAGCGAGTCCTGACGCACACGG
CCT1032sgEF	CG8422	AGGGTACCGCGAGCTGTCCTCGG	CCT1140sgEF	CG7918	GCTCAAGGGTTATTGGGACCTGG
CCT1033sgEF	CG12370	GCTGTTGACACTGTAGCGTGCGG	CCT1141sgEF	CG11144	GTTGAGGCCGGTGATACTTGAGG
CCT1033sgEF	CG12370	AGACGACGATTTGAGGGCACTGG	CCT1141sgEF	CG11144	GCGACCAAACGACTGAGACAAGG
CCT1033sgEF	CG12370	TAGTGATCCCACGTTCCGTTTGG	CCT1141sgEF	CG11144	CAAAAGAAGCCTAACGCTCGCGG
CCT1034sgEF	CG13480	CAGCGATTCCACTCGTGGGGCGG	CCT1142sgEF	CG4322	TATCCAATACGGAAACATAGGGG
CCT1034sgEF	CG13480	GGCTGGCTCCATAGACTTGACGG	CCT1142sgEF	CG4322	GGCCCTGCTGAAATGTCCCAAGG
CCT1034sgEF	CG13480	GGTGGGGCGTAGTGCCGGAAGGG	CCT1142sgEF	CG4322	GGAGGACGGCTATCCCCCCCTGG
CCT1035sgEF	CG10626	GGAATTCCTGCCCGGAGCCGAGG	CCT1143sgEF	CG8985	GATATTCAAGGTATTCGCGATGG
CCT1035sgEF	CG10626	TACACTCAGGGCCTGGACGAAGG	CCT1143sgEF	CG8985	GAAACTGAGCCGCTCTACTGCGG
CCT1035sgEF	CG10626	CTATGGGGGAATCAGTATCGTGG	CCT1143sgEF	CG8985	GATGTAGTCGTGTATGGTGTAGG
CCT1036sgEF	CG4128	GTGCTCTTGAAGATACCAGGGGG	CCT1144sgEF	CG17061	GCACAGCGAGGAGTAACCCACGG
CCT1036sgEF	CG4128	CAATACGCTGGAGCGACCCGTGG	CCT1144sgEF	CG17061	CCTGGAGGATCCCTATACTGCGG
CCT1036sgEF	CG4128	AACGGAATACGGCGGGGTCAAGG	CCT1144sgEF	CG17061	GAACGGATCCATGCTCCGTGTGG
CCT1037sgEF	CG33976	GCCCGGAGCCACCGCGGCAAAGG	CCT1145sgEF	CG32853	GCTGACGGATCCAACTTTAGCGG
CCT1037sgEF	CG33976	AACATTGGCGCGGGTCACGGCGG	CCT1145sgEF	CG32853	TCTTTATCCCGAAATCTACTCGG
CCT1037sgEF	CG33976	CAACATCGTTTGGGTGTTCAAGG	CCT1145sgEF	CG32853	GAAATTCCTGCCAACCTGACCGG
CCT1038sgEF	CG13758	TCTACGCCATGAAAGCCGCCAGG	CCT1147sgEF	CG30018	ACTCGATGATAATTCGACAGAGG
CCT1038sgEF	CG13758	GCATCGAAATCGTGCAGTAGTGG	CCT1147sgEF	CG30018	CTTGTGTGATATAATCCATATGG
CCT1038sgEF	CG13758	GACGCAAGCGTTAGATTCCAGGG	CCT1147sgEF	CG30018	TATGGATGAACTACGATTGTTGG
CCT1039sgEF	CG14358	GCTCATGGCAAGCGGTCCGGCGG	CCT1148sgEF	CG17795	GATACCGTTGATATCTCGGAAGG
CCT1039sgEF	CG14358	GAATACGGACATTCGTGTTGGGG	CCT1148sgEF	CG17795	GGTGCAAAGGCACTATAAGAAGG
CCT1039sgEF	CG14358	TCAGGTTCCTGCCTGGAATACGG	CCT1148sgEF	CG17795	TCATTAGCTTCTTAACGCACAGG
CCT1040sgEF	CG30106	GAGACACCCTACGTGCCCTACGG	CCT1149sgEF	CG6536	GTGATTGCAGTCATGATTAGCGG
CCT1040sgEF	CG30106	CATCCTTCATGAACTCCGACAGG	CCT1149sgEF	CG6536	GCATACAACTTATACGCCTGGGG
CCT1040sgEF	CG30106	TTCGCATCTGTCGCACACTGAGG	CCT1149sgEF	CG6536	GACTAAACTTAATCCGCAAGTGG
CCT1041sgEF	CG13575	GCTCGAGTTGTACCTAGAATGGG	CCT1150sgEF	CG6965	CCGATGTTCACCAGCTATGGAGG
CCT1041sgEF	CG13575	CCAGTGAGATGAGGCAGGCCCGG	CCT1150sgEF	CG6965	ACCAGTCATGTCACTAGCGCCGG
CCT1041sgEF	CG13575	CCCTCGATCCAGCCGTATCCGGG	CCT1150sgEF	CG6965	TGGCCAATATACCACTATGCTGG
CCT1042sgEF	CG13995	TCTAGGCAATCCGTATGACGTGG	CCT1151sgEF	CG16992	GAATTCGGATCTTCCAAACGGGG
CCT1042sgEF	CG13995	TTGCCATAGTCGTAGTCCGCGGG	CCT1151sgEF	CG16992	GATTAGCTCCTCGTACGCATAGG
CCT1042sgEF	CG13995	GAGGGCGAGATGCAGCTCCGCGG	CCT1151sgEF	CG16992	GAAGGTTGTTTCGGTACAGGAGG
CCT1043sgEF	CG33495	CTAAACTTAGGACCCTACCTCGG	CCT1152sgEF	CG7476	TGAGTGGTACTCGTGCCTGTAGG
CCT1043sgEF	CG33495	AGGATCGAAATGATACGGAGTGG	CCT1152sgEF	CG7476	CTAAGGATCCAGGAGATATGTGG
CCT1043sgEF	CG33495	ACGACCAAGAGGAGAAATAGCGG	CCT1152sgEF	CG7476	GTGTCGTAGTAGTTGCACCCGGG
CCT1044sgEF	CG31720	GGTTCCATCGATCTTGCAATAGG	CCT1153sgEF	CG32475	GCAAACATAACGGGGAGCTACGG

CCT1044sgEF	CG31720	TACGAATACTCAGTACTGCGTGG	CCT1153sgEF	CG32475	GAGGCAGTGCTTAGTCCCTGTGG
CCT1044sgEF	CG31720	AAACGTAAATAAATCCCTGTGGG	CCT1153sgEF	CG32475	GATGGTCTACCTTATGTGTTCGG
CCT1045sgEF	CG30361	ATGCACCGCGACCTGTGCGGCGG	CCT1154sgEF	CG12414	ACATCTGTCGTATTAACAACAGG
CCT1045sgEF	CG30361	AGTACACCGAGGGCGAGCTGCGG	CCT1154sgEF	CG12414	AATATAATAATACCGTGCATGGG
CCT1045sgEF	CG30361	CATCCACTTCAAGCAGTCCCAGG	CCT1154sgEF	CG12414	TTGGCAGTTGGACTTATGATGGG
CCT1046sgEF	CG10342	GCCGGCGGCTAGGAGGGCAAGGG	CCT1155sgEF	CG32975	CGTGCTGATGTACAACAGTGCGG
CCT1046sgEF	CG10342	TTGACATCGTTCTTTCGCGGAGG	CCT1155sgEF	CG32975	AATACTGAACTCATTGTCGCTGG
CCT1046sgEF	CG10342	GACAGAGCCCGCGTTCGGTTCGG	CCT1155sgEF	CG32975	GTCATTGCTTCTACCGTGGTTGG
CCT1047sgEF	CG1147	TGGACCCGGTGCTTATCGATAGG	CCT1156sgEF	CG32538	ATCTCGTTCTATCCTGACCAGGG
CCT1047sgEF	CG1147	GCTGATGAGCATGTGGTACCAGG	CCT1156sgEF	CG32538	TTGGTTCGTGGACCTACGATGGG
CCT1047sgEF	CG1147	GCGTGCGCTATCTGGACGACCGG	CCT1156sgEF	CG32538	TGGAGTAGCCGCTTCTCATGGGG
CCT1048sgEF	CG13061	AGAGGAGATCCGACAACGGTGGG	CCT1157sgEF	CG11822	GGACGCGGGTGTGTAGATGACGG
CCT1048sgEF	CG13061	CAGAGGAGAAGGATGCACCTGGG	CCT1157sgEF	CG11822	GATCGGCTCCTGGGGCCTGAAGG
CCT1048sgEF	CG13061	GATCAAGAGCGTCCATGGCCTGG	CCT1157sgEF	CG11822	AGTTCGTGAACAGGCCGGCGTGG
CCT1049sgEF	CG8795	GGTGTCATCGGGGTCACCGTGGG	CCT1158sgEF	CG34388	AGGCGGCCTTGAGCCACCAACGG
CCT1049sgEF	CG8795	AAATCATGTCGGATATAGCGAGG	CCT1158sgEF	CG34388	GGAGGAGCTGGCCCCAGAATCGG
CCT1049sgEF	CG8795	GGAGAGCGTTCTCTCGGAAACGG	CCT1158sgEF	CG34388	GCTGGCCCCAATACCGATGAGGG
CCT1050sgEF	CG16752	GATCCGCGTCAGATGGTCCGCGG	CCT1159sgEF	CG3441	GCACTCACAATAATGGACCGTGG
CCT1050sgEF	CG16752	GGCATACAGTAGCCATAGAGCGG	CCT1159sgEF	CG3441	GGAGGAGGACAAACGTTCGGTGG
CCT1050sgEF	CG16752	GCTCAAAACGAGCACAATCAGGG	CCT1159sgEF	CG3441	GAAGCTGGTACTCGGGACTGGGG
CCT1051sgEF	CG14871	TTATGGCCTGCGAACTGGGGGGG	CCT1160sgEF	CG11051	GAATTCGTTGAAATCACCCTGGG
CCT1051sgEF	CG14871	GTAGTTAAAGCAGCATGTGCTGG	CCT1160sgEF	CG11051	CAGGATTGGATTCCTCACGGGGG
CCT1051sgEF	CG14871	TGACTAAGACAACGATGCATTGG	CCT1160sgEF	CG11051	GTCCGCCCGCGTCCCCCGTGAGG
CCT1052sgEF	CG34381	TCCGTCCCCCGAGAGTCCGGTGG	CCT1161sgEF	CG15361	GATTGGGGCGGGATTGGCACGGG
CCT1052sgEF	CG34381	CCACCGGACAACAACCGCCCCGG	CCT1161sgEF	CG15361	CTAGCTCCGTAGTAGTACTGGGG
CCT1052sgEF	CG34381	AGTGGACAAACTGGTACATGCGG	CCT1161sgEF	CG15361	AGCAAACAACATGTTCAAGCTGG
CCT1053sgEF	CG16720	GGAGCGGAATCTACAAAACGTGG	CCT1162sgEF	CG3856	GATGAACTCGAGTACGGCCAGGG
CCT1053sgEF	CG16720	GGCCACCAGATGCAAAATCGAGG	CCT1162sgEF	CG3856	GGCCAAACCCACCAGAAGATCGG
CCT1053sgEF	CG16720	TGGTCCTGACCATCTACATTCGG	CCT1162sgEF	CG3856	TCTCTGGTGCCGCATTTGGCTGG
CCT1054sgEF	CG15113	TGGTCGATGACGAACAAGAGCGG	CCT1163sgEF	CG7485	GGCGGCGGCTCTAACCGCTGCGG
CCT1054sgEF	CG15113	TCTATTTCCAAAATGCTCGCTGG	CCT1163sgEF	CG7485	ACTCAATGCCGCGGTAACGGTGG
CCT1054sgEF	CG15113	AATGGCCACCAGGTGCAGTATGG	CCT1163sgEF	CG7485	CAACGTGGCTTACTCGATCCTGG
CCT1055sgEF	CG12073	CAGCTGGATAGCCTATGCGGCGG	CCT1164sgEF	CG13565	GCGTTAAGAGAATTGTGTAACGG
CCT1055sgEF	CG12073	GCAAATTCCTCCAGGAGCAAAGG	CCT1164sgEF	CG13565	GGAACACCGATACCACCGCCAGG
CCT1055sgEF	CG12073	TCCGTCTCGCCTTCCACGAGCGG	CCT1164sgEF	CG13565	CATTCACGCAGCGCCCGGTGTGG
CCT1056sgEF	CG14919	GGTCCTGTTTCGGCACCCGAAGG	CCT1165sgEF	CG15284	GAACTGCGAGACTCTCAAGTCGG
CCT1056sgEF	CG14919	CCTCGCTGAGGGCAAAGAACAGG	CCT1165sgEF	CG15284	AGGGCATTGCGATATAGCCAAGG
CCT1056sgEF	CG14919	GACGTGCGAGGCGCCTATGGAGG	CCT1165sgEF	CG15284	GCATTGGGGCACTAGGATCGCGG
CCT1057sgEF	CG14575	TCCTCTCCAAATCCATGGGATGG	CCT1166sgEF	CG31660	CGATGAGCCGACACGTGCGGAGG
CCT1057sgEF	CG14575	GGTCTGTGGTCCAAGCACAAAGG	CCT1166sgEF	CG31660	TGTGTCCGCTCTCAGTCGGGCGG
CCT1057sgEF	CG14575	TAAGAGATTACCAACGACCCCGG	CCT1166sgEF	CG31660	CAACATTATCCGAATCCACTAGG
CCT1058sgEF	CG33344	TGCGATATCACACGTGATGCTGG	CCT1167sgEF	CG7105	GCTGTGGAAGTGGACACAGGTGG
CCT1058sgEF	CG33344	GGACGCCAGCCCCGAGGATTCGG	CCT1167sgEF	CG7105	GCGACCTTGTCGGCAGGTAACGG
CCT1058sgEF	CG33344	GTCAAATTCGCCGGGGTCGCTGG	CCT1167sgEF	CG7105	CTCCACAATGAGGCCACCGGTGG

CCT1059sgEF	CG13579	GTATGTAGGCCGCATAGCGGCGG	CCT1168sgEF	CG6986	AGTCCAATAACAAAAACGCACGG
CCT1059sgEF	CG13579	GGAAAGCGCCCCTCGGAGCAGGG	CCT1168sgEF	CG6986	GTAGAGCTTGAAATGATACTTGG
CCT1059sgEF	CG13579	TGACAGAAGATCTCTCCGTATGG	CCT1168sgEF	CG6986	GATTAACTGGCACGTCAGGTAGG
CCT1060sgEF	CG31760	GATAGGGCTCCGCCTCGCATTGG	CCT1169sgEF	CG10537	GGTGTAGAAACACTATCGGTTGG
CCT1060sgEF	CG31760	GCCCACTTCCTGGAGTATCGAGG	CCT1169sgEF	CG10537	ACGGATCCATACAGTGCAAGCGG
CCT1060sgEF	CG31760	GTCCTACGTCTGGTGGGTCAAGG	CCT1169sgEF	CG10537	TTTGTCGTAACTAACACTAAAGG
CCT1061sgEF	CG32547	GTAGGGCGAGAGCTGCGTACTGG	CCT1170sgEF	CG8930	GAAAACCTCCCAGGTCCAGGAGG
CCT1061sgEF	CG32547	GTTGACATGGAGCGACTTAGTGG	CCT1170sgEF	CG8930	AAGTCCTTGCAGGAATACCATGG
CCT1061sgEF	CG32547	CAGATTGATGATGAACGCATGGG	CCT1170sgEF	CG8930	GCGCAGGGTAGAAAAGGTCCTGG
CCT1062sgEF	CG18314	GCAGGAAATGAGCTACCTACAGG	CCT1171sgEF	CG40733	AGAAAGAAATGCTCGTTTCGAGG
CCT1062sgEF	CG18314	GTAGTAGTTGATCACCTCTGTGG	CCT1171sgEF	CG40733	TTCTTTCTTGGCTCTCGGTACGG
CCT1062sgEF	CG18314	TATCGGTATACACCTTCATGTGG	CCT1171sgEF	CG40733	AGGTACGATGAAAATGCGTCTGG
CCT1063sgEF	CG9652	GGATGTTTCCGGCCACCGAAAGG	CCT1172sgEF	CG5811	CGACTATGACCTTCTATCGGAGG
CCT1063sgEF	CG9652	AATCACACCAGTGGGAGCACCGG	CCT1172sgEF	CG5811	GACCGTGCGCATGCGAGGTGTGG
CCT1063sgEF	CG9652	CGTCGAGCACATGACATCAAAGG	CCT1172sgEF	CG5811	GACGATGAAGGGTCCAACTATGG
CCT1064sgEF	CG3022	ATACGGTCCATGGCCGGCCGTGG	CCT1173sgEF	CG4545	GAGAGGACTCGCGAGACCTGGGG
CCT1064sgEF	CG3022	CGTCCGTTTGTACTTCCAATCGG	CCT1173sgEF	CG4545	GGGATTCGAGCGGCCCGTCGTGG
CCT1064sgEF	CG3022	GGCCCTTGCCTGGGCAACGTCGG	CCT1173sgEF	CG4545	TGGACTGCCCCTGTTCTACATGG
CCT1065sgEF	CG3454	CTATATGCGCCAGTTACTGCCGG	CCT1174sgEF	CG33527	AAGATGCTGCCGTTGAACGGAGG
CCT1065sgEF	CG3454	GACAGTACTCACCCCTTTGGCGG	CCT1174sgEF	CG33527	GCTCCAGTGAGGCAGCCTACAGG
CCT1065sgEF	CG3454	GCAGGCCGGCGAGCTCGCCCAGG	CCT1174sgEF	CG33527	CTGCGACCAGGATCGTGACCAGG
CCT1066sgEF	CG4395	TGACTCAGCACAGTGCCGGCCGG	CCT1175sgEF	CG10823	GCTGGGCACGGTTCTCACTACGG
CCT1066sgEF	CG4395	GCGGCATTCTCCAGATATCGCGG	CCT1175sgEF	CG10823	CCATTCCGACCATGGCGCCGGGG
CCT1066sgEF	CG4395	CCAGAATGTCACATACGATACGG	CCT1175sgEF	CG10823	GTAGGCCACGCAGTAGACCATGG
CCT1067sgEF	CG4356	CGGGCTATACGATCCCTATTCGG	CCT1176sgEF	CG3171	ATGCGGGTAGATCGATTGCGTGG
CCT1067sgEF	CG4356	GCCAATGCCAGACTCATGACCGG	CCT1176sgEF	CG3171	ACATTGCCATAGAAGATCACCGG
CCT1067sgEF	CG4356	AGCCAGGTGTCGCAGACGATGGG	CCT1176sgEF	CG3171	GCTCAAGAGCCCCACGATACGGG
CCT1068sgEF	CG6456	CTATGGCTCACACTAAGACGCGG	CCT1177sgEF	CG7431	GTAGGAGGTGGATATCCCAGCGG
CCT1068sgEF	CG6456	CCACCCTCTAATGAACCAGGAGG	CCT1177sgEF	CG7431	GTAGAAGTGCGCCCATTCGGCGG
CCT1068sgEF	CG6456	ACGGCAACAATAAGCGCGCCTGG	CCT1177sgEF	CG7431	GAAGATGCCCACGAGAAGGTCGG
CCT1069sgEF	CG4521	GGATCCTCCAGAGCATTGATCGG	CCT1178sgEF	CG16766	GGCGTGTGGTCAGAACGGCGAGG
CCT1069sgEF	CG4521	GCATGGTGATAGCAAGCGTATGG	CCT1178sgEF	CG16766	CAGACCAGTGCGGCACCAGGTGG
CCT1069sgEF	CG4521	GGCAGCTATCAGACTAGCTACGG	CCT1178sgEF	CG16766	GGATGGAGCCGCTGCAGAGCAGG
CCT1070sgEF	CG6530	GCCGCTAAATGAATTCCAGAGGG	CCT1179sgEF	CG8394	CATTCCGGAACGCCGGTAGCTGG
CCT1070sgEF	CG6530	GAAATATCCCAGGAACAAGGAGG	CCT1179sgEF	CG8394	AAAGACTACGAGCAACCGCCGGG
CCT1070sgEF	CG6530	CATTTAGCGGCAACTCCAGCTGG	CCT1179sgEF	CG8394	CCTTCAATGAGTACGACGGCAGG
CCT1071sgEF	CG5610	GCAGAAGGATTTGTAAATGGCGG	CCT1180sgEF	CG3822	GCGAGGTCACCAGGTAGCTATGG
CCT1071sgEF	CG5610	GACCGTCTCACCGTCAAGATGGG	CCT1180sgEF	CG3822	GGACATTGTCGAGCTCACTCCGG
CCT1071sgEF	CG5610	ACTACTACATCTCCGTGGAGTGG	CCT1180sgEF	CG3822	TCCCCACTTGGAGAATCGCTGGG
CCT1072sgEF	CG6844	GTGACGCCGCCATACTCCGAGGG	CCT1182sgEF	CG5549	ATAGACGGCCACGGGACCCAGGG
CCT1072sgEF	CG6844	GGATACGGTTCGGCACAGCAGGG	CCT1182sgEF	CG5549	TCGCTGCTCGGATACTCAGTGGG
CCT1072sgEF	CG6844	TCGCCTGAACGGTTTCGCAGAGG	CCT1182sgEF	CG5549	AGGCGTGGTCTGCCCCTCTACGG
CCT1073sgEF	CG2302	GAGCTCCTGCGAAATCGACGTGG	CCT1183sgEF	CG5621	GATGCTCATCGCGTGACGGGCGG
CCT1073sgEF	CG2302	GTCCGGACGCCAGATGTGATCGG	CCT1183sgEF	CG5621	GGTCTCCTTTAGCATGCCATAGG

CCT1073sgEF	CG2302	TTCGACGGACGTATAGAACTCGG	CCT1183sgEF	CG5621	CAAACCGAATGGGTCCCGTGAGG
CCT1074sgEF	CG11348	GGCTTCCAAACCTTGTCGGGGGG	CCT1184sgEF	CG7446	GATCCGGGGCCGATGGACCAGGG
CCT1074sgEF	CG11348	ATGTGATGTCAGTCTCCGTGGGG	CCT1184sgEF	CG7446	GGTGGCTCGGGGTCGACCACCGG
CCT1074sgEF	CG11348	ATAACGGCCCTTGCCCGAAAGGG	CCT1184sgEF	CG7446	CGTCGGATGTCATCTACCGTTGG
CCT1075sgEF	CG6798	GGAGTATTACCCCGATACACTGG	CCT1185sgEF	CG7589	GTCTTTCCAGTCGATCATAGCGG
CCT1075sgEF	CG6798	TTCTCCCGTATACTTCAGAGTGG	CCT1185sgEF	CG7589	GATCATCTCCACGCGCATGCAGG
CCT1075sgEF	CG6798	ACTTGCACTAGGTTACTGCCAGG	CCT1185sgEF	CG7589	TCGTAGTGTTGTGCCAGAACTGG
CCT1076sgEF	CG6919	GACCACGTCTTCAACGGATACGG	CCT1186sgEF	CG8681	GGTCGAGGCCAACATAACTACGG
CCT1076sgEF	CG6919	TTCGTCAAGTGTTTCATTATTGG	CCT1186sgEF	CG8681	TTTATTGTATCCTCACGCCTGGG
CCT1076sgEF	CG6919	TAATGCTTCCGTCATGATCTCGG	CCT1186sgEF	CG8681	ACAGTAAAACAACTGGGGCCGGG
CCT1077sgEF	CG9918	GGCCGTAATCGTTAGCACCGTGG	CCT1187sgEF	CG9935	GAACTTCTCCGTGAAATGACCGG
CCT1077sgEF	CG9918	GGCCATCGTGATACCCGTAACGG	CCT1187sgEF	CG9935	GGGCAGACCGGCCTATGTTTGGG
CCT1077sgEF	CG9918	CCTGCGGAACGCCCGACAACAGG	CCT1187sgEF	CG9935	CCAGCCTGGAATGTATAACTCGG
CCT1078sgEF	CG7395	GGACATTTCCGAAGACACCCAGG	CCT1188sgEF	CG11155	TCTTCTTTAACCATAACATACGG
CCT1078sgEF	CG7395	ATGGCACAGACTCCTGCCGAAGG	CCT1188sgEF	CG11155	ATCATTCCAGGTTTGGTCGGAGG
CCT1078sgEF	CG7395	CAACTGGAGCCTAACGTCGCCGG	CCT1188sgEF	CG11155	CTAGCTAAAAGAGCATCTGTTGG
CCT1079sgEF	CG11895	GTCTCCGTGAATCACAAGGATGG	CCT1189sgEF	CG12344	TTAGGCGGAAGAACTACTCGCGG
CCT1079sgEF	CG11895	TTTAAGGTAGATTCCAGGACAGG	CCT1189sgEF	CG12344	CTACGTGACGCTGCTTCCAGAGG
CCT1079sgEF	CG11895	GAGATCCGTCGATGCAGGGCGGG	CCT1189sgEF	CG12344	CGAAGCGGAAGTATACGGTGAGG
CCT1080sgEF	CG9122	GTTTCCCACCTGGTTACGCAGGG	CCT1190sgEF	CG32848	GGGCTATCGATACAATCACGAGG
CCT1080sgEF	CG9122	CTACACTTCCGTGAACACGCAGG	CCT1190sgEF	CG32848	CCCGTGATATTATCCCTCAACGG
CCT1080sgEF	CG9122	CAGGCCCAGAAGACTCTTCCCGG	CCT1190sgEF	CG32848	TCGACGGCAGTCTTTGCTTGTGG
CCT1081sgEF	CG1056	TTTCTGGACTACAGTCCCCACGG	CCT1191sgEF	CG7535	GCCTTCGTATAGGAAACGGGCGG
CCT1081sgEF	CG1056	ACTGTTGCGATGGCCGTACGAGG	CCT1191sgEF	CG7535	GAGCAGATCTGTCTATCCAGCGG
CCT1081sgEF	CG1056	ATGCAAAGCTACTCTGGTCGTGG	CCT1191sgEF	CG7535	AAAGTATCTGACCCTGACGGAGG
CCT1082sgEF	CG42796	GCACCTGGTCCTGTGGGAGGAGG	CCT1192sgEF	CG17336	GAGGCGCTGATAGACTCCAGTGG
CCT1082sgEF	CG42796	CATCCAGGCAGATCCAGGTGAGG	CCT1192sgEF	CG17336	GTAGTGCAGATCCATCATGCAGG
CCT1082sgEF	CG42796	TCGTCCTGGGAACAGCGGCCGGG	CCT1192sgEF	CG17336	GTATTGGCGCGACGAGCGTTTGG
CCT1083sgEF	CG9753	GTTTCTGGGTAGTCCCATGGAGG	CCT1194sgEF	CG11236	ACTGGCAACACCATTAACCCCGG
CCT1083sgEF	CG9753	GGTGTAGGGTATGTTCAGCTCGG	CCT1194sgEF	CG11236	TGGGGTCCGTACCTTCTGGGCGG
CCT1083sgEF	CG9753	GGCGTCGCAACTTTCTTTCCCGG	CCT1194sgEF	CG11236	CATAAAGGTGACGATCATATCGG
CCT1084sgEF	CG18208	CGTCTTCTCGACCGGAAAGCCGG	CCT1195sgEF	CG12338	CTCCTTCTGGAGTTCTAAGGCGG
CCT1084sgEF	CG18208	TCGCTGGCCAATGAGCTAATGGG	CCT1195sgEF	CG12338	TAGTGGCATAGGGCAAGAAGAGG
CCT1084sgEF	CG18208	CGAATCACACAGAAGTCCACTGG	CCT1195sgEF	CG12338	ATCCCAGTAGTTGAAGGCATCGG
CCT1085sgEF	CG18741	AGGAGCCGGCGCGCCCCTCCTGG	CCT1196sgEF	CG4827	GGTGCCCTTCCTAAATGCCGTGG
CCT1085sgEF	CG18741	CCGTGTGCAAGTACCGCTCCCGG	CCT1196sgEF	CG4827	GAATCCCATTGCACCCCGGGCGG
CCT1085sgEF	CG18741	CCTCCTGTTGCCACCATCGCAGG	CCT1196sgEF	CG4827	GTTCCGAAAGGCAAGCACCTTGG
CCT1086sgEF	CG32476	AGACAACCCGTTAGATCCGGCGG	CCT1197sgEF	CG30104	TATCGTAAGGAGGCTCAGGAGGG
CCT1086sgEF	CG32476	GCAAATAACTAACTAATAGCAGG	CCT1197sgEF	CG30104	TCAGTTGGGGAACCTTGCTTAGG
CCT1086sgEF	CG32476	CAACGAATCATACACTGTGAAGG	CCT1197sgEF	CG30104	TGGCCACTCGGGTTATTTGAAGG
CCT1087sgEF	CG42244	CATTGCGGTGGATAACCAGGCGG	CCT1198sgEF	CG8129	GGCCATGCGAATGTCCCGCGAGG
CCT1087sgEF	CG42244	GCCTATAACATCGCAATTTGTGG	CCT1198sgEF	CG8129	ATCTATTAGCGGCATTGCGGTGG
CCT1087sgEF	CG42244	AACGCCTCCGTGGAACTGTCCGG	CCT1198sgEF	CG8129	TTTAACGGCTGTGGCAATACCGG
CCT1088sgEF	CG7411	GGAATACCGCCTGCTCGAGGTGG	CCT1199sgEF	CG3011	GGCCTGGATCTGCCCGATGGCGG

CCT1088sgEF	CG7411	GGGGCGTTGTTGGATCCCACTGG	CCT1199sgEF	CG3011	AGGGATATCCCGGCAAGAGGTGG
CCT1088sgEF	CG7411	GTTCACCCTTAAGCGTCGTTTGG	CCT1199sgEF	CG3011	GTCTCCGGGTTCACTTTGTACGG
CCT1089sgEF	CG1543	GGTGAGACGGGACTACCAGCAGG	CCT1200sgEF	CG13317	GCCGCTGATACCCACGCCGGAGG
CCT1089sgEF	CG1543	CAATGTGACGGCACCGCACGAGG	CCT1200sgEF	CG13317	TTTTGTTGCGCCGTGTCAGTCGG
CCT1089sgEF	CG1543	TGTGATGATGATAAGCCAGTTGG	CCT1200sgEF	CG13317	AGTTGACAACTCACCGCTCGCGG
CCT1090sgEF	CG10118	GGAGTCCCGTCAGTCGCGCGTGG	CCT1201sgEF	CG14049	GATATGCGTAAGCGGAACGGTGG
CCT1090sgEF	CG10118	GAGGCGTGCTTGGGGAACCACGG	CCT1201sgEF	CG14049	TATCACATCGCTGAGGCCGGTGG
CCT1090sgEF	CG10118	ATCCCGCCGTCGCAGCCTGGTGG	CCT1201sgEF	CG14049	GGCCACCTTGTTCGCCGTGGCGG
CCT1091sgEF	CG7285	TGTCCTCCAGTTTGTGAAAGGGG	CCT1202sgEF	CG14059	GTGCGAGCACCTCTTTCAGGCGG
CCT1091sgEF	CG7285	GCTATGCAATGTTGATAGGTGGG	CCT1202sgEF	CG14059	ACTCGATGGACCTTCTGTCGCGG
CCT1091sgEF	CG7285	ATATATCCTGAATCTGGCGGTGG	CCT1202sgEF	CG14059	CATCGGAGTCTGTTGCCTGATGG
CCT1092sgEF	CG13702	CATACTGAATCTGGCTATCGCGG	CCT1203sgEF	CG14167	CTACTAATCCTTATGATCGGCGG
CCT1092sgEF	CG13702	TGTAGCTGTACGAACAGTCCGGG	CCT1203sgEF	CG14167	GCGGCCGCACAACTTCATGGTGG
CCT1092sgEF	CG13702	GTCCAGGTGGGGTCGCACACTGG	CCT1203sgEF	CG14167	GTAGGAGTAGGCTAGGTAGCAGG
CCT1093sgEF	CG13968	TTATCATAGAGATTGCTCAGGGG	CCT1204sgEF	CG14173	CCCGGAAACCACAAACTCTGCGG
CCT1093sgEF	CG13968	GATGCAGCAGCCCGCCCAGGCGG	CCT1204sgEF	CG14173	TGCAGGATGATAGCAGCATGTGG
CCT1093sgEF	CG13968	ACTGAGTCAAGGCTGCGCCTTGG	CCT1204sgEF	CG14173	GCATGTGGCAGACACTGGACGGG
CCT1094sgEF	CG11937	TACAACGCGTCGCCGCAACGCGG	CCT1205sgEF	CG14920	AAATCTCCTCCGGCTGACTGGGG
CCT1094sgEF	CG11937	TTCGGCTCTCTCTCTTCGGCTGG	CCT1205sgEF	CG14920	AGAAGTTGCACAAGTCTTGCCGG
CCT1094sgEF	CG11937	TTCGAAAGGTAGCGCAGCACTGG	CCT1205sgEF	CG14920	AGCCGGAGAGGTGACATTGCCGG
CCT1096sgEF	CG13419	GCTCCGCCACGAGAACAACAAGG	CCT1206sgEF	CG17673	TCCAGGCCTGGGAATGGCCGTGG
CCT1096sgEF	CG13419	TCAAATACCATTATCCGTGGCGG	CCT1206sgEF	CG17673	TTTGTAGGCTTCCTATTCCACGG
CCT1096sgEF	CG13419	CAGCATTCTGAAACTCTGCACGG	CCT1206sgEF	CG17673	ACTCGGCTTGGTCCAGGCCTGGG
CCT1097sgEF	CG15520	GACCACGACAAGAACCGACGAGG	CCT1207sgEF	CG17878	CATTGGCCAACGCTCACCACTGG
CCT1097sgEF	CG15520	GAAGGCATAGAGCCCCATGTTGG	CCT1207sgEF	CG17878	CAGTTGAGAAGACCCCATCTCGG
CCT1097sgEF	CG15520	ATCGCCGAATTCAGTACAGCTGG	CCT1207sgEF	CG17878	ACTCAATGGGAAAGGACGCTTGG
CCT1098sgEF	CG4910	CGTCCATGAGGATTTCCCTGAGG	CCT1208sgEF	CG33273	GGAGAACTGGGATCACGGAGCGG
CCT1098sgEF	CG4910	AGCTAAGTGGCGTTATACAATGG	CCT1208sgEF	CG33273	TCAGCATGTCCATCAAGGCGGGG
CCT1098sgEF	CG4910	GAACAACGAGGGCACCAATATGG	CCT1208sgEF	CG33273	AGCTATCCAAATCCGCCAAGTGG
CCT1099sgEF	CG11318	GTACGTTTCCACTCCAGTAGTGG	CCT1209sgEF	CG40041	TATACGTGTATACACGACGATGG
CCT1099sgEF	CG11318	TATGAAACCTGGTCAACTGAGGG	CCT1209sgEF	CG40041	GTTGGGACTATGTAAGCGTTTGG
CCT1099sgEF	CG11318	TGGAGAGGAACGTAATTCATCGG	CCT1209sgEF	CG40041	CGCTGGGCGTGGACACAAACAGG
CCT1100sgEF	CG12290	GCAGTCCCAGGAACAAAGTGGGG	CCT1210sgEF	CG6736	GATTTACACGCCGTGTCAGGCGG
CCT1100sgEF	CG12290	CTCCGTGGGTAAGCTCTCAAAGG	CCT1210sgEF	CG6736	CGGCTGCAGTAACTGCGACACGG
CCT1100sgEF	CG12290	GGGATCCGTAACGGCACACCAGG	CCT1210sgEF	CG6736	GTGCGGCGAGGCTCTGATCCAGG
CCT1101sgEF	CG12796	GATTGGAGATGACCGATCGCAGG	CCT1211sgEF	CG8167	CTGCAGTGAAAAGCTCAACGAGG
CCT1101sgEF	CG12796	GAGCTTCGATAATCCCAAGCGGG	CCT1211sgEF	CG8167	GAAGGACAAAGGCTTGCTCATGG
CCT1101sgEF	CG12796	CAGCAGGCAGGGACCTCTCATGG	CCT1211sgEF	CG8167	GCGCGCTTGTGTGGAATCACGGG
CCT1102sgEF	CG13229	TGTCGTTGAAAGGAACCCGCTGG	CCT1212sgEF	CG17777	TATGGACACGGTCACTACGGCGG
CCT1102sgEF	CG13229	AGATTTGAGCTACACCTGGGCGG	CCT1212sgEF	CG17777	CGTCTTCTTCTCATCCACGGCGG
CCT1102sgEF	CG13229	TTCCAGCATCACAAACATATCGG	CCT1212sgEF	CG17777	CGCCGTAGCCGCCATAGCCGTGG
CCT1103sgEF	CG15556	GGATCACGTGACCTGTAGGTCGG	CCT1213sgEF	CG45777	CGTGTCTTGGGCGAGCACGGAGG
CCT1103sgEF	CG15556	TATGAGACCTGGCTTAGCGATGG	CCT1213sgEF	CG45777	GGAGGCGAGTGCCGTGCCCACGG
CCT1103sgEF	CG15556	TGAGTCGGAACGATGTACTCTGG	CCT1213sgEF	CG45777	GGAGCGTTGCTAAAGGAAGCGGG

CCT1104sgEF	CG15614	GATGCAGTCCATCCACGAAAGGG	CCT1214sgEF	CG34136	GAAGAATGCAAGGCACAGTAGGG
CCT1104sgEF	CG15614	TCACCAGCTCAGAATCCGGTTGG	CCT1214sgEF	CG34136	GAATGAGGTGAGCGGAAGACAGG
CCT1104sgEF	CG15614	AAAGTTCGTACACAGTCCAAAGG	CCT1214sgEF	CG34136	TTGCCCAAGCGAAGAATGCAAGG
CCT1105sgEF	CG15744	GCTCTCCCTGGGCACACCAATGG	CCT1215sgEF	CG43117	GAATTGGTCTGGGCTGAGGAAGG
CCT1105sgEF	CG15744	GCCATTAGCCACATCTATGAGGG	CCT1215sgEF	CG43117	ATCCACCAACACCACAACCACGG
CCT1105sgEF	CG15744	CGCCTGGCCCCCCTCTGCTGCGG	CCT1215sgEF	CG43117	GCAGGCAGAATCCGGCGAATAGG
CCT1107sgEF	CG30340	CTGGCTGCACAAGCCCAATGGGG			
CCT1107sgEF	CG30340	GACTACCGAGAGATTGAGCACGG			
CCT1107sgEF	CG30340	CTTCTATCAGAACTACCAGTTGG			

Table S4 CCT gene expression profile of clock neuron

	s-LNv		l-LNv		5th		LNd		LPN		DN1		DN2		DN3	
Gene symbol	GFP+	N#	GFP+	N#	GFP+	N#	GFP+	N#	GFP+	N#	GFP+	N#	GFP+	N#	GFP+	N#
AstC	/	/	/	/	/	/	1 ± 0	6	/	/	/	/	1.83 ± 0.41	6	*1 ± 0*	*1*
CCHa1	/	/	/	/	/	/	/	/	/	/	**1.6 ± 0.55**	5	/	/	/	/
ChAT	*3 ± 1.41*	*2*	/	/	/	/	**2.3 ± 1.06**	10	*1 ± 1*	*1*	***1 ± 0***	*1*	1 ± 0	10	**1 ± 0**	7
CNMa	/	/	/	/	/	/	/	/	/	/	**4 ± 1.41**	2	/	/	1 ± 0	2
Dh31	3.64 ± 0.5	11	/	/	/	/	1.2 ± 0.42	10	/	/	**3.8 ± 0.63**	10	/	/	/	/
Dh44	/	/	1.67 ± 0.58	3	/	/	**3 ± 1**	3	/	/	**5 ± 0**	3	1.67 ± 0.58	3	**1.67 ± 0.58**	3
GlyT	2.8 ± 1.64	5	3.88 ± 0.35	8	1 ± 0	3	1 ± 0	3	/	/	**1.57 ± 0.79**	7	1 ± 0	6	2 ± 0.93	8
ITP	/	/	/	/	/	/	/	/	/	/	/	/	/	/	1 ± 0	2
NPF	1 ± 0	2	/	/	/	/	**1 ± 0**	3	/	/	/	/	/	/	/	/
Nplp1	/	/	/	/	/	/	/	/	/	/	**5 ± 0**	2	/	/	**2 ± 0**	2
Proc	/	/	/	/	/	/	**1 ± 0**	12	/	/	/	/	/	/	/	/
sNPF	**4 ± 0**	7	/	/	/	/	**1.63 ± 0.52**	8	/	/	/	/	/	/	/	/
TH	1.5 ± 0.71	2	/	/	/	/	1 ± 0	2	/	/	3.5 ± 0.71	2	/	/	/	/
Trh	/	/	/	/	/	/	/	/	/	/	1.75 ± 0.5	4	/	/	/	/
Trissin	/	/	/	/	/	/	**1.82 ± 0.4**	11	/	/	/	/	/	/	/	/
VGlut	/	/	1.2 ± 0.45	5	/	/	1.17 ± 0.41	6	/	/	**3.5 ± 0.55**	6	*2 ± 0*	*1*	2.2 ± 0.45	5
CG13229	/	/	**3.5 ± 0.55**	6	*1 ± 0*	*1*	**1.5 ± 0.55**	6	/	/	/	/	/	/	1 ± 0	3
CG32547	/	/	**2.71 ± 0.95**	7	/	/	**1.86 ± 0.9**	7	/	/	**3.29 ± 1.8**	7	1 ± 0	5	/	/
CG43795	/	/	/	/	/	/	/	/	/	/	/	/	1 ± 0	6	/	/
5-HT2B	/	/	/	/	/	/	**1.62 ± 0.65**	13	/	/	/	/	*1 ± 0*	*1*	/	/
CCHa1-R	1.5 ± 0.71	2	/	/	/	/	/	/	/	/	/	/	/	/	/	/
CNMaR	/	/	/	/	/	/	/	/	/	/	/	/	/	/	15.67 ± 0.58	3
CrzR	/	/	/	/	/	/	/	/	/	/	**2 ± 0**	2	1.5 ± 0.71	2	**2.5 ± 0.71**	2
D2R	/	/	/	/	/	/	1 ± 0	6	/	/	/	/	/	/	/	/
Dh31-R	***2 ± 0***	*2*	**3.43 ± 0.53**	7	*1 ± 0*	*2*	/	/	/	/	**1 ± 0**	3	/	/	/	/
Dh44-R2	/	/	/	/	/	/	1 ± 0	6	/	/	/	/	/	/	/	/
FMRFaR	/	/	/	/	/	/	/	/	/	/	/	/	1 ± 0	6	/	/
GABA-B-R2	3.43 ± 0.53	7	3.63 ± 0.52	8	1 ± 0	4	4.29 ± 1.7	7	/	/	3 ± 0	6	*1 ± 0*	*1*	*1 ± 0*	*1*
GABA-B-R3	/	/	/	/	/	/	1 ± 0	4	/	/	/	/	/	/	/	/

GluRIB	/	/	/	/	/	/	/	/	/	/	**1.56 ± 1.01**	9	1.5 ± 0.58	4	*1 ± 0*	*2*
mAChR-B	1.33 ± 0.58	3	3.33 ± 0.87	9	/	/	1.5 ± 0.53	8	/	/	3.38 ± 2.33	8	1 ± 0	5	/	/
MsR1	/	/	**3.29 ± 0.49**	7	/	/	**1 ± 0**	7	*1 ± 1*	*1*	/	/	2 ± 0	1	/	/
nAChRα1	3 ± 0	2	/	/	/	/	**5.6 ± 0.89**	5	2 ± 1	3	**12.4 ± 1.52**	5	/	/	1 ± 0	2
nAChRα2	/	/	3.8 ± 0.45	5	*1 ± 0*	*1*	2 ± 0.89	6	/	/	2.17 ± 1.17	6	/	/	2 ± 0.71	5
nAChRβ2	/	/	3 ± 1	3	/	/	/	/	/	/	1 ± 0	2	/	/	1 ± 0	5
Nmdar1	*1 ± 0*	*2*	3.64 ± 0.5	11	/	/	1.88 ± 0.35	8	/	/	1.5 ± 0.58	4	1.11 ± 0.33	9	1.4 ± 0.84	10
NPFR	/	/	/	/	/	/	1 ± 0	10	/	/	/	/	/	/	**1.14 ± 0.38**	7
Oct-TyrR	/	/	/	/	/	/	/	/	/	/	/	/	/	/	2 ± 0	2
Octβ2R	/	/	/	/	/	/	/	/	/	/	**10.5 ± 0.71**	2	**1.5 ± 0.71**	2	2.5 ± 0.71	2
Pdfr	/	/	1.14 ± 0.38	7	/	/	***1 ± 0***	*2*	/	/	**2.29 ± 1.11**	7	1 ± 0	6	1.33 ± 0.58	3
PK2-R1	/	/	/	/	/	/	**1.5 ± 0.71**	2	/	/	/	/	1 ± 0	3	/	/
SIFaR	/	/	**3.21 ± 0.43**	14	/	/	**2 ± 0.39**	14	/	/	**1 ± 0**	5	1 ± 0	6	**1.22 ± 0.44**	9
spab	/	/	/	/	/	/	1 ± 0	4	/	/	/	/	1 ± 0	2	/	/

$N^{\#}$ represents GFP positive brain number. The largest N# number indicates total brains analyzed for certain CCT line.

/ represents no GFP found in corresponding clock neuron subset

The *italic* values indicate that the number of positive brains is less than 1/3 of the total analyzed brains

The **bolder** values (41/127) indicate that genes were also reported in transcriptome analysis (Ma et al., 2021)

Table S5 List of CCT genes intersected with Clk856 drivers

RaoLab Stock No.	CG No.	Gene Symbol	Driver	Intersection with Clk856
DKI0289	CG42796	5-HT2B	LexA	Clk856-GAL4
DKI0317	CG14919	AstC	LexA	Clk856-GAL4
DKI0292	CG43795	CG43795	LexA	Clk856-GAL4
DKI0303	CG13229	CG13229	LexA	Clk856-GAL4
DKI0073	CG13995	CG13995	LexA	Clk856-GAL4
DKI0110	CG12345	ChAT	LexA	Clk856-GAL4
DKI0254	CG32547	CG32547	LexA	Clk856-GAL4
DKI0121	CG33517	Dop2R	LexA	Clk856-GAL4
DKI0309	CG12370	Dh44-R2	LexA	Clk856-GAL4
DKI0060	CG13094	Dh31	LexA	Clk856-GAL4
DKI0105	CG32843	Dh31-R	LexA	Clk856-GAL4
WCKI1122	CG2114	FMRFaR	LexA	Clk856-GAL4
DKI0305	CG5549	GlyT	LexA	Clk856-GAL4
DKI0322	CG6706	GABA-B-R2	LexA	Clk856-GAL4
DKI0312	CG3022	GABA-B-R3	LexA	Clk856-GAL4
DKI0191	CG43743	GluRIB	LexA	Clk856-GAL4
DKI0212	CG6798	nAChRβ2	LexA	Clk856-GAL4
DKI0221	CG7918	mAChR-B	LexA	Clk856-GAL4
DKI0201	CG6844	nAChRα2	LexA	Clk856-GAL4
WCKI1173	CG8985	MsR1	LexA	Clk856-GAL4
WCKI1006	CG1147	NPFR	LexA	Clk856-GAL4
WCKI1018	CG7105	Proc	LexA	Clk856-GAL4
DKI0093	CG2902	Nmdar1	LexA	Clk856-GAL4
WCKI1089	CG10823	SIFaR	LexA	Clk856-GAL4
WCKI1080	CG8784	PK2-R1	LexA	Clk856-GAL4
DKI0059	CG13968	sNPF	LexA	Clk856-GAL4
DKI0082	CG14871	Trissin	LexA	Clk856-GAL4
DKI0248	CG9122	Trh	LexA	Clk856-GAL4
DKI0265	CG9887	VGlut	LexA	Clk856-GAL4
DKI0165	CG13586	ITP	Gal4	Clk856-p65AD
DKI0111	CG10118	TH	Gal4	Clk856-p65AD
DKI0168	CG3441	Nplp1	Gal4	Clk856-p65AD
DKI0287	CG14723	HisCl1	Gal4	Clk856-p65AD
DKI0203	CG5610	nAChRα1	Gal4	Clk856-p65AD
WCKI1015	CG10342	NPF	LexA	Clk856-GAL4
DKI0099	CG14358	CCHa1	LexA	Clk856-GAL4
WCKI1017	CG33976	Octβ2R	Gal4	Clk856-p65AD
WCKI1019	CG10698	CrzR	Gal4	Clk856-p65AD
DKI0078	CG30106	CCHa1-R	LexA	Clk856-GAL4
DKI0029	CG13936	CNMa	p65AD	Clk856-GAL4
DKI0288	CG33696	CNMaR	p65AD	Clk856-GAL4
WCKI1095	CG8348	Dh44	GAL4	Clk856-p65AD

DKI0134	CG13758	Pdfr	LexA	Clk856-GAL4
WCKI1199	CG7485	Oct-TyrR	Gal4	Clk856-p65AD
DKI0262	CG8216	spab	LexA	Clk856-GAL4
DKI0013	CG10537	Rdl	LexA	Clk856-GAL4
DKI0069	CG1056	5-HT2A	LexA	Clk856-GAL4
WCKI1162	CG10626	Lkr	LexA	Clk856-GAL4
DKI0251	CG11318	CG11318	LexA	Clk856-GAL4
WCKI1030	CG11325	AkhR	LexA	Clk856-GAL4
WCKI1201	CG1171	Akh	LexA	Clk856-GAL4
DKI0215	CG11822	nAChRβ3	LexA	Clk856-GAL4
CG11883-L-LexA	CG11883	CG11883	LexA	Clk856-GAL4
CG11883-S-LexA	CG11883	CG11883	LexA	Clk856-GAL4
WCKI1180	CG11937	amn	LexA	Clk856-GAL4
DKI0307	CG12344	CG12344	LexA	Clk856-GAL4
Nplp3-LexA	CG13061	Nplp3	LexA	Clk856-GAL4
L53-T5-W-	CG13480	Lk	LexA	Clk856-GAL4
DKI0302	CG13565	Orcokinin	LexA	Clk856-GAL4
DKI0050	CG13575	CG13575	LexA	Clk856-GAL4
DKI0160	CG13579	CG13579	LexA	Clk856-GAL4
DKI0286	CG13579	CG13579-RB	LexA	Clk856-GAL4
DKI0091	CG13633	AstA	LexA	Clk856-GAL4
DKI0096	CG14375	CCHa2	LexA	Clk856-GAL4
DKI0086	CG14575	CapaR	LexA	Clk856-GAL4
DKI0007	CG14593	CCHa2-R	LexA	Clk856-GAL4
DKI0094	CG14734	Tk	LexA	Clk856-GAL4
DKI0020	CG14994	gad1	LexA	Clk856-GAL4
DKI0089	CG15113	5-HT1B	LexA	Clk856-GAL4
DKI0187	CG15274	GABA-B-R1	LexA	Clk856-GAL4
DKI0055	CG15284	Pburs	LexA	Clk856-GAL4
Tβh-LexA	CG1543	Tβh	LexA	Clk856-GAL4
DKI0143	CG15520	Capa	LexA	Clk856-GAL4
WCKI1196	CG15614	CG15614	LexA	Clk856-GAL4
DKI0159	CG15744	CG15744	LexA	Clk856-GAL4
DKI0030	CG16720	5-HT1A	LexA	Clk856-GAL4
DKI0146	CG16752	SPR	LexA	Clk856-GAL4
DKI0156	CG16992	mthl6	LexA	Clk856-GAL4
DKI0294	CG17061	mthl10	LexA	Clk856-GAL4
WCKI1120	CG17084	CG17084	LexA	Clk856-GAL4
DKI0031	CG17795	mthl2	LexA	Clk856-GAL4
DKI0196	CG18039	GluRIID	LexA	Clk856-GAL4
DKI0148	CG18090	Dsk	LexA	Clk856-GAL4
WCKI1097	CG18208	CG18208	LexA	Clk856-GAL4
DKI0321	CG18314	DopEcR	LexA	Clk856-GAL4
DKI0123	CG18741	DopR2	LexA	Clk856-GAL4

DKI0205	CG2302	nAChR α3	LexA	Clk856-GAL4
WCKI1184	CG2346	FMRFa	LexA	Clk856-GAL4
DKI0225	CG2872	AstA-R1	LexA	Clk856-GAL4
DKI0290	CG30018	mthl13	LexA	Clk856-GAL4
DKI0066	CG30340	CG30340	LexA	Clk856-GAL4
DKI0151	CG31096	Lgr3	LexA	Clk856-GAL4
DKI0231	CG31147	mthl11	LexA	Clk856-GAL4
DKI0232	CG31760	CG31760	LexA	Clk856-GAL4
DKI0234	CG32447	CG32447	LexA	Clk856-GAL4
DKI0259	CG32475	mthl8	LexA	Clk856-GAL4
WCKI1107	CG32476	CG32476	LexA	Clk856-GAL4
DKI0252	CG32540	CCKLR-17D3	LexA	Clk856-GAL4
DKI0206	CG32975	nAChR α5	LexA	Clk856-GAL4
DKI0101	CG33344	CCAP-R	LexA	Clk856-GAL4
DKI0284	CG33495	Dup99B	LexA	Clk856-GAL4
DKI0087	CG33495	Dup99B	LexA	Clk856-GAL4
DKI0128	CG33513	Nmdar2	LexA	Clk856-GAL4
DKI0315	CG33527	SIFa	LexA	Clk856-GAL4
DKI0180	CG33639	CG33639	LexA	Clk856-GAL4
DKI0246	CG34388	natalisin	LexA	Clk856-GAL4
DKI0175	CG34411	CG34411	LexA	Clk856-GAL4
DKI0102	CG3454	HDC	LexA	Clk856-GAL4
WCKI1101	CG3856	oamb	LexA	Clk856-GAL4
DKI0208	CG4128	nAChR α6	LexA	Clk856-GAL4
WCKI1044	CG42244	Octβ3R	LexA	Clk856-GAL4
DKI0193	CG4226	GluRIIC	LexA	Clk856-GAL4
DKI0173	CG42301	CCKLR-17D1	LexA	Clk856-GAL4
WCKI1166	CG4313	CG4313	LexA	Clk856-GAL4
DKI0276	CG4356	mAChR-A	LexA	Clk856-GAL4
DKI0016	CG43745	MsR2	LexA	Clk856-GAL4
WCKI1169	CG4395	hec	LexA	Clk856-GAL4
NT5E1-lexA	CG4827	NT5E-1	LexA	Clk856-GAL4
WCKI1176	CG5400	Eh	LexA	Clk856-GAL4
WCKI1203	CG5811	RYa-R	LexA	Clk856-GAL4
WCKI1205	CG5911	ETHR	LexA	Clk856-GAL4
WCKI1055	CG6371	CG6371	LexA	Clk856-GAL4
WCKI1009	CG6440	Ms	LexA	Clk856-GAL4
WCKI1011	CG6456	Mip	LexA	Clk856-GAL4
WCKI1192	CG6530	mthl3	LexA	Clk856-GAL4
WCKI1194	CG6536	mthl4	LexA	Clk856-GAL4
WCKI1049	CG6919	oa2	LexA	Clk856-GAL4
WCKI1118	CG6965	CG6965	LexA	Clk856-GAL4
DKI0192	CG6992	GluRIIA	LexA	Clk856-GAL4
WCKI1093	CG7285	AstC-R1	LexA	Clk856-GAL4

DKI0071	CG7411	Ort	LexA	Clk856-GAL4
DKI0311	CG7431	TyrR	LexA	Clk856-GAL4
DKI0299	CG7446	Grd	LexA	Clk856-GAL4
DKI0320	CG7497	CG7497	LexA	Clk856-GAL4
WCKI1094	CG7665	Lgr1	LexA	Clk856-GAL4
DKI0240	CG8380	DAT	LexA	Clk856-GAL4
DKI0047	CG8394	vGAT	LexA	Clk856-GAL4
WCKI1181	CG8422	Dh44-R1	LexA	Clk856-GAL4
DKI0269	CG8442	GluRIA	LexA	Clk856-GAL4
WCKI1174	CG8795	PK2-R2	LexA	Clk856-GAL4
WCKI1060	CG10001	CG10001	Gal4	Clk856-p65AD
DKI0130	CG14723	HisCl1	Gal4	Clk856-p65AD
DKI0041	CG15361	Nplp4	Gal4	Clk856-p65AD
WCKI1198	CG15556	CG15556	Gal4	Clk856-p65AD
DKI0255	CG18105	ETH	Gal4	Clk856-p65AD
DKI0198	CG31201	GluRIIE	Gal4	Clk856-p65AD
WCKI1164	CG3171	Tre1	Gal4	Clk856-p65AD
DKI0300	CG4910	CCAP	Gal4	Clk856-p65AD
DKI0226	CG6936	mth	Gal4	Clk856-p65AD
WCKI1178	CG6986	Proc-R	Gal4	Clk856-p65AD
DKI0297	CG7476	mthl7	Gal4	Clk856-p65AD
WCKI1053	CG9918	PK1-R	Gal4	Clk856-p65AD

Table S6 Phenotypes of CCT genes knocking out in clock neurons

Target Gene	LD condition				DD conditon		
	MAI	MAPI	EAI	EAPI	Power	Period	AR
Pdfr	**0.087 ± 0.119**	-0.047 ± 0.175	0.34 ± 0.076	**0.101 ± 0.071**	**3.45 ± 7.54**	**22.41 ± 0.51**	17/22
Pdf	**0.11 ± 0.124**	0.026 ± 0.12	0.383 ± 0.065	**0.114 ± 0.094**	**15.46 ± 34.25**	**22.31 ± 0.4**	13/23
nAChRα1	0.316 ± 0.121	**0.14 ± 0.145**	0.352 ± 0.094	-0.094 ± 0.068	**37.83 ± 27.68**	**23.18 ± 0.43**	1/14
Dh44	0.339 ± 0.111	0.042 ± 0.106	0.367 ± 0.09	-0.138 ± 0.088	**44.22 ± 45.84**	23.55 ± 0.24	7/19
CNMaR	0.345 ± 0.063	0.062 ± 0.129	0.342 ± 0.132	-0.042 ± 0.061	**71.37 ± 39.43**	24.01 ± 0.8	1/22
SIFaR	0.296 ± 0.076	0.062 ± 0.098	0.381 ± 0.08	-0.041 ± 0.078	**75.56 ± 66.38**	23.32 ± 0.33	4/24
ITP	0.277 ± 0.103	0.015 ± 0.106	0.357 ± 0.058	-0.06 ± 0.075	80.74 ± 39.06	23.75 ± 0.29	2/24
CG17777	0.272 ± 0.096	-0.025 ± 0.18	0.453 ± 0.068	-0.114 ± 0.048	81.81 ± 49.34	23.74 ± 0.29	1/22
Dh31	**0.205 ± 0.122**	-0.035 ± 0.134	0.405 ± 0.075	-0.092 ± 0.094	82.44 ± 51.16	23.5 ± 0.29	1/22
CG13995	0.346 ± 0.087	0.011 ± 0.152	0.414 ± 0.055	-0.072 ± 0.099	87.7 ± 36.53	23.56 ± 0.33	1/24
nAChRα2	0.26 ± 0.1	0 ± 0.145	0.348 ± 0.088	-0.042 ± 0.078	88.15 ± 50.2	23.7 ± 0.24	1/22
NPFR	0.269 ± 0.174	0.042 ± 0.092	0.403 ± 0.089	-0.072 ± 0.073	88.69 ± 46.62	23.35 ± 0.33	2/24
CrzR	0.324 ± 0.087	0.026 ± 0.122	0.415 ± 0.068	-0.028 ± 0.083	91.63 ± 54.11	23.35 ± 0.39	2/24
HisCl1	0.306 ± 0.075	0.08 ± 0.097	0.398 ± 0.04	-0.04 ± 0.096	93.7 ± 48.07	23.8 ± 0.39	1/23
AstC-R2	0.363 ± 0.074	-0.073 ± 0.164	0.465 ± 0.082	-0.136 ± 0.073	94.45 ± 57.72	24.04 ± 0.38	1/24
VGAT	0.249 ± 0.093	0.078 ± 0.118	0.402 ± 0.054	-0.106 ± 0.078	98.11 ± 52.33	23.42 ± 0.36	1/21
MsR1	0.31 ± 0.069	0.091 ± 0.089	0.336 ± 0.086	-0.099 ± 0.077	99.46 ± 46.48	24.14 ± 0.65	1/24
CCAP	0.321 ± 0.075	-0.028 ± 0.191	0.464 ± 0.06	-0.105 ± 0.074	99.76 ± 57.98	23.84 ± 0.37	0/22
CG34136	0.278 ± 0.084	0.022 ± 0.099	0.388 ± 0.052	-0.037 ± 0.085	101.43 ± 54.01	23.7 ± 0.43	1/22
GABA-B-R2	0.277 ± 0.078	-0.016 ± 0.108	0.337 ± 0.074	-0.084 ± 0.071	101.92 ± 30.51	23.95 ± 0.4	0/20
Hug	0.337 ± 0.073	0.013 ± 0.093	0.41 ± 0.042	-0.059 ± 0.081	102 ± 51.47	23.55 ± 0.39	1/23
nAChRβ2	0.254 ± 0.095	0.035 ± 0.121	0.355 ± 0.079	**-0.011 ± 0.07**	104.34 ± 42.52	23.91 ± 0.3	0/22
AstC	0.329 ± 0.102	-0.005 ± 0.178	0.36 ± 0.098	-0.017 ± 0.057	104.4 ± 48.76	23.71 ± 0.4	2/23
Nplp3	0.38 ± 0.06	0.023 ± 0.102	0.415 ± 0.041	-0.124 ± 0.076	105.02 ± 47.1	23.66 ± 0.35	1/22
Ptth	0.377 ± 0.069	-0.028 ± 0.127	0.409 ± 0.057	-0.061 ± 0.085	105.4 ± 35.61	23.49 ± 0.32	0/24
GluRIB	0.317 ± 0.079	-0.016 ± 0.137	0.363 ± 0.057	-0.059 ± 0.077	106.25 ± 41.48	23.78 ± 0.25	0/18
CCHa1-R	0.307 ± 0.1	0.052 ± 0.088	0.419 ± 0.041	-0.064 ± 0.073	106.83 ± 46.29	**23.28 ± 0.4**	0/23
TβH	0.257 ± 0.103	0.037 ± 0.123	**0.31 ± 0.061**	-0.05 ± 0.079	107.86 ± 44.06	23.74 ± 0.38	0/19
Oct-TyrR	0.343 ± 0.085	0.013 ± 0.107	0.387 ± 0.061	-0.088 ± 0.1	108.19 ± 56.73	23.94 ± 0.32	2/22
Clk856-GAL4>Cas9.M9	***0.3 ± 0.076***	***0.016 ± 0.09***	***0.38 ± 0.048***	***-0.066 ± 0.074***	***108.37 ± 30.19***	***23.8 ± 0.25***	***0/24***
Dop2R	0.357 ± 0.075	0.063 ± 0.137	0.425 ± 0.084	-0.076 ± 0.073	109.27 ± 69.88	23.51 ± 0.51	2/24
Mip	0.316 ± 0.052	0 ± 0.134	0.402 ± 0.048	-0.068 ± 0.066	111.37 ± 42.75	23.47 ± 0.42	1/22
TrH	0.26 ± 0.124	0.05 ± 0.124	0.365 ± 0.051	-0.024 ± 0.07	111.5 ± 41	23.7 ± 0.44	0/23
Trissin	0.261 ± 0.086	0.056 ± 0.116	0.362 ± 0.065	-0.073 ± 0.056	111.89 ± 54.79	23.4 ± 0.29	2/22
CG43795	0.333 ± 0.113	0.007 ± 0.114	0.415 ± 0.054	-0.099 ± 0.071	111.9 ± 57.29	23.57 ± 0.35	0/22
CG7589	0.327 ± 0.061	0.013 ± 0.12	0.474 ± 0.065	-0.092 ± 0.07	112.13 ± 45.66	23.8 ± 0.38	0/23
CNMa	0.284 ± 0.086	0.082 ± 0.12	0.364 ± 0.041	-0.091 ± 0.085	112.6 ± 41.9	23.97 ± 0.22	0/24
CG32547	0.249 ± 0.098	-0.015 ± 0.116	0.344 ± 0.078	-0.049 ± 0.072	112.98 ± 63.4	23.69 ± 0.29	2/23
CG45777	0.36 ± 0.067	-0.047 ± 0.154	0.484 ± 0.065	-0.119 ± 0.077	113.47 ± 68.45	23.55 ± 0.25	0/24
Octβ2R	0.319 ± 0.081	0.028 ± 0.065	0.434 ± 0.07	-0.061 ± 0.071	114.28 ± 63.82	23.55 ± 0.41	1/24
Dh44-R2	0.357 ± 0.058	0.054 ± 0.067	0.403 ± 0.047	-0.039 ± 0.07	115.91 ± 61.1	23.51 ± 0.39	1/23
VAChT	0.284 ± 0.095	-0.118 ± 0.116	0.401 ± 0.084	-0.154 ± 0.058	116.69 ± 74.92	23.93 ± 0.3	1/21
CCHa1	0.352 ± 0.058	0.002 ± 0.086	0.39 ± 0.062	-0.119 ± 0.081	116.75 ± 44.06	23.73 ± 0.32	1/22
mGluRA	0.321 ± 0.065	-0.005 ± 0.078	0.49 ± 0.047	-0.062 ± 0.073	116.82 ± 50.26	24.04 ± 0.25	1/23
PK2-R1	0.333 ± 0.079	0.037 ± 0.121	0.429 ± 0.046	-0.099 ± 0.093	117.33 ± 50.14	23.95 ± 0.27	1/22
spab	0.253 ± 0.08	-0.005 ± 0.094	0.363 ± 0.046	**0.002 ± 0.057**	117.38 ± 46.52	23.64 ± 0.26	0/22

Dh31-R	0.321 ± 0.103	-0.021 ± 0.161	0.412 ± 0.043	-0.09 ± 0.072	118.71 ± 50.62	23.6 ± 0.23	1/20
FMRFaR	0.294 ± 0.092	-0.013 ± 0.099	0.373 ± 0.033	-0.111 ± 0.074	119.47 ± 42.54	23.86 ± 0.32	0/21
CG13229	0.359 ± 0.069	0.059 ± 0.098	0.421 ± 0.049	-0.068 ± 0.066	122.46 ± 60.2	23.36 ± 0.37	2/21
mAChR-B	0.242 ± 0.112	0.09 ± 0.087	0.388 ± 0.037	-0.047 ± 0.081	122.88 ± 40.64	23.77 ± 0.42	0/23
5-HT2B	0.293 ± 0.085	0.035 ± 0.123	0.373 ± 0.042	-0.095 ± 0.084	124.65 ± 34.31	24.03 ± 0.29	0/24
TH	0.3 ± 0.101	0.016 ± 0.131	0.349 ± 0.11	-0.032 ± 0.086	125.71 ± 44.74	23.94 ± 0.33	1/23
Proc	0.362 ± 0.072	0.028 ± 0.142	0.437 ± 0.03	-0.086 ± 0.095	128.13 ± 61.01	23.57 ± 0.37	0/23
AstA	0.312 ± 0.092	-0.025 ± 0.113	0.412 ± 0.051	-0.082 ± 0.089	131.22 ± 35.09	23.63 ± 0.31	0/24
5-HT1B	0.313 ± 0.072	0.047 ± 0.117	0.402 ± 0.062	-0.083 ± 0.091	132.29 ± 41.37	23.5 ± 0.29	0/20
sNPF-R	0.283 ± 0.112	0.035 ± 0.069	0.387 ± 0.035	-0.089 ± 0.056	133.38 ± 41.77	23.74 ± 0.4	0/21
CG43117	0.285 ± 0.084	-0.03 ± 0.134	0.333 ± 0.081	-0.095 ± 0.092	134.98 ± 58.52	23.72 ± 0.33	0/21
NMDAR1	0.341 ± 0.066	0.065 ± 0.134	0.408 ± 0.052	-0.084 ± 0.083	135.01 ± 45.81	23.76 ± 0.23	1/19
GABA-B-R3	0.314 ± 0.104	0.041 ± 0.097	0.362 ± 0.061	-0.081 ± 0.056	135.49 ± 37.61	23.79 ± 0.24	0/23
CG12344	0.327 ± 0.062	-0.043 ± 0.154	0.465 ± 0.099	-0.121 ± 0.067	138.31 ± 63.27	23.98 ± 0.35	0/23
Gpb5	0.268 ± 0.058	-0.006 ± 0.12	0.424 ± 0.077	-0.078 ± 0.068	138.41 ± 42.42	23.69 ± 0.29	0/23
Nplp1	0.248 ± 0.115	0.072 ± 0.087	0.414 ± 0.023	-0.071 ± 0.103	138.54 ± 40.39	23.92 ± 0.3	0/23
Grd	0.26 ± 0.091	0.008 ± 0.132	0.448 ± 0.075	-0.065 ± 0.064	139.49 ± 78.28	23.65 ± 0.39	1/24
NPF	0.329 ± 0.086	0.007 ± 0.147	0.404 ± 0.067	-0.071 ± 0.05	139.57 ± 44.27	23.72 ± 0.3	0/23
sNPF	0.346 ± 0.084	-0.007 ± 0.118	0.414 ± 0.062	-0.111 ± 0.065	146.16 ± 58.23	23.6 ± 0.45	0/17
GlyT	0.273 ± 0.111	-0.119 ± 0.117	0.395 ± 0.076	-0.193 ± 0.105	105.325 ± 60.615	23.548 ± 0.245	5/43

1. VGlut and ChAT presented in Table S7

2. Genotype for each experimental group is Clk856-GAL4/UAS-sgRNA^{TargetGene}; UAS-Cas9.M9/+. Genotype for control group is Clk856-GAL4/+; UAS-Cas9.M9/+

3. Value in bolder indicate they are outside of one standard deviation (SD) compared to control group

Table S7 arrhythmicity related to Figure 6R

Genotype	arrhythmicity	Arrhythmic rate
+;UAS-Pdfr/+	2/44	4.55%
Pdfr-attpKO;UAS-Pdfr/+	29/44	65.91%
Pdfr-attpKO;;R79A11-GAL4/+	38/47	80.85%
Pdfr-attpKO;UAS-Pdfr/+; R79A11-GAL4/+	5/40	12.50%
Pdfr-attpKO;;R91F02-GAL4/+	36/48	75.00%
Pdfr-attpKO;UAS-Pdfr/+;R91F02-GAL4/+	9/40	22.50%
Pdfr-attpKO;;R51H05-GAL4/+	36/46	78.26%
Pdfr-attpKO;UAS-Pdfr/+; R51H05-GAL4/+	20/43	46.51%

Table S7 Phenotypes of candidate CCT genes knockout in clock neurons

Genotype	LD condition				DD condition		
	MAI	MAPI	EAI	EAPI	Power	Period	AR
sgRNA^{Dh44}, Cas9.M6	0.329 ± 0.086	-0.058 ± 0.119	0.38 ± 0.058	-0.081 ± 0.065	66.38 ± 40.4	23.18 ± 0.31	2/22
Clk856> sgRNA^{Dh44}	0.354 ± 0.093	0.03 ± 0.131	0.444 ± 0.045	-0.085 ± 0.066	94 ± 45.35	23.61 ± 0.34	2/20
Clk856> sgRNA^{Dh44}, Cas9.M6	0.346 ± 0.096	-0.02 ± 0.165	0.397 ± 0.059	-0.085 ± 0.077	74.64 ± 27.25	23.75 ± 0.31	0/20
sgRNA$^{nAChR\alpha1}$, Cas9.M6	0.29 ± 0.089	-0.064 ± 0.139	0.363 ± 0.056	-0.071 ± 0.064	58.35 ± 43.82	23.53 ± 0.45	2/13
Clk856> sgRNA$^{nAChR\alpha1}$	0.318 ± 0.096	0.019 ± 0.137	0.401 ± 0.052	-0.08 ± 0.071	56.89 ± 45.03	23.66 ± 0.43	1/12
Clk856> sgRNA$^{nAChR\alpha1}$, Cas9.M6	0.307 ± 0.154	-0.031 ± 0.099	0.381 ± 0.056	-0.074 ± 0.074	69.21 ± 52.1	23.71 ± 0.29	2/13
sgRNA^{ChAT}, Cas9.M6	0.292 ± 0.096	0.026 ± 0.155	0.291 ± 0.092	-0.1 ± 0.055	91.48 ± 55.18	23.43 ± 0.41	3/19
Clk856> sgRNA^{ChAT}	0.298 ± 0.098	-0.016 ± 0.157	0.353 ± 0.071	-0.079 ± 0.051	78.66 ± 41.65	23.54 ± 0.25	1/22
Clk856> sgRNA^{ChAT}, Cas9.M6	0.22 ± 0.137	0.003 ± 0.123	0.318 ± 0.078	-0.124 ± 0.075	49.35 ± 42.11	23.7 ± 0.2	4/14
sgRNA^{CNMa}, Cas9.M6	0.342 ± 0.076	-0.141 ± 0.138	0.35 ± 0.091	-0.088 ± 0.079	92.81 ± 39.89	23.98 ± 0.44	1/23
Clk856> sgRNA^{CNMa}	0.355 ± 0.181	0.019 ± 0.093	0.431 ± 0.05	-0.121 ± 0.079	18.96 ± 22.19	23.8 ± 0.27	7/14
Clk856> sgRNA^{CNMa}, Cas9.M6	0.354 ± 0.11	0.113 ± 0.169	0.353 ± 0.086	-0.072 ± 0.066	93.51 ± 48.39	24.17 ± 0.42	1/20
sgRNA^{VGlut}, Cas9.M6	0.254 ± 0.114	-0.115 ± 0.14	0.32 ± 0.066	-0.073 ± 0.043	56.28 ± 39.85	23.41 ± 0.38	1/20
Clk856> sgRNA^{VGlut}	0.306 ± 0.102	-0.026 ± 0.146	0.369 ± 0.074	-0.104 ± 0.067	63.82 ± 48.6	23.6 ± 0.36	5/20
Clk856> sgRNA^{VGlut}, Cas9.M6	0.179 ± 0.1**	-0.087 ± 0.107	0.27 ± 0.07	-0.158 ± 0.063	45.09 ± 41.35	23.7 ± 0.27	6/21
sgRNA$^{mAChR\text{-}B}$, Cas9.M6	0.37 ± 0.062	-0.047 ± 0.109	0.374 ± 0.064	-0.076 ± 0.054	110.16 ± 32.99	23.78 ± 0.47	0/21
Clk856> sgRNA$^{mAChR\text{-}B}$	0.358 ± 0.095	-0.003 ± 0.109	0.442 ± 0.038	-0.143 ± 0.087	73 ± 36	23.48 ± 0.45	0/17
Clk856> sgRNA$^{mAChR\text{-}B}$, Cas9.M6	0.259 ± 0.1	-0.109 ± 0.139	0.357 ± 0.066	-0.088 ± 0.074	109.35 ± 45.07	23.71 ± 0.36	0/22
sgRNA^{MsR1}, Cas9.M6	0.339 ± 0.078	-0.011 ± 0.175	0.368 ± 0.061	-0.072 ± 0.087	55.68 ± 49.3	23.77 ± 0.55	5/22
Clk856> sgRNA^{MsR1}	0.378 ± 0.098	-0.023 ± 0.114	0.4 ± 0.036	-0.143 ± 0.075	55.05 ± 43.19	23.89 ± 0.4	3/19
Clk856> sgRNA^{MsR1}, Cas9.M6	0.276 ± 0.085	-0.04 ± 0.123	0.313 ± 0.063	-0.085 ± 0.083	78.21 ± 50.06	23.85 ± 0.48	2/21
sgRNA^{SIFaR}, Cas9.M6	0.254 ± 0.104	-0.075 ± 0.14	0.34 ± 0.047	-0.072 ± 0.052	82.85 ± 42.29	23.63 ± 0.35	0/23
Clk856> sgRNA^{SIFaR}	0.329 ± 0.122	-0.058 ± 0.121	0.375 ± 0.059	-0.096 ± 0.05	81.71 ± 41.2	23.82 ± 0.36	0/21
Clk856> sgRNA^{SIFaR}, Cas9.M6	0.219 ± 0.143	-0.142 ± 0.172	0.299 ± 0.095	-0.117 ± 0.088	94.45 ± 32.78	24.04 ± 0.38	0/19
Clk856> Cas9.M6	0.295 ± 0.12	-0.043 ± 0.109	0.325 ± 0.081	-0.118 ± 0.048	90.64 ± 43.86	23.7 ± 0.27	1/16

Clk856> sgRNA^{VGlut}, Cas9.M6 vs Clk856> sgRNA^{VGlut} , ** $P < 0.01$

Clk856> sgRNA^{VGlut}, Cas9.M6 vs Clk856> Cas9.M6 , ** $P < 0.01$

Clk856> sgRNA^{VGlut}, Cas9.M6 vs sgRNA^{VGlut}, Cas9.M6, $P = 0.0921$

Table S8 Conditional knockout of VGlut in DN1s

Genotype	LD condition				DD condition		
	MAI	MAPI	EAI	EAPI	POWER	PERIOD	AR
sgRNA^{VGlut},Cas9.M6	0.268 ± 0.124	-0.072 ± 0.106	0.328 ± 0.071	-0.065 ± 0.035	79.06 ± 49.45	22.89 ± 0.19	1/23
R18H11>sgRNA^{VGlut}	0.258 ± 0.085	-0.093 ± 0.104	0.327 ± 0.05	-0.124 ± 0.069	67.49 ± 42.52	23.38 ± 0.36	1/21
R18H11>sgRNA^{VGlut},Cas9.M6	**0.136 ± 0.148 ****	-0.109 ± 0.116	0.284 ± 0.106	-0.084 ± 0.061	61.9 ± 42.35	23.18 ± 0.27	4/24
R18H11>Cas9.M6	0.25 ± 0.093	-0.068 ± 0.124	0.387 ± 0.055	-0.048 ± 0.057	55.46 ± 49.14	23.33 ± 0.43	5/20
R51H05>sgRNA^{VGlut}	0.348 ± 0.067	-0.078 ± 0.078	0.398 ± 0.051	-0.103 ± 0.047	122.02 ± 38.89	23.4 ± 0.37	0/20
R51H05>sgRNA^{VGlut},Cas9.M6	0.26 ± 0.097	-0.16 ± 0.116	0.312 ± 0.073	-0.062 ± 0.059	82.56 ± 48.06	23.23 ± 0.33	2/22
R51H05>Cas9.M6	0.251 ± 0.098	-0.118 ± 0.143	0.349 ± 0.087	-0.055 ± 0.072	45.76 ± 41.2	23.19 ± 0.39	3/17
R79A11>sgRNA^{VGlut}	0.172 ± 0.131	-0.11 ± 0.102	0.378 ± 0.055	-0.087 ± 0.062	88.87 ± 40.43	23.43 ± 0.31	1/21
R79A11>sgRNA^{VGlut},Cas9.M6	0.178 ± 0.11	-0.131 ± 0.083	0.325 ± 0.08	-0.068 ± 0.037	75.67 ± 45.37	23.3 ± 0.29	1/19
R79A11>Cas9.M6	0.19 ± 0.132	-0.128 ± 0.114	0.346 ± 0.052	-0.082 ± 0.065	31.29 ± 32.62	23.16 ± 0.47	3/21
R91F02>sgRNA^{VGlut}	0.233 ± 0.099	-0.108 ± 0.1	0.341 ± 0.069	-0.081 ± 0.049	97.13 ± 41.94	23.73 ± 0.39	0/21
R91F02>sgRNA^{VGlut},Cas9.M6	0.301 ± 0.109	-0.109 ± 0.056	0.381 ± 0.071	-0.061 ± 0.042	112.28 ± 47.81	23.45 ± 0.31	0/24
R91F02>Cas9.M6	0.26 ± 0.166	-0.078 ± 0.107	0.366 ± 0.065	-0.035 ± 0.04	72.82 ± 45.83	23.43 ± 0.41	2/22
CNMa-KI-GAL4>sgRNA^{VGlut}	0.28 ± 0.123	-0.058 ± 0.088	0.357 ± 0.043	-0.063 ± 0.019	54.7 ± 43.96	23.03 ± 0.33	3/23
CNMa-KI-GAL4>sgRNA^{VGlut},Cas9.M6	0.268 ± 0.094	-0.117 ± 0.119	0.331 ± 0.055	-0.048 ± 0.086	51.21 ± 36.91	22.83 ± 0.29	3/18
CNMa-KI-GAL4>Cas9.M6	0.261 ± 0.066	-0.155 ± 0.114	0.342 ± 0.051	-0.088 ± 0.08	54.14 ± 36.21	22.85 ± 0.21	2/24
Clk4.1M>sgRNA^{VGlut}	0.281 ± 0.116	-0.052 ± 0.102	0.4 ± 0.057	-0.174 ± 0.043	61.29 ± 46.5	23.45 ± 0.39	3/23
Clk4.1M>sgRNA^{VGlut},Cas9.M6	0.181 ± 0.111	-0.074 ± 0.07	0.313 ± 0.101	-0.112 ± 0.047	77.13 ± 38.86	23.44 ± 0.38	0/21
Clk4.1M>Cas9.M6	0.294 ± 0.102	-0.096 ± 0.098	0.41 ± 0.035	-0.087 ± 0.051	80.18 ± 40.76	23.51 ± 0.25	0/24

***** P <0.01***